THESIS FOR THE DEGREE OF LICENTIATE OF ENGINEERING

Geodetic analysis for the Very Long Baseline Interferometry Global Observing System

NIKO KAREINEN

CHALMERS

Department of Earth and Space Sciences
CHALMERS UNIVERSITY OF TECHNOLOGY
Göteborg, Sweden 2016

Geodetic analysis for the Very Long Baseline Interferometry Global Observing System
NIKO KAREINEN

Space Geodesy and Geodynamics Group
Department of Earth and Space Sciences
Chalmers University of Technology
SE–412 96 Göteborg, Sweden
Phone: +46 (0)31–772 1000

Contact information:
Niko Kareinen
Chalmers University of Technology
Onsala Space Observatory
SE–439 92 Onsala, Sweden

Phone: +46 (0)31–772 5566
Email: niko.kareinen@chalmers.se

Printed by Chalmers Reproservice
Chalmers University of Technology
Göteborg, Sweden 2016

Geodetic analysis for the Very Long Baseline Interferometry Global Observing System

NIKO KAREINEN
Department of Earth and Space Sciences
Chalmers University of Technology

Abstract

Very Long Baseline Interferometry (VLBI) is an essential technique for space-geodesy. It realizes the International Celestial Reference Frame (ICRF) and provides a link between the Earth- and space-fixed coordinate systems by directly observing all Earth Orientation Parameters (EOP) simultaneously. In particular, it is the only technique available that can directly measure UT1-UTC and nutation. This of special importance to satellite-based techniques, which need regular input from VLBI observations to account for drifts in their derived UT1-UTC estimates. Currently, daily UT1-UTC estimates from VLBI are provided by 1-hour Intensive sessions with three regular baseline configurations, which provide UT1-UTC with an appropriate accuracy of 20 μs. Increased UT1-UTC accuracy is given by bi-weekly 24-hour Rapid turnaround sessions for EOP determination, which employ a network of at least 8 stations. However, the typical delay for the results obtained from these sessions is close to the specified upper limit of 15 days.

The VLBI Global Observing System (VGOS) is the upcoming VLBI component of the Global Geodetic Observing System (GGOS) of the International Association of Geodesy (IAG). It represents a complete redesign of the current VLBI system to meet the requirements for a system capable of observing phenomena with a magnitude of a few millimetres.

For VGOS the main goals are a global accuracy of 1 mm for positions and 1 mm/y for velocities and continuous monitoring of EOP and station positions. Major effort in hardware and software across the whole signal chain are needed to accomplish these goals. This includes investments in, to name a few, new telescopes, front- and backends, recording systems, correlation, and data analysis. Most of the related systems need to be automated to ensure reliable continuous operations. In this thesis the aspects of geodetic VLBI data analysis related to the transition to VGOS are investigated through two practical cases.

The VGOS requirements necessitate upgrades in the station hardware. In 2011 Onsala Space Observatory installed a digital backend (Digital Base-Band Converter (DBBC) system) alongside the operational analogue Mark IV system. The effect of this hardware change on the VLBI observables and estimated geodetic parameters is investigated through analysing a series of sessions recorded in parallel on both the old and the new systems.

Automated near-real time VLBI analysis is studied using the Intensive sessions on the Kokee–Wettzell baseline. The impact in terms of availability of a priori data for the

analysis are investigated to determine the most crucial factors for high-accuracy UT1-UTC production in an automated near-real time mode.

Keywords: VLBI; VGOS; GGOS; digital back-ends; DBBC; Earth rotation; EOP; UT1; automated analysis

List of appended papers

This thesis is based on the following papers. References to the papers will be made using the Roman numerals associated with the papers.

I Kareinen, N. and Haas, R. (2015), 'Experience from geodetic very long baseline interferometry observations at Onsala using a digital backend', *Journal of Geodetic Science* **5**(1), pp. 26–34.

II Kareinen, N., Hobiger, T. and Haas, R. (2015), 'Automated analysis of Kokee–Wettzell Intensive VLBI sessions—algorithms, results, and recommendations', *Earth, Planets and Space* **67**(1), p. 181.

Acknowledgements

I would like to thank my supervisor Rüdiger Haas for his unwaivering support, without which this work would have not been possible. Also a big thank you goes to my co-supervisor Thomas Hobiger. A sincere thank you also goes to all the PhD students at the department of Earth and Space Sciences, who have made these 2.5 years go by in a blink of an eye.

Niko

Contents

List of Figures

List of Tables

Chapter 1

Introduction

The Earth is a system of complex interactions driven by a multitude of underlying physical forces. With increased understanding of these processes, the possibilities of using geodesy to help studying these phenomena become increasingly diverse. The shape, gravity field, and orientation of the Earth in time and space make up the three pillars of geodesy. These elements are all but static. Variations are caused by the composition of Earth itself – its geometric shape, internal structure, and ongoing dynamic processes – as well as the gravitational effect exerted by the Sun, Moon and planetary bodies in our solar system. The mass distribution of the Earth is governed by secular processes such as plate tectonics, and dynamical ones such as the weather. The redistribution of the air masses driven mainly by solar radiation happen in cyclic and predictable as well as chaotic manner. The mass and volume of the oceans are subject to changes connected to prevailing temperature conditions and sea water composition. Depending on the interplay with other geophysical processes such as land uplift or sinking, sea-level variations can have drastic local and global consequences for the nature and human lives. Global warming is the observed long-term rise in the trend of global mean surface temperature since the start of the 20^{th} century (Hartmann et al., 2013). This increase in the energy of the system is mainly being stored into the oceans. On a global scale this is detected as an increase in the mean sea level. According to Bindoff et al. (2007) between the years 1993 and 2010 the global mean sea level rose by 3.2 ± 0.4 mm. Interpreting and forecasting the effect of these changes is a difficult task due to the complexity and numerous feedback loops in the Earth system. All of these changes in the mass distribution of the Earth have an effect on the gravity field and the angular momentum vector of the Earth, which can be observed with geodetic techniques. As such geodesy provides an indispensable tool to directly study the geophysical processes affecting and affected by these global changes. Moreover, by establishing accurate reference frames, geodesy pro-

vides a reliable framework in which different fields of Earth sciences can refer, compare, and validate their observations. Today there are multiple available techniques with varying properties for monitoring Earth rotation. The technique used within this thesis is the geodetic Very Long Baseline Interferometry (VLBI) (Sovers et al., 1998). It is unique among space-geodetic techniques in the sense that it is the only one capable of determining all the five Earth Orientation Parameters (EOP) simultaneously. This is of particular importance to satellite-based techniques, which rely on VLBI to determine the phase of the Earth's rotation (i.e. UT1). The satellite-techniques themselves are only capable of directly observing the changes in UT1-UTC (i.e. its time derivative). Timely VLBI observations are needed in order to observe drift-free UT1.

Geodetic VLBI is moving towards a new observing infrastructure defined in the VLBI Global Observing System (VGOS) (Petrachenko et al., 2009) project, which is an element in the Global Geodetic Observing System (GGOS) (Plag and Pearlman, 2009). The growing requirements for e.g. data rates and bandwidth necessitate a shift from analogue legacy hardware towards modern digitized alternatives, which provide better controllability and flexibility. The subject of this thesis concerns the existing challenges in low-latency monitoring of the EOP, with emphasis on Universal Time (UT1), using geodetic VLBI as well as the transition to the VGOS with continuous observations and minimal latency.

1.1 Thesis structure

EOP and UT1 are parameters which describe the movement of the Earth's rotation vector. They are observed within the Earth system and they are thus dynamically connected by a wide range of interacting phenomena. The structure of the thesis aims at first to define and describe the Earth system and the phenomena that are the underlying causes for the variations in the geodetic parameters. The focus of this thesis is on the technique of VLBI. First, it is discussed in terms of its basic principle, practice, technical aspects, and modelling. Then the methods of VLBI processing used in the analysis of the research conducted in the context of this thesis are introduced. Finally, results connected to the papers appended to this thesis are discussed. The chapter structure of the thesis is as follows.

- Chapter 2 discusses the different processes ongoing within system Earth, as well as their monitoring. First, the practical monitoring of system Earth is discussed. The organised global geodetic effort is introduced through the International Association of Geodesy (IAG) the GGOS and its relation to the Global Earth Observing System of Systems (GEOSS). Secondly, the different geophysical phenomena observed within system Earth with var-

ious geodetic observations are categorized and discussed, with an emphasis on Earth rotation.

- Chapter 3 describes the practical and theoretical aspects of VLBI. Firstly, the motivation and the basic principles of VLBI and geodetic VLBI are briefly introduced. Then, the organization, namely the International VLBI Service for Geodesy and Astrometry (IVS) (Schuh and Behrend, 2012), and its components which organize and coordinate the international efforts of Earth observation and monitoring with VLBI are discussed. This includes introducing IVS components and current types of routine observing session. Moreover, the VLBI contribution to GGOS, namely VGOS and its specifications, requirements, and objectives are discussed.

  Finally, the theoretical aspects of geodetic parameters estimation in geodetic VLBI are discussed. The delay model for VLBI observations is introduced. This includes the model of observation geometry and description of the error sources affecting the parameter estimation.

- Chapter 4 introduces general aspects and methods of VLBI data processing. Available VLBI analysis software packages are briefly introduced with an emphasis on the two software packages used in the context of this thesis. This is followed by the common VLBI data analysis approaches needed to process different session types. Furthermore, VLBI data processing aspects related to the work done in the included papers are discussed.

- Chapter 5 summarises and discusses the results from the analysis done within this work. The main results from *Papers I* and *II* are discussed as well as some views of the future.

Chapter 2

Monitoring system Earth

Earth is a dynamical system consisting of complex interactions between a wide range of phenomena. This system consists of everything contained in Earth and its sphere of influence: geophysical phenomena, weather and climate, water masses contained in oceans and hydrological cycles, biosphere and its ecosystems. Furthermore, the interests of mankind also lie in managing the natural resources that form the basis of our survival. An important aspect is also the capability to understand and predict natural hazards that can have immense impact on the civilization. This includes recognizing our own influence on the nature. The main elements driving these physical processes in this system are the gravitational attraction exerted by the Sun and the Moon, the solar radiation emitted by the Sun, and the inner structure of the Earth. Planet Earth is influenced by its biosphere, which includes a vastly complex layer to the geological Earth. Life on Earth interacts with the surrounding environment both on geological and short time scales. Most recently humankind has contributed to the global warming by releasing large quantities of green house gases to the atmosphere (Cook et al., 2013). System Earth is a sum of multiple subsystems. The hierarchy between these systems is intricate due to feedback loops and complex interactions. In general these systems are characterized both by their internal processes as well as interaction with other subsystems. The following listing summarizes some of the main components of system Earth (Chernicoff, 1999, Ratcliffe, 1972, Peixoto and Oort, 1992, Barry and Chorley, 1992, Vaughan et al., 2013).

- Earth structure: inner and outer core, mantle, crust
  - Lithosphere: includes portions of mantle and the crust. It consists of tectonic plates moving on top the Earth's mantle and is driven by a heat-flow emanating from the mantle. Plate tectonics are intrinsically linked with seismic events and volcanism.

- Hydrosphere: contains the combined water masses of Earth. Ocean currents transport large amounts of mass and heat around the planet. The hydrological cycle of water in and on the earth top layer is closely linked to weather systems in the atmosphere.
  - Cryosphere: consist of the frozen mass of the hydrosphere, including snow and ice. The largest part is formed by the continental glaciers. Cryosphere is intrinsically linked with the albedo of Earth and global warming through its melting response.
- Atmosphere: the mass of gases that surround planet Earth. The atmosphere is divided into different layers and section based on composition, temperature, and air movement. It consists of five main layers.
  - Troposphere (0–20 km): contains approximately 99 % of atmospheric water content and 80 % of the atmosphere's mass. The main weather phenomena take place in the troposphere.
  - Stratosphere (20–50 km): has 19 % of atmospheric gases and contains the ozone layer.
  - Mesosphere (50–85 km): a region with planetary scale winds caused by atmospheric tides.
  - Thermosphere (85–600 km): contains the ionosphere – a layer of ionized gas molecules, which is important to space geodesy due to its effect on electromagnetic signal propagation.
  - Exosphere (600–10000 km): region where the gas particles escape the gravitational pull of the Earth. Contains the inner part of the Van Allen Radiation belt.
  - Magnetosphere: the magnetic field surrounding Earth generated by the flow of the molten outer core.
- Biosphere: the system which includes all living organisms and their interaction with the environment.
  - Antroposphere: subsystem of the biosphere and its components which include and are influenced by humankind.

In order to understand this system it is necessary to monitor both its subcomponents and their interactions. In 2005 a plan on international collaboration in global earth observation was adopted by nearly 60 governments and the European Commission (Battrick, 2005). The plan involves a Global Earth Observation System of Systems (GEOSS), which aims to coordinate the effort on combining the effort and output from existing Earth observation systems into an interoperating system of systems. A 10-year implementation plan defined

the first measures to take in forming a functioning collection of organizations and agencies from local to global scale that would form the GEOSS. The main purpose of GEOSS is to provide reliable, accurate, and timely information on phenomena within system Earth that influence humankind. This will form a basis of informed decision making that is based on accurate data. GEOSS will thus act as a link between different research fields by providing an infrastructure of collaboration and data sharing. The main objectives of GEOSS emphasize using high-quality data to achieve societal benefits. The improvement goals include resource management, reducing loss of life, weather prediction, ecosystem management, conservation of biodiversity, and sustainable practices in agriculture.

Monitoring the changes in this system requires a highly accurate and stable infrastructure in which to perform these observations. This infrastructure is provided by geodesy through its study of Earth's motion, gravity field, and dimensions. The total mass distribution of Earth is connected with its deformation and rotation in space. By connecting observations of these displacements, gravity field, and spatial dimensions we are able to establish reference frames in which changes in these quantities can be measured accurately. Through these measurements it is possible to gain insight into the geophysical characteristics of the Earth.

2.1 Global Geodetic Observing System

The Global Geodetic Observing System (GGOS) is an observing system of the International Association of Geodesy (IAG) that brings together different areas and techniques of geodesy as a combined system. The decision to establish GGOS was made in 2003 and in 2007 it became an official IAG component. As an organizational layer GGOS acts as the link between the needs of GEOSS and the contributions of the geodetic services provided by various IAG components. In 2005 it was recognized in Plag et al. (2005) that, within the framework of the 10-year implementation plan of GEOSS, geodesy will provide GEOSS components with accurate reference frames. Furthermore, it will contribute to all GEOSS areas of societal benefits. The main operational structure of GGOS is formed by the 15 IAG services. Table 2.1 summarizes these IAG components and their functions.

2.1.1 GGOS techniques

The techniques involved with the services in Table 2.1 include e.g. the space-geodetic techniques that are involved with monitoring Earth rotation and its geometry, satellite gravimetry missions, absolute and relative gravimeters, tide

gauges, satellite altimetry, and Interferometric Synthetic Aperture Radar (InSAR). GGOS seeks to combine these systems into a consistent single system. Figure 2.1 illustrates the connections between the three pillars of geodesy and their respective techniques.

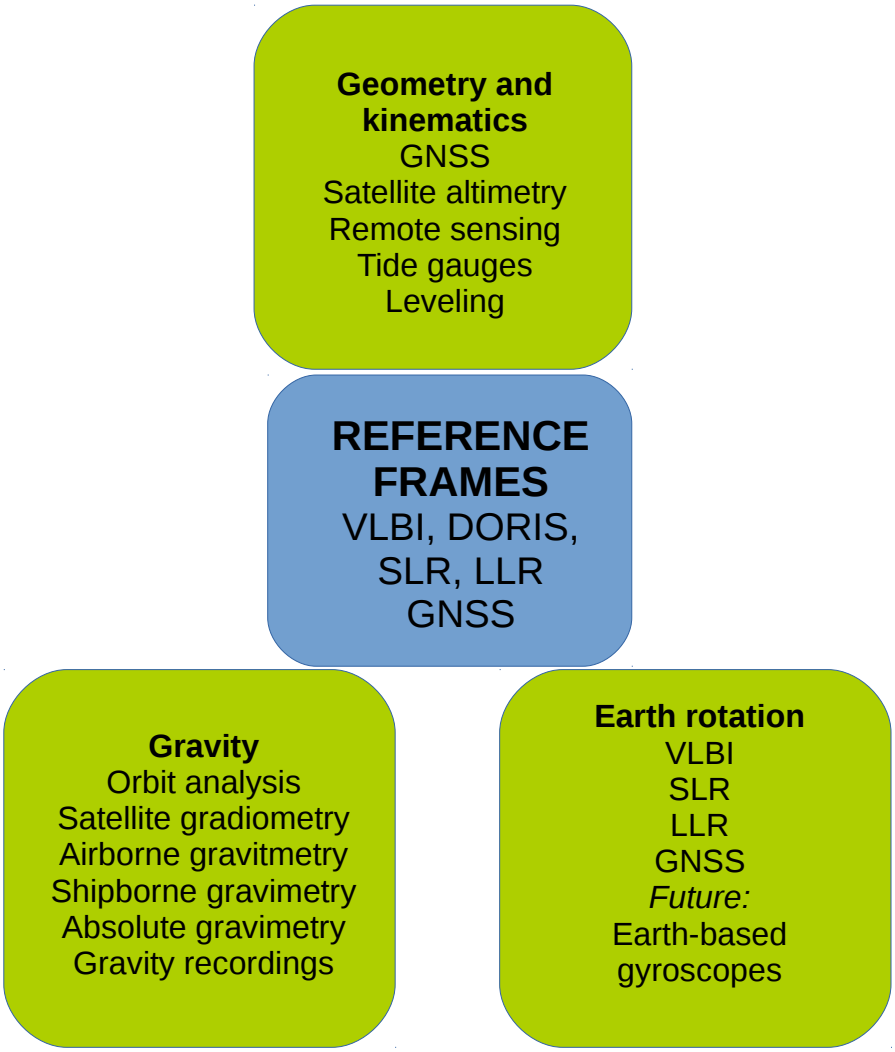

Figure 2.1: The three pillars of geodesy. GGOS observation techniques and their connections to establishing reference frames. The diagram is adapted from Plag and Pearlman (2009).

The four geometric space-geodetic techniques involved with monitoring Earth rotation are Very Long Baseline Interferometry (VLBI), Global Navigation Satellite Systems (GNSS), Doppler Orbitography and Radiopositioning Integrated by Satellite (DORIS), and Satellite/Lunar Laser Ranging (SLR, LLR). In addition to these traditional methods terrestrial ring laser gyroscopes are a

promising new addition to the well-tested existing techniques. In theory ring lasers enable the direct measurement of the instantaneous angular velocity of Earth (Plag and Pearlman, 2009). However, the method currently suffers from insufficient sensor stability and resolution. VLBI and ring laser observations have been successfully combined in e.g. Parselia et al. (2014). Since the VLBI accuracy outperformed that of the ring laser, only modest improvement could be obtained with a combined solution.

In the context of this thesis in the following emphasis will be given to Earth rotation monitoring. However, it is important to note that even though Earth rotation is primarily measured with geometric space-geodetic techniques, the underlying phenomena which influence the temporal variations in Earth rotation are connected with geophysical processes that can be observed by other GGOS techniques. Earth rotation, its gravity field, and deformations influence one another through a complex network of interactions. As such a complete picture of the system Earth will contribute to the accuracy of Earth rotation monitoring and vice versa.

2.2 Earth rotation and geophysical models

Earth rotation and its variations are a combination of contributions from a wide array of geophysical phenomena, which also affect Earth's gravitational field and deform its shape. Earth is neither solid or regular, but closer to an irregular rotational ellipsoid that consist of different layers of solid and viscous material. Thus, in the presence of both external torques from the Sun, the Moon, and the planets, and inner material fluctuations, Earth is not a rigid body, but deforms in response to excitations by these forces. Furthermore, Earth is covered by dynamic layers of fluid and gas, which are also affected by these external torques, as well as dynamics driven by e.g. diurnal solar radiation and internal composition. The resulting changes in the mass distribution of the Earth are reflected in the changes of the direction of its rotation vector. In general the rotation of a non-rigid Earth system can be described by Eulerian equations with time varying angular momentum and external torques. The movement of the Earth's rotational axis relative to the space-fixed frame is affected by long-term variation in the form of precession and nutation. Earth's rotation axis is inclined approximately 23.5° relative to the celestial plane. It rotates around this pole with a main period of 26000 years. This motion is superimposed with minor terms, which together constitute the precession-nutation of the Earth's axis of rotation (Lambeck, 1988).

The angular velocities of the Earth-fixed axes about themselves are assumed to be small variations in the direction cosines of the angular velocity vector with respect to the rotation axis of the Earth. The dynamical Liouville equations of

motion for non-rigid Earth are given by

$$\frac{\mathrm{d}}{\mathrm{d}t}[\mathbf{I(t)}\boldsymbol{\omega} + \mathbf{h}(t)] + \boldsymbol{\omega} \times [\mathbf{I}(t)\boldsymbol{\omega} + \mathbf{h}(t)] = \mathbf{L}, \tag{2.1}$$

where $\mathbf{I}(t)$ is the time-dependent inertia tensor, $\mathbf{h}(t)$ is the angular momentum vector relative to Earth-fixed axes, $\mathbf{L}$ is the applied torque. The $\boldsymbol{\omega}$ is the angular rotation vector of the Earth, given by

$$\boldsymbol{\omega} = \omega_0[m_1\hat{\mathbf{x}}_1 + m_2\hat{\mathbf{x}}_2 + (1 + m_3)\hat{\mathbf{x}}_\mathbf{3}], \tag{2.2}$$

where ω_0 is the mean angular velocity of the Earth, $\hat{\mathbf{x}}_{1,2,3}$ are the Earth-fixed axes, and $m_{1,2,3}$ are small disturbances in the non-rigid motion of the rotation vector. The latter are angular displacements that describe the position of the instantaneous rotation axis $\boldsymbol{\omega}$ with respect to the Earth-fixed axes $\hat{\mathbf{x}}$ on the equator plane of x_3. m_1 and m_2 correspond to counter-clockwise rotations around x_1 and x_2, respectively. The movement described by these two is called the polar motion, giving the position of the instantaneous rotation axis. The m_3 describes the difference from the uniform speed of rotation ω_0. It is connected to the Length-Of-Day (LOD), the excess of day measured by UT1 with respect to 86400 s. LOD and UT1 are related by

$$m_3 = \frac{\mathrm{LOD}}{86400\ \mathrm{s}} = -\frac{d}{dt}(\mathrm{UT1} - \mathrm{UTC}). \tag{2.3}$$

Formulating in terms of the three axes, Equation 2.1 can be written as

$$\begin{aligned} \frac{\boldsymbol{i}\dot{m}_1 - \dot{m}_2}{\sigma_r} + m_1 + \boldsymbol{i}m_2 &= \psi_1 + \boldsymbol{i}\psi_2, \\ m_3 &= \psi_3, \end{aligned} \tag{2.4}$$

where $\boldsymbol{i}$ denotes imaginary unit and σ_r is the rigid-body wobble frequency.
The $\psi_{1,2,3}$ are excitation functions, which characterise the torques, relative motions, and changes in the inertial tensor of the system. This formulation describes the Earth rotation response to the geophysical phenomena included in the excitation functions. Furthermore, it separates polar motion and the variations in the rate of rotation. The rigid-body wobble frequency includes information on the constant terms of the inertial tensor components. The excitation functions include the time-dependent changes in the inertial tensor and angular momentum vector (Lambeck, 1988).

2.2.1 Tides and station displacements

The combined gravitational pull of the Sun, the Moon, and to some extent other planets, cause angular torques and a series of tidal forces that through their

impact on the solid Earth, atmosphere, and oceans disturb the orientation of the Earth's rotation axis, change the Earth's gravitational field, and deform the solid Earth. The tides consist of both permanent and periodic parts. The tide that has all the observed periodic variation removed is referred to as mean tide. In addition to the direct response to gravitational changes, the crustal deformation is also driven by plate tectonics, which in turn are closely connected with volcanism and seismic activity. Furthermore, the global distribution of ground water, snow, and ice masses cause crustal loading and relaxation effects.

Major changes in the cryosphere are caused by the phase in the global cooling and warming cycles, mainly driven by the precession of the Earth's axis of rotation. We are currently in an ongoing interglacial period. This has released water locked in glaciers and polar ice caps. The removal of these ice masses causes the previously compressed crust to rebound, which can be detected through glacial isostatic adjustment as post-glacial uplift. Moreover, short-term variations in the cryosphere, e.g. snowfall, also contribute to crustal loading. Furthermore, changes in the biosphere and ground water deposits contribute to the seasonal variation seen in various loading phenomena. The following sections will describe the main tidal responses.

Solid Earth tides

The combined effect of the tidal potential caused by the Sun, the Moon, and the planets exert forces that deform Earth. The tidal forces in combination with the orbital acceleration and rotation of the Earth lead to two main tidal bulges. This leads to a deformation of the Earth's crust and consequently displacement of observing sites, e.g. GNSS and VLBI instrumentation. The geopotential field V(r,λ,ϕ) expanded into spherical harmonics is given by

$$V(r,\lambda,\phi) = \frac{GM}{r}\sum_{n=0}^{N}\left(\frac{a_e}{r}\right)^n \sum_{m=0}^{n}[\overline{C}_{nm}\cos m\lambda + \overline{S}_{nm}\sin m\lambda]\overline{P}_{nm}(\sin\phi), \qquad (2.5)$$

where GM and a_e are geocentric gravitational constant and the Earth radius consistent with EGM2008, respectively. r, ϕ and λ are the geocentric distance, latitude and longitude. The $\overline{P}_{nm}$ are fully normalized spherical harmonic functions. $\overline{C}_{nm}$ and $\overline{S}_{nm}$ are the fully normalized geophysical spherical harmonic coefficients (Petit and Luzum, 2010). The harmonic coefficients describe the contributions of the sum terms to Earth's potential, where the zero-degree term corresponds to that of the spherical Earth (Torge and Müller, 2012). Harmonic expansion of the potential leads to three main frequencies for the tidal potential, which represent long periodic, diurnal, and semi-diurnal tides. The crustal deformation response to the tidal potential depends on its composition. The maximum amplitude of solid Earth tides reach amplitudes of 50 cm (Sovers

et al., 1998). The solid tides have to be modelled and accounted for in precise geodetic applications by appropriate observing instrument displacements. The solid Earth tide is the primary tidal effect affecting the observed positions.

Ocean loading

Similarly to Earth tides, the ocean masses also respond to the tidal forces caused be the Sun and the Moon. These shifting water masses deform the underlying crust, and cause an effect called ocean loading. This leads to horizontal and vertical station displacements on a centimetre level (Petit and Luzum, 2010). This effect is largely affected by the stations proximity to water and local flow patterns. In general the ocean tides constitute 11 main tidal components. The associated station displacement is computed as a sum of these tidal constituents, accounting for the amplitude and phase of the loading components, and lunar nodes longitudes (Scherneck, 1999). The IERS Conventions 2010 also recommend an inclusion of 342 constituent waves, which are based on the 11 main tides.

Solid Earth pole tide

The polar motion causes a centrifugal force, which is observed as pole tides. This causes an elastic response in Earth's crust, which causes station displacement in vertical and horizontal directions. The station displacements computed with respect to the mean pole have amplitudes of 2 cm in radial and a few millimetres in lateral directions (Petit and Luzum, 2010).

Ocean pole tide

The parallelism of the Earth and ocean tidal effects continues with the ocean pole tide. It is the ocean counterpart to tidal response caused by the centrifugal polar motion, which also contributes the site displacement. The amplitudes of the displacements range from 2 mm in radial to sub-millimetre in lateral directions. They were included in the IERS 2010 Conventions modelled according to Desai (2002). This model takes into account the continental boundaries, mass conservation, self-gravitation, and ocean floor loading. The effect on geopotential coefficients and station displacements are modelled in terms of the m_1 and m_2 parameters.

Atmospheric loading

The air masses in the atmosphere are redistributed due to dynamical changes in e.g. air pressure and temperature. The pressure variations in the atmosphere are driven by the diurnal heating of the atmosphere (Petrov and Boy, 2004).

The mass transport of the atmosphere (i.e. atmospheric pressure) cause a loading effect, which leads to displacements of the station positions. The amplitude of the effect is in millimetre range (Petit and Luzum, 2010). The effect of the pressure loading is highly dependent on the station location. Maximum amplitudes are detected in regions with high variation in the governing atmospheric pressure systems. The displacement in the vertical direction can be modelled as function of the local barometric pressure deviation from a standard pressure and a pressure anomaly around the site. As such a gridded model is needed, from which the values can be interpolated to the site location. The atmospheric loading has two strong diurnal and semi-diurnal tides, S1 and S2, respectively. The IERS 2010 Conventions include these two tides in the recommended atmospheric loading computation.

2.2.2 Earth orientation parameters

The parameters that describe the relation between an Earth-Centred Earth-Fixed (ECEF) and Earth-Centred Inertial (ECI) coordinate system are called the Earth Orientation Parameters (EOP). They arise from the formulation in Equation 2.4 and the external torques caused by the Sun, the Moon and the planetary bodies, which change the orientation of the Earth's rotational axis in the space-fixed frame. The changes in the external torques and Earth's mass distribution are reflected in the irregular rotation (hence also in the EOP). The International Earth Rotation and Reference Systems Service (IERS) publishes the EOP through various predicted, rapid, monthly, and long-term data products[1]. The following subsections will discuss EOP in terms of their response to the geophysical excitations discussed in the previous sections. Explanation on their implementation in the coordinate transforms between the terrestrial and celestial systems is further discussed in Section 3.5.

Precession and nutation

The precession and nutation of the origins associated with the celestial reference systems are described according to the IAU2006/2000 precession/nutation model (Capitaine and Soffel, 2015). This includes the orientation of the Earth's rotation axis in space via the Celestial Intermediate Pole (CIP) and the direction of the Celestial Intermediate Origin (CIO) on the equator of CIP. The latest IERS Conventions (Petit and Luzum, 2010) define precession-nutation as the motion of the CIP in the GCRS, which includes Free Core Nutation (FCN) and other standard corrections. In this definition precession includes the 26000 year term and the secular part of the motion and nutation is the residual motion that is not included in precession. IERS published the position of the CIP both consistent

[1] `http://www.iers.org/IERS/EN/DataProducts/EarthOrientationData/eop.html`

with the IAU1980 and IAU2006/2000 precession/nutation models. The offset parameters with respect to the IAU1980 model are given by nutations in longitude $\Delta\epsilon$ and obliquity $\Delta\psi$. The IAU2006/2000 nutation/precession parameters are given as celestial pole offsets dX, dY to the CIP location (X, Y) in an ECI reference system (Capitaine and Wallace, 2006). The precession/nutation amplitudes are within tens of arcseonds per year. The origin of longitude varies within milliarcseond per century and it stays aligned to 0.1 as within a century relative to the initially defined alignment (Petit and Luzum, 2010).

FCN is a motion caused by the interaction of the mantle and the Earth's fluid core. The observed motion is free and thus difficult to model and predict. It has a period of approximately 431 sidereal days (Malkin, 2007). It is not included in the IAU2006/2000 precession/nutation model, and causes an additional CIP motion on the order of a few hundred μas. FCN can be predicted with an accuracy of approximately 100 μs RMS and its period and amplitude has been estimated from VLBI observations, e.g. Krasna et al. (2013).

Polar motion

The polar motion describes the motion of the Earth's rotation axis in the terrestrial reference system. Its main components consist of an annual period and the Chandler wobble with a period of approximately 435 days. Additionally, polar motion includes daily and sub-daily terms, excited by tidal motions and gravitational torques. Generally, it is relatively difficult to predict polar motion. The polar motion components are given by x_p and y_p, which describe the direction of the rotation axis in the terrestrial system. They are related to the formulation in Equation 2.4 by appropriate mean components via $m_1 = x_p - \overline{x}_p$ and $m_2 = -(y_p - \overline{y}_p)$. The x_p polar motion axis is aligned with the terrestrial x-axis, whereas the y_p axis has for historical reasons opposite sign with respect to the y-axis. The amplitude of the polar motion components are below 1 as with an additional long-term drift. These amplitudes translate to several meters on the surface of the Earth (0.5 arcsecond $\sim$ 15 m). The polar motion values published by the IERS do not include corrections for the diurnal and semi-diurnal tide and the libration terms, which have to be added afterwards. The effect of the sub-daily tides and libration to polar motion are on the order of 0.5 μs (Petit and Luzum, 2010) and 60 μs (Chao et al., 1991), respectively.

UT1

Universal Time (UT1) measures the diurnal rotation of the Earth relative to the sun. It is defined to be connected with a linear relationship to the sidereal Earth Rotation Angle (ERA) (see Chapter 3 Section 3.5). The observations are referred to some external time reference, thus technically the observed parameter is typ-

ically either LOD or UT1-UTC, where UTC is the Coordinated Universal Time. It is defined to be within 1 second of the UT1, with leap seconds added when needed to compensate the slowing UT1.

UT1 is a difficult parameter to model or predict, thus in general it has to be determined from observations. In this the technique of geodetic VLBI has a unique role. It is the only space-geodetic technique capable of directly observing UT1-UTC. On the contrary, satellite-techniques only have access to LOD.

Similar to polar motion UT1 is also affected by libration and tidal variations. The axial libration causes UT1 variations up to several microseconds. The effect of sub-daily tides to UT1 is on the order of 50 μs, whereas the effect of fortnightly tides goes up to 785 μs (Petit and Luzum, 2010).

Table 2.1: IAG services as GGOS components. The table lists the services, their respective techniques, and field of applications (Plag and Pearlman, 2009). The abbreviations in the first column from top to bottom correspond to: Bureau Gravimétrique International, Bureau International des Poids et Mesures, International Altimetry Service, IAG Bibliographic Service, International Centre for Earth Tides, International Centre for Global Earth Models, International DORIS Service, International Earth Rotation and Reference Systems Service, International Geoid Service, International Gravity Field Service, International GNSS Service, International Laser Ranging Service, International VLBI Service for Geodesy and Astrometry, The Permanent Service for Mean Sea Level, International Digital Elevation Model Service.

IAG Service	Techniques and responsibilities
BGI	Compiles and stores all gravity measurements and gravity field information.
BIPM	Responsible for realizing, maintaining and providing users with UTC and TAI.
IAS	Service for altimetry. Collects and distributes satellite altimetry related data from multiple satellite missions.
IBS	Maintains bibliographic services and collects literature related to geodesy.
ICET	Provides Earth tide data products.
ICGEM	Provides services for gravity field products. Long-term archiving of gravity field models.
IDS	Responsible for the DORIS service. Contributes to EOP determination.
IERS	Collects data from different services to monitor Earth rotation. Provides EOP, geophysical data, standards and constants, realizations for ICRS, ITRS.
IGeS	Collects geoid data. Produces geoid models for global and local use.
IGFS	Coordinates the collection of gravity field related data. Unify gravity products for GGOS.
IGS	Produces high quality GNSS data and products. Provides accurate GNSS satellite ephemerides and contributes to EOP determination, global coordinate systems, time scale, and atmospheric studies.
ILRS	Coordinates LLR and SLR observations. Contributes e.g. to EOP determination and study of Earth-Moon dynamics.
IVS	Coordinates VLBI for geodesy and astrometry. Essential to EOP determination and realizing the ICRS. Long-term nutation time-series.
PSMSL	Permanently monitors and determines mean sea-level.
IDEMS	Collects and distributes digital elevation models.

Chapter 3

Very Long Baseline Interferometry

Very Long Baseline Interferometry (VLBI) is an interferometric technique in which simultaneous observations from two or more radio telescopes are combined in an interferometric sense. This is done to achieve increased effective angular resolution. When the observed signals are combined into an interferometric pattern the angular resolution of the interferometer greatly outperforms a single-dish antenna. The relationship between the angular resolution of the telescope, antenna size, and observed signal for a single-dish telescope can be approximated by

$$\theta = \frac{\lambda}{D}, \tag{3.1}$$

where θ is the angular resolution, λ is the observed wavelength, and D is the diameter of the antenna aperture (Karttunen et al., 2007). This form of an approximation can also be used to describe the angular resolution of a telescope array, where the antenna aperture D in Equation (3.1) is replaced by the linear size of the antenna, i.e. the physical distance between the telescopes. For fully steerable reflectors the structural limitations with current materials limit the size of single reflector to around 100 m. Currently the largest of this kind is the Green Bank Telescope[1] (Green Bank, West Virginia, the United States of America) with a collecting area of 100 meter in diameter. The baseline length is limited in theory only by the diameter of the Earth, approximately 12,000 km. In practice the possible baseline length is also restricted by the source positions and the locations of suitable telescopes. Regardless of these limitations, a telescope array allows an improvement of 4–5 orders of magnitude in angular resolution compared to a single telescope. For a frequency range of 1 MHz to 300 GHz ($\approx$ 300 m to 1 mm) and baseline length of 100–10,000 km the angular resolution power of a two-telescope array ranges from 6–600 arcseconds for

[1] `https://science.nrao.edu/facilities/gbt`

1 MHz to 0.02–2 milliarcseconds for 300 GHz. Generally, the limiting factors for the observing frequencies are the ionosphere in the low-frequencies and absorption lines of oxygen and hydrogen in the high-frequency bands (Karttunen et al., 2007).

In astronomy this capability is used for high-resolution imaging of radio sources otherwise unattainable with other methods. Geodetic VLBI can be in some sense thought of as an inverse process to the astronomical case, where instead of source imaging the goal is to accurately determine the baselines between the observing stations. Another important field utilizing VLBI is astrometry, which is involved with determining the distance and movement of celestial bodies. VLBI astrometry is closely related to geodetic VLBI via the realization of the International Celestial Reference System (ICRS), called International Celestial Reference Frame (ICRF).

3.1 Basic principle of geodetic VLBI

The basic principle of geodetic VLBI is to observe extra-galactic radio sources, quasi-stellar objects (quasars) and active galactic nuclei (Fey et al., 2009), and measure the time delay between the arrival times of the radio signal at two antennas, which comprise a single baseline. When several telescopes observe the same source simultaneously the baselines between these stations form an observation network.

Due to the vast distance of billions of light years to the radio sources they form a quasi-inertial reference frame. This feature is extremely useful in geodesy because it allows realizing the Celestial Reference System (CRS) and the motion of the Earth relative to this coordinate system. The movement of the solar system around the galactic centre causes the so-called secular aberration drift of approximately 5 μas in the apparent motion of the radio sources (Titov et al., 2011). The observed extra-galactic sources have a high visibility in the radio frequencies. In geodetic VLBI these radio sources are normally considered to be point sources. However, as the accuracy of the VLBI observations increases and the effect of now dominant error sources become smaller the effect of the radio source structure can become significant (Souchay and Feissel-Vernier, 2006). Some radio sources exhibit structural variation on a milliarcseond level. This makes it difficult to rigorously refer the position of the radio source to a single point. Further complications are caused by sources which in addition to extended structure exhibit temporal variations in flux. These variations can require correction by modelling the source structure. The accuracy in which the source positions are known is connected to the accuracy obtainable with geodetic VLBI. In addition to defining the Celestial Reference System (CRF), VLBI also has an important role in producing the International Terrestrial Reference Frame

(ITRF), which realizes the International Terrestrial Reference System (ITRS), by providing a stable scale (Sovers et al., 1998). Furthermore, as a technique VLBI is unique within the space-geodetic techniques due to the possibility of simultaneously and directly observing all five Earth Orientation Parameters (EOP). The EOP serve as rotational parameters in the coordinate transformation between the ITRF and ICRF.

The radio signals from the radio sources are recorded at both stations. The time delay between time signal arrival times is determined by correlating the recorded signals, which requires that the observations are time-tagged with high accuracy. The accuracy level is realized by frequency standards such as hydrogen masers, which have a stability of approximately 10^{-14}. The correlation is performed at correlation centres using a software correlator. Advances in affordable, scalable, and high-performance consumer electronics and software correlation software have replaced the old purpose-built hardware correlators. Because the signal travels at the speed of light the time delays can be converted into distances. Thus, from these delay observations it is subsequently possible to solve the vector between the antennas. The VLBI observation schematics is illustrated in Figure 3.1. In geodetic VLBI the radio signals have typically been observed on two frequency bands, S-band centred around 2.3 GHz and X-band centred around 8.4 GHz. The dual-frequency observations are motivated by their capability to mitigate the effect of ionosphere on the observed delays. Because the ionosphere is a dispersive medium for electromagnetic radiation, observing on two frequencies makes it possible to define an observable which is nearly free of ionospheric influence. This approach requires sufficiently high signal-to-noise (SNR) ratios on both channels. The implications of using alternative observing band configurations and SNR levels are investigated in more detail in Section 3.4.

The general process of producing the delays from VLBI observations for geodetic analysis is divided into multiple stages. Broadly these include scheduling, observations, correlation, post-processing, and the processing with VLBI analysis software to estimate various parameters of interest such as EOP or station coordinates. To achieve the best possible accuracy levels in the observations and estimated parameters it is necessary to aim for good global coverage of the radio telescope locations. Thus, VLBI is an international effort which requires high level of organizing and collaboration. To realize the limitations and possibilities of such a system it is necessary to understand the contribution of different elements in the product chain.

In the following sections the elements of the organized international VLBI effort as well as VLBI product chain are discussed in more detail.

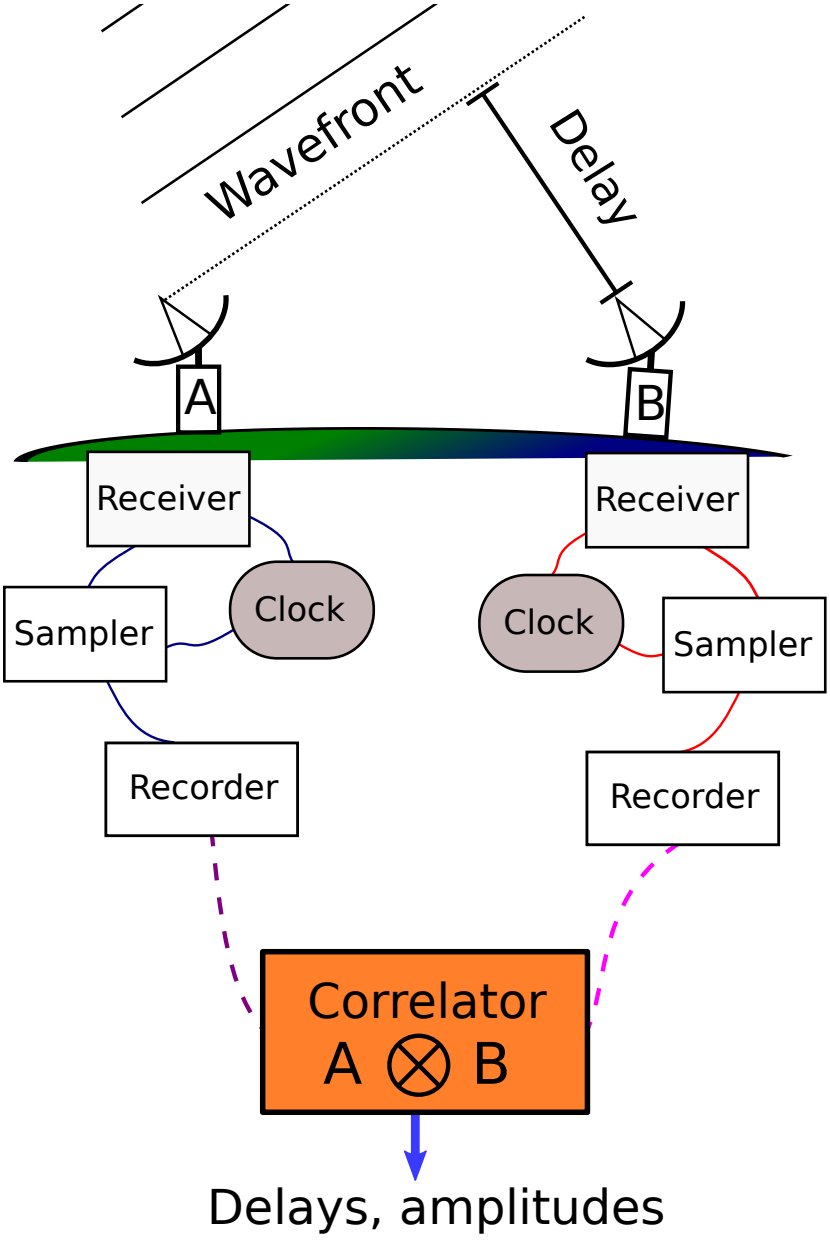

Figure 3.1: VLBI observing principle. Two radio telescopes separated by a baseline **b** simultaneously observe signals from an extra-galactic source. The signals are sampled, digitized, and recorded at the stations. The time and frequency information is provided by high-precision frequency standards (hydrogen maser) at the stations. The recorded signals are sent to a correlator that produces the cross-correlation functions, which are processed to find fringes to determine the delays and amplitudes.

3.2 Geodetic VLBI experiment flow

The quality of the geodetic parameters estimated in the VLBI analysis is connected to the choices made in the pre-analysis stages of a VLBI experiment. Naturally the overall quality is also impacted by the success of the stations to execute the observation plan from a technical point of view.

3.2.1 Scheduling

Before any actual observations take place the VLBI experiment needs to be scheduled. The schedule file includes instructions for the VLBI antennas participating in the experiment. The instructions include the sequence of sources to be observed and associated observing configurations. The schedule contains information on scans in the sessions, source positions and models, observation masks, antenna parameters, antenna specific equipment and frequency configurations. The frequency setup includes channel number and spacing, frequencies, bandwidths, 1 or 2 bit sampling, and recording mode. A scan consists of all the simultaneous observations on the same source made by two or more antennas in the observation network. Depending on the network geometry multiple sub-networks may also participate in different scans simultaneously.

Multiple conditions have to be satisfied when composing the observation schedule. This includes selecting sources that are visible to all stations wanted in a scan, computing the estimated flux densities for each baseline, and the resulting Signal-to-Noise Ratio (SNR) of an observation. The SNR of a VLBI observation can be approximated by (Thompson et al., 2008)

$$\mathrm{SNR} = \frac{\nu F \sqrt{2 \cdot B \cdot T}}{\sqrt{\mathrm{SEFD}_1 \cdot \mathrm{SEFD}_2}}, \tag{3.2}$$

where $\mathrm{SEFD}_{1,2}$ are the System Equivalent Flux Densities (SEFD) for antennas 1 and 2, F is the source flux, T is the integration time, B is the observed bandwidth, and ν includes instrumental correction factors and correlation coefficient. The factor 2 in the square root is due to the Nyquist sampling criterion. Thus, better SNR can be achieved via better antennas (larger size, higher SEFD), observing stronger sources, or increasing the recorded bandwidth.

The schedule structure depends on the conditions that it tries to meet and to optimise. Typically VLBI observation schedules try to maximise the number of scans per stations. Sometimes this can be a balancing act of both minimising the slewing time but still achieving good sky coverage. Only maximising the number of scans and hence trying to minimise slewing time can lead to clustering of sources and subsequently to sub-optimal sky coverage. Furthermore, the schedules try to attain good sky coverage usually in 1 hour time span. Effects such as atmospheric delay become easier to resolve, when there is good (or at

the least necessary) temporal coverage during the typical variation period of the phenomena. Furthermore, observations on low elevations further help in separating the tropospheric effects from e.g. station clocks (Gipson, 2010).

A widely used scheduling package for geodetic VLBI is Sked (Vandenberg, 1999) created at NASA Goddard Space Flight Center (GSFC). More recent alternatives include the scheduling module VIE_Sched (Sun et al., 2011) in the Vienna VLBI Software (VieVS) (Böhm et al., 2012).

3.2.2 Data acquisition

The VLBI observations are carried out according to the schedule previously created for the experiment. Because VLBI does not require identical antennas, the stations participating in the observation network might have different receiver architectures. However, the most general features are common within receiver systems, which are described in some detail in the following. First, the plane wave fronts are observed by the individual telescopes. Typically Cassegrain telescopes are the most commonly used telescope type in geodetic VLBI (see e.g. Baver et al. (2013, 2014, 2015)). The signals are reflected via main and sub-reflectors into the waveguide/antenna feed. From there the signals travel through multiple intermediate stages in the VLBI back-end before the sampled product is recorded and/or transferred in real-time. Together with the received signals, phase calibration signals are injected. Next, the signal is amplified with a Low-Noise Amplifier (LNA) and mixed with a Local Oscillator (LO) signal. The resulting radio frequency signal is heterodyned to multiple Intermediate Frequencies (IF), and down-converted to base-band frequency channels (BBC)/video frequency channels (VC). For geodetic VLBI typically 8 channels for X-band and 6 channels for S-band are used. The base-band signals are limited to channels with a width of a few MHz, sampled, and digitised. The digitised signals are then formatted and recorded. The data are time-tagged using precise local frequency standards (hydrogen masers) (Sovers et al., 1998). In case of a more modern Digital Back-End (DBE), described in more detail in the following, the digitisation is done before the signals are split into multiple IF frequencies.

The development in circuit technology during the previous years has made it possible to replace the Analogue Back-End (ABE) with its digital counterpart, Digital Back-End (DBE). Several DBEs have been developed during the last years.[2] One such product line is the Digital Base-Band Converters (DBBC). Conceived by Gino Tuccari, the DBBCs are produced by HAT-Lab[3]. The development of the DBBC started in 2004 (Tuccari, 2004) and so far includes three generations, DBBC1 (2004–2008), DBBC2 (2007-) and DBBC3 (2015-) (Tuccari et al.,

[2] `http://ivs.nict.go.jp/mirror/technology/vlbi2010-docs/dbe_comparison_130121.pdf`
[3] `http://www.hat-lab.com/hatlab/`

2006, 2010, 2014). Additionally, an enhanced version of DBBC2, DBBC2010, has been available since 2009. In 2011 the Onsala Space Observatory (OSO) acquired a DBBC2, which was installed and operated during tests in parallel with an old setup using a MarkIV (Whitney, 1993) analogue back-end. The data gathered with these systems were studied in *Paper I* attached to this thesis.

The formatted data are recorded to hard disk drives (HDD). The traditional workhorse of VLBI data recording has been the Mark 5 VLBI data system[4] series (Whitney, 2002) developed at the Massachusetts Institute of Technology (MIT), Haystack Observatory. The Mark 6 VLBI data system has been developed as the next-generation replacement to Mark 5. General information of the existing Mark 5/6 systems is listed in Table 3.1, see e.g. Whitney (2002, 2004), Whitney et al. (2010), Whitney and Lapsley (2012). These systems house detachable disk banks, which can be shipped to the correlator physically. However, nowadays the data are normally transferred via high-speed internet connections (in VLBI context referred to as e-transfer). Alternative systems include e.g. FlexBuff (Mujunen and Salminen, 2013), which is a system capable of simultaneously recording and streaming the data to the correlator. Instead of a fixed hardware solution FlexBuff is a combination of guidelines and software on which the users can construct their recording machines according to general FlexBuff specifications.

Table 3.1: General information on Mark 5/6 VLBI data systems.

Model	Introduced	Recording rate (Gbps)
Mark 5A	2002	1
Mark 5A+	2006	1
Mark 5B	2005	1
Mark 5B+	2006	2
Mark 5C	2011/2012	4
Mark 6	2012	16

3.2.3 Correlation and post-processing

Once a session (or as little as a single observation in case of real-time correlation) is recorded, it is transferred to the correlator. Because the observed radio sources are extremely weak when compared to the noise generated by the receiver, the received signal is essentially dominated by Gaussian noise. In order to extract the weak radio source signal the observed signals are combined in an interferometer where the Gaussian noise is averaged out. The main task of

[4] `http://www.haystack.edu/tech/vlbi/mark5/`

the correlator is to combine the recorded signals in pairwise manner to produce an interferometer pattern for each baseline. More specifically, the correlator produces the complex correlation functions, which are then processed by a post-processing such as the Haystack Post-Processing System (HOPS) to find the fringes of the correlation and to produce the phase- and amplitude VLBI observables.

The cross-correlation function is a function of arrival time difference τ of the signals

$$R = \frac{1}{T}\int_0^T V_1(t)V_2^*(t-\tau)dt, \tag{3.3}$$

where T is the averaging interval, $V_{1,2}$ are bit-streams of the recorded voltages at stations 1 and 2. The correlator finds this peak by testing different values (lags) for the time delays, τ. The behaviour of the cross-correlation function is dominated by three effects: the changes in the baseline geometry, the clock offset between the stations, and the Doppler shift caused by the rotation of the Earth during the observation. The baseline geometry is corrected prior by shifting the bit-streams by applying a correlator delay model. This models the observed delay within an accuracy level that the delay and delay rate are found within the correlation window. The correlation is done simultaneously for all the observed frequency channels on X- and S-band. Typical integration times are between 1–2 s. The effect of the Doppler shift is removed by multiplying the cross-correlated bits with a sine and cosine terms. The resulting terms are averaged to produce the phase and amplitude for each channel per integration period.

The phase samples $\phi(\omega_i, t_j)$ collected from all frequency channels are then fitted with a phase, group delay, and phase rate. The process involves Fourier transforming the phase samples to the delay and delay rate domain. A correlation amplitude peak is searched in this domain to supply an initial guess to a bilinear least-squares fit for the measured phases

$$\phi(\omega, t) = \phi_0(\omega_0, t_0) + \frac{\partial\phi}{\partial\omega}(\omega-\omega_0) + \frac{\partial\phi}{\partial t}(t-t_0), \tag{3.4}$$

where the phase delay is defined as $\tau_{pd} = \phi_0/\omega_0$, the group delay as $\tau_{gd} = \partial\phi/\partial\omega$ and the phase delay rate as $\dot{\tau}_{ph} = (1/\omega_0)(\partial\phi/\partial t)$.

3.3 International VLBI Service for Geodesy and Astrometry

The International VLBI Service for Geodesy and Astrometry (IVS) (Schuh and Behrend, 2012) is an best effort international collaboration of organizations which are involved in VLBI activities. The IVS is one of the four autonomous technique

centres contributing to the International Earth Rotation and Reference System Service (IERS). The goal of IVS is to work as a service which supports research and operational activities in geodesy, geophysics, and astrometry. IVS as a service is committed to supporting contributors and providing the data to end-users. It also acts as a contact hub for collaborating organizations. With these activities IVS will represent and help the integration of the VLBI component with other elements in GGOS.

3.3.1 IVS components

The IVS has seven components responsible for different tasks within the VLBI service. These include the coordinating centre, network stations, operating centres, correlators, data centres, analysis centres, and technology and development centres.

Coordinating centre and master schedule

The coordinating centre is responsible for coordinating IVS operations on both short- and long-term time scale. This includes for example the development of standards, communication within and outside IVS, resource allocation, organizing trainings and meetings, as well as coordinating and maintaining the observation program. The latter is particularly important for the continuity and success of regular VLBI observations. The observation schedule is maintained in a form of master schedules. These schedules are produced for each year and they contains the basic information on the IVS observing sessions: session identification, date, participating stations, scheduler, correlator, and status of correlation. This status shows whether the data are waiting to be or currently being processed, or correlated. Moreover, the delay between the observing date and release of the correlated data are logged. The turnover time goals vary between different session types, but in general the aim is to provide the results in as timely manner as possible.

Network stations

The IVS network stations include VLBI stations which comply with the performance criteria agreed by the IVS Directing Board. This includes standards for station reliability and data quality. Moreover, each station is required to provide timing data, local meteorological observations, and local tie information. The collected auxiliary data are supplied further in the product chain to the IVS Data Centres. A map[5] (Baver et al., 2015) of the IVS network stations is shown in Figure 3.2. An issue which is immediately evident from this map is that

[5] http://ivscc.gsfc.nasa.gov/stations/ns-map.html

the station distribution is currently focused on the Northern hemisphere. To achieve stronger network geometry and thus improved accuracies in e.g. CRF determinations (Jacobs et al., 2013) the stations should ideally be distributed more evenly on the surface of the Earth. Naturally, this is limited by available resources, environmental factors, and the fact that there is more available land mass on the Northern hemisphere. There is an ongoing research into determining the optimal locations for new telescopes to be added to the permanent observing network, see for example Hase et al. (2012).

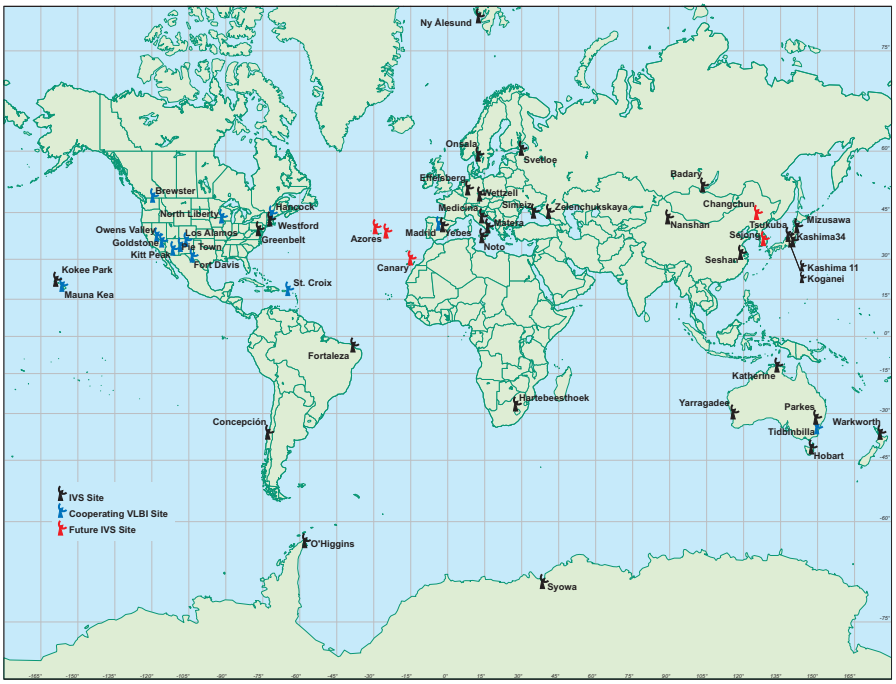

Figure 3.2: Distribution of IVS Network Stations. Black telescope icons denote current IVS sites, blue icons show co-operating sites, and red icons are sites that are future IVS sites. After the release of the map the network some of the sites marked as "Future IVS Sites" have been inaugurated. These include the RAEGE VGOS station in Santa Maria, Azores and the Korea Geodetic VLBI station Sejong.

Operating Centres

The routine operations for the network stations are planned in detail by the operating centres. They produce the session-wise observation schedules, which contain the set of observation instructions for each participating station. The stations also receive feedback on their performance from the operating centres, which in turn will help the individual network stations to meet and maintain the criteria defined by the IVS. In addition to this routine procedural support

the operation centres are also planning observation programs. The composition of an observation network varies e.g. in geometry, antenna properties, and source visibility. With these factors and practical considerations in mind the observation network must be designed so that it meets the requirements of the task. This can be for example monitoring a geophysical phenomena or reference frame determination.

Correlators

Once the session is observed the data are sent to the assigned correlator. Currently there are six correlators functioning within the IVS. The Geospatial Information Authority of Japan (GSI) operates a correlator at Tsukuba. The United States of America has two operational correlators, namely the MIT Haystack Correlator and the Washington Correlator. Germany, Russia, and China and have one correlator each. These correlators support global and more localized observing programs to a varying degree. Moreover, some correlators are dedicated for only geodetic activities while others share their time with other efforts, such as astronomical VLBI. The Washington Correlator (The United States of America) is used solely for geodetic VLBI. It handles the correlation of IVS-R4 sessions, observed on Thursdays, which make up one half of the so-called rapid-turnaround sessions. The Bonn Astro/Geo Correlator (Germany) is responsible for the IVS-R1, observed on Mondays, as well as T2 and EUR sessions. In total the majority of geodetic VLBI sessions are currently correlated at Bonn.

Besides producing the correlation results from the recorded data the correlators also serve as a feedback channel to the observing stations. This includes analysis on data quality of individual stations as well as comparing the output between the correlators. Correlators facilitate the electronic data transfer of VLBI data, which has largely replaced the old way of physically sending the data recorded on disk or magnetic tape to the correlators.

Data centres

The data centres are responsible for storing and distributing all data important to the end-users. This includes the data products, observation schedules, and auxiliary files such as station log files. Reliable archiving of all necessary data is extremely important for the success of VLBI derived products. It provides the users with an extremely long-term data sets, which are vital for understanding low-frequency geophysical phenomena. Moreover, the long-term data sets facilitate the continual development of the related analysis techniques.

Analysis centres

The analysis centres provide the users with various products from the VLBI data analysis. Operational analysis centres provide the typical VLBI analysis products generated on a regular basis. These include the EOP, station coordinates, and source coordinates. Similar to the other components in the product chain, analysis centres also provide station-specific performance feedback. Although the data analysis is coordinated by the IVS, the individual analysis centres are not tied to a specific procedure rather than specifications on quality in data production. Thus, for example different software used for the VLBI analysis by the analysis centres can lead to small biases between the solutions. The EOP series can be compared in the EOP series comparison service[6]. The individual solutions from the operational centres are combined into a technique-specific VLBI product at combination centres. The combined products represent the official IVS VLBI data products. This includes for example the EOP series as generated by VLBI, which can be then further combined with input from other techniques. One such combined product being the latest version of combined IERS EOP series C04 that is consistent with ITRF2008 (Bizouard and Gambis, 2011). Contrary to the operational analysis centres, associate and special analysis centres are directed towards production of specialized VLBI products. The associate analysis centres participate in production of special-purpose products. These include regular products related to e.g. reference frames maintenance and regional studies as well as research on new ways to utilize VLBI. The special analysis centres focus on a few certain types of observation and the analysis associated with them.

Technology development centres

At the moment there are seven operational IVS Technology Development Centres (TDC), that contribute in different areas relevant to current development efforts in IVS VLBI activities (Baver et al., 2015). These are located in Canada, USA (2), Spain, Sweden, Russia, and Japan. The TDCs and their current focus areas are listed in Table 3.2.

3.3.2 IVS observing program

The IVS observing program is maintained by the Coordinating centre. It includes a wide range of different session types. The typical session length is 24 h but the program also includes so-called Intensive Sessions (INT), which currently have a duration of only 1 h. The sessions are observed on different intervals depending on the scientific goals, user needs, and resources. Two most

[6] `http://hpiers.obspm.fr/eop-pc/index.php?index=operational`

Table 3.2: Current IVS Technology Development Centres and their main activities during 2014.

IVS Component	Country	Activity
Canadian VLBI Technology Development Center	Canada	VGOS development (e.g. VGOS observing plan, VGOS feeds, DBEs, recorders.
National Institute of Information and Communications Technology	Japan	Broadband VLBI system Gala-V development and testing including new wideband feed NINJA.
Institute of Applied Astronomy Technology Development Center	Russia	Tri-band receiving system for the interferometer, broadband acquisition system (BRAS), multipurpose digital backend MBDE.
IGN Yebes Observatory	Spain	RAEGE radio telescopes, LNA development, Tri-band S/X/Ka receiver, broadband feed, control software development.
Onsala Space Observatory	Sweden	Onsala Twin-Telescope project (OTT), broadband feed for VGOS, new 4.00-12.25 GHz front-end for the 20-m radio telescope, FlexBuff and FILA40G.
Goddard Space Flight Center	USA	Field System, scheduling software, hardware (e.g. station timing and meteorology).
Haystack Observatory	USA	KPGO 12-m signal chain, VLBI data acquisition module, Mark 6.

observed session types are the rapid turnaround and intensive sessions. These are accompanied with among others regional campaign and reference frame maintenance sessions.

Rapid turnaround sessions

The IVS-R1 and IVS-R4 sessions are observed every week on Monday and Thursday, respectively. This makes a total of 104 R-sessions per year. The R refers to rapid turnaround. This means that the components in the product chain, i.e. stations, correlators, and analysis centres, have a responsibility to ensure the timely release of the results. In practice this means the aim to minimize the time that it takes from end of observations to uploading the final databases to the IVS file servers. The target maximum delay is currently 15 days, which is realized to a moderate degree. For example during the year 2014 the median delays for IVS-R1 and IVS-4 sessions were 14 days and 20 days, respectively. [7] Both IVS-R1 and IVS-R4 sessions have a duration of 24 hours and are mainly aimed for EOP determination. IVS-R1 and IVS-R4 sessions are correlated at the Bonn correlator (Germany) and the Washington Correlator (The United States of America), respectively. The observation networks for the sessions consists of a set of core stations, which participate on a regular basis. These stations are joined by a few alternating additional stations. Occasionally, stations are dropped out due to e.g. technical maintenance or unforeseen problems with the equipment. In 2014 the median number of observing stations in the network was 9 for IVS-R1 and 8 for IVS-R4 sessions.

Intensive sessions

The IVS Intensive sessions (henceforth referred to as INT) are daily 1-hour observation sessions, which typically involve 2–3 stations. The purpose of the INT sessions is to provide a daily estimate for the value of UT1. Currently, there are three types of intensive sessions: IVS-INT1, IVS-INT2, and IVS-INT3. Together these sessions cover a duration of the entire week. Normally the INT sessions incorporate the following four stations: Kokee Park, (Hawaii, the United States of America), Wettzell (Germany), Ny-Ålesund (Svalbard, Norway), and Tsukuba (Japan). IVS-INT1 are carried out at 17:30 UTC from Monday to Friday on the Kokee–Wettzell baseline. IVS-INT2 sessions are observed on weekends at 7:30 UTC on Tsukuba–Wettzell. IVS-INT3 are observed only on Mondays at 7:00 UTC with stations Wettzell, Tsukuba, and Ny-Ålesund. This fills the otherwise lengthy gap in observations between Sunday morning (INT2) and Monday evening (INT1). Thus in total there are 416 scheduled INT sessions every year.

[7] `http://lupus.gsfc.nasa.gov/sess/master14.html`

The participating stations and baselines are illustrated in Figure 3.3. The baselines are oriented on the East-West direction, because this makes them sensitive in particular to changes in UT1. On the other hand, separating the effect of polar motion from this geometry is difficult. Because INT sessions are carried out to produce daily UT1 values in a timely manner, the product delivery time from end of observations to database creation is of particular importance. The data are transferred via internet to the correlator and subsequently to the appropriate analysis centre. In order to reach minimal latencies for the UT1 estimates there have been efforts in automating different stages in the analysis chain (see e.g. Hobiger et al. (2010)). Due to the daily schedule and routine nature of the observations the analysis of INT sessions can benefit significantly from automation. When analysis steps are performed automatically the product chain is not dependent on human interaction, which in turn can improve the reliability in terms of data latency. However, it is important that the automated methods perform reliably quality-wise as well.

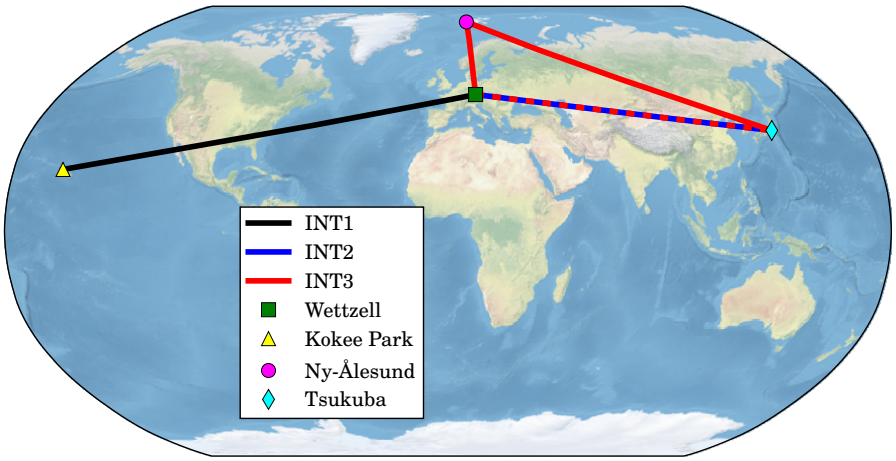

Figure 3.3: The participating stations and baselines observed in INT sessions. Wettzell (green square), Kokee Park (yellow triangle), Ny-Ålesund (magenta circle), Tsukuba (cyan diamond). INT1: Kokee–Wettzell (black line). INT2: Tsukuba–Wettzell (blue line). INT3: Ny-Ålesund–Tsukuba, Ny-Ålesund–Wettzell, Wettzell–Tsukuba (red line).

Reference frame sessions

The reference frame sessions organised by the IVS can be divided into two groups, the CRF and TRF sessions.

The CRF sessions are intended for maintaining and improving the current CRF as realized by VLBI. Additionally, new sources (i.e. sources not currently included in the ICRF) are included in the observations. For accurate CRF determination it is important to have as good as possible sky coverage and source

distribution. The CRF sessions are further divided into IVS-CRF, IVS-CRFDS, and IVS-CRFMS sessions. These sessions are observed with sources on the Northern hemisphere, median-south (MS), and deep-south (DS), respectively. Due to both geographical and economical reasons the VLBI antenna distribution has become concentrated on the Northern hemisphere. For this reason the source distribution in the ICRF has not been optimally homogeneous. There are still areas in the southern hemisphere sky where relatively few sources are observed. New telescopes are expected to mitigate this situation in the future. In 2013 a total of 16 CRF sessions were observed (Dick and Thaller, 2014).

The IVS-T2 sessions are intended for regular monitoring of the VLBI contribution to the TRF. The sessions are organised bi-monthly and they involve an extended network of global geodetic VLBI stations. In 2013 the average number of participating stations was 18 (Dick and Thaller, 2014). Regular observation campaigns involving a large number of stations have their organisational difficulties. Thus, in general the IVS-T2 sessions emphasize robust networks over the total number of observing sessions (Bernhart et al., 2013).

Regional sessions

In addition to global observations a number of networks focus on regional monitoring and studies. This includes regional networks in Europe (EUROPE), Australia and New Zealand (AUSTRAL), Japan (JADE), the Southern hemisphere including Antarctica (IVS-OHIG), and Asia-Pacific region (APSG). Generally, the main objective of these sessions is to strengthen the local TRF by observing station coordinate evolution with high precision. The APGS network spans four tectonic plates: the Eurasian, North American, Pacific, and the Australian plate. This includes areas that have historically been extremely seismologically active. Thus, the data from APGS network provide a valuable resource in studying the particular geodynamics of the area (Dick and Thaller, 2014). The IVS-OHIG sessions utilise the O'Higgins radio telescope situated at the German Antarctic Research Site (GARS) in Antarctica to tie together observations on the Southern hemisphere. Currently, 20 % of the telescope time is allocated for geodetic activities. The number of observed sessions is fairly limited, between 1–6 per year. Ongoing efforts to increase the remote capabilities of the station aim to increase the efficiency of the observations.

VLBA sessions

The National Radio Astronomy Observatory (NRAO) (The United States of America) operates the Very Long Baseline Array (VLBA) which consists of 10 radio telescopes in the USA. The VLBA is used to jointly observe with a variable network (normally 6–10 stations) of geodetic stations in a set of RDV ses-

sions. The RDV sessions are observed every two months for a total of six times per year. One of the advantages in these sessions is the ability to image the source and correct for the source structure. RDV sessions have been successful in producing highly accurate EOP measurements and strengthening the CRF (Gordon, 2005).

Research & Development sessions

The IVS research and development sessions (IVS-R&D) are directed towards addressing specific scientific or technical goals. Individual sessions may be devoted to testing new network geometries or the R&D sessions might have more common theme, such as preparing for the CONT14 campaign in 2013 (Dick and Thaller, 2014). Other R&D sessions concentrate e.g. on observations of Gaia transfer sources (Bourda et al., 2015) or observations of the Chinese Lunar Lander.

CONT campaigns

An important series of special VLBI campaigns are the so-called CONT-campaigns. It is an continuous VLBI observation campaign observed over the period of 15 days. The first one was carried out in 1994. Since 2002 it has been repeated approximately every three years. The purpose of CONT is to produce a data set that reflects the state-of-the-art capabilities of VLBI. These data sets have proven extremely useful for the VLBI community e.g. in testing new analysis strategies. Furthermore, the continuous observation periods are useful for repeatability testing. The number of stations and their distribution in CONT sessions is significantly better compared to regular observing networks. The continuous observations and strong network geometry provide an excellent test-bed for model testing with high precision as well as investigating high-frequency variations and global scale phenomena.

The latest CONT campaign (CONT14) was carried out during the month of May in 2014. In total 16 network stations took part in the observations. In addition to VLBI observations data was simultaneously collected with GNSS for comparison purposes. Three stations (HartRAO, Wettzell, and Yarragadee) also observed with SLR during the campaign. Furthermore, as during CONT11, on the Onsala–Tsukuba baseline the data recorded at Onsala were transferred to the correlator at Tsukuba. The observations on this this baseline were correlated in near real-time to determine UT1-UTC estimate. The latency for the estimates was most of the time between 3 and 10 minutes [8].

[8] `http://sgdns.spacegeodesy.go.jp/vlbi/dUT1/cont14/#latency`

3.4 VLBI Global Observing System

The VLBI Global Observing System (VGOS) is a VLBI observation system that represents the VLBI component in the GGOS (Schuh and Behrend, 2012). It was initially conceived as a response to the need for increasingly accurate observations on a global scale in order to monitor both scientifically and societally important phenomena such as sea-level rise. The project started out with a title VLBI2010, but has since been renamed to VGOS in order to have consistent naming convention and emphasize its role as a component of GGOS. Because the targeted phenomena have magnitudes on the order of a few millimetres, the accuracy of the VLBI observation needs to reach millimetre in order to monitor them. It became apparent that these requirements could not be reached with the existing legacy equipment and observation systems. Furthermore, the existing VLBI products were not in compliance with the aim of continuous monitoring of the system Earth.

3.4.1 Goals

The main goals of the VGOS system are based on both scientific and practical points of view. Between 2003 and 2005 IVS Working Group 3 (WG3) for VLBI2010 was established (Niell et al., 2005). The working group set out to recognize and postulate the goals and their requirements to make a concrete road map of what are the societal and scientific needs for next generation VLBI and what is the feasible way to fulfil these goals. Based on their work (Niell et al., 2005) the following goals have been stated as the guideline for VGOS:

- Accuracy of 1 mm in position and 0,1 mm/year in station velocities
- Continuous monitoring of station positions (baselines) and EOP
- Turnaround time of less than 24 hours for initial geodetic results
- Easy implementation to facilitate timely introduction of the system

The first three out of the four objectives can be regarded as the main technical goals. However, easy implementation of the system is also crucial for the success of the project. In this context easy implementation means keeping the construction and operational expenses to a sufficiently low level. There has to be willingness within the participating organisations to invest into a new system based on the promise of improved scientific capability. On the other hand, having affordable specifications will enable more participants to invest into new antennas. Finding this balance is important to the realization of a full VGOS network.

While postulating the goals for the new system, WG3 also stressed the importance on continuing to provide the products that are technique-specific to VLBI – UT1 and nutation, CRF determination. The full set of goals specify accuracy, timeliness, frequency, and resolution targets for TRF, CRF, EOP, physical and geophysical parameters. An overview of these goals in terms of accuracy and timeliness are presented in Table 3.3, derived from the goal table in Niell et al. (2005).

Table 3.3: VGOS objectives for parameter accuracy and latency. The accuracy targets, frequency, temporal resolution, and turnaround time goals for the different parameters and VLBI products. These include TRF, CRF, EOP, and geophysical and physical parameters. The table is derived from Niell et al. (2005).

	Product	Accuracy	Timeliness
TRF	X,Y,Z time series (session)	2–5 mm	1 day
	Annual coordinates	1–2 mm	1 month
	Annual Velocities	0.1–0.3 mm/y	1 month
CRF	Source coordinates	0.25 mas	1 month
	α & δ time series	0.5 mas	1 month
EOP	UT1-UTC	5 μs	Near real time
	Precession/nutation	20–50 μas	Near real time
	Polar motion	20–50 μas	Near real time
Geodynamics	Solid Earth tides	0.1 %	1 month
	Ocean loading	1 %	1 month
	Atmosphere loading	10 %	1 month
Atmosphere	Tropospheric parameters	1–2 mm	Near real time
	Zenith delay gradients	0.3–0.5 mm	Near real time
	Ionosphere mapping	0.5 TECU	Near real time

Achieving these goals poses challenges in all aspects of the VLBI observation process. At the time of the conception of VGOS, and still today, the struggle to realize these goals can be attributed to generally ageing VLBI infrastructure, insufficient level of automation, increased radio-frequency interference (RFI), and uneven global telescope distribution.

The telescope distribution issue means that improvement has to be pursued by not only upgrading existing telescopes/sites, but also modernising the analysis chain and supplementing the existing observation network with new stations. With Southern hemisphere having historically been under-represented in the global station distribution it is one of the main areas of focus for new telescopes (Petrachenko et al., 2009). The IVS network station distribution shown in Figure 3.2 shows that the majority of the network stations are located in Eu-

rope and North America. With increase in regularity within the global coverage, the sensitivity of the network to variations in EOP is improved. Moreover, when selecting new sites for telescopes the data transfer infrastructure should be considered. Reducing turnaround times means that the observation data must be transferred to the correlators via high-speed broadband connections. Even though many countries nowadays have relatively comprehensive broadband coverage around heavily populated areas, the telescopes usually reside in more secluded places to avoid RFI. This so called last-mile connectivity has to be taken into account when selecting sites for new telescopes. Moreover, increasing data rates put strain also on the existing broadband capabilities. This is pronounced at the correlators, who have be able to handle the traffic when receiving raw data from the observation network during or after the experiment.

In addition to improving the number of and spatial distribution of the telescopes, also noted was the need to reduce the random errors of the delay observable. This includes contribution from the errors in individual observations, stochastic effects of both the troposphere and instrumental errors including frequency standards. The 1 mm accuracy requirement corresponds roughly to 4 ps of observation noise per baseline (Niell et al., 2005).

Furthermore, when the observation error is reduced the systematic errors affecting the system need to be taken into account with increased care. This includes for example errors in the instrumentation and the telescope structure. The sensitivity of the instrumentation to external and internal variables such as temperature and component quality must be taken into account. Furthermore, these variations can be specific to a certain design. The telescope structure is affected by its environment via thermal and gravitational deformation as well as other weather phenomena. Moreover, local and global phenomena of different loading mechanics connected to ocean masses, hydrology, and atmosphere will manifest themselves through systematic effects. The increase in accuracy will also see the effect of source structure becoming a factor in the overall accuracy.

The impact of random errors in the observed delays can be further reduced by increasing the observation density. By having an increased number of observations per unit of time is directed towards increasing the robustness, precision, estimation strength, and decorrelation of variables in the VLBI observations. If the overall model is not changed the increase in observation density will increase the overall degrees of freedom. Generally, VLBI observations have relatively small degrees of freedom. With increased number of observations the detection of unmodeled effects will also improve. Especially important are the improvements in the estimation of tropospheric parameters. With increased number of observations it is possible to observe on a wider range of azimuths and elevations, thus building a better overall picture of the surrounding atmospheric conditions. The observations must also sample the atmosphere often enough so that it is able to capture its short term variations. This will also help

to decorrelate the effects of troposphere, station clocks, and the apparent local vertical movement of the station (Niell et al., 2005).

In addition to error reduction the need for improved observation and analysis strategies was also recognized. To benefit from the increased accuracy the existing geophysical, astronomical, and mechanical models need to be improved. Furthermore, investigating the differences in VLBI data analysis processes with different collaborators using varying analysis software packages is needed.

3.4.2 Technical requirements and strategies

Based on the identified limitations, and strategies to address them, WG3 prepared a list of recommendations for the VGOS system that could fulfil the given requirements in overall accuracy. The plan involves the whole VLBI observing system with upgrades to data acquisition, signal chain, and data analysis. The feasibility of these recommendations posed in Niell et al. (2005) was investigated in multiple studies and simulations. The results and conclusions of the investigations were released in Petrachenko et al. (2009).

VGOS Simulations

The impact of scheduling strategies, network size, and different sources of error in the VLBI observation process was investigated by extensive Monte Carlo simulations. The studied error processes were related with troposphere, frequency standards at the stations, and measurement noise associated with the delay. The Monte Carlo simulations incorporated these stochastic effects in a delay model, in which the difference between observed and modelled delay was computed as follows

$$\Delta_{oc} = mf_{w,2} \cdot \mathrm{ZWD}_2 + \tau_{c,2} - (mf_{w,1} \cdot \mathrm{ZWD}_1 + \tau_{c,1}) + n_w, \tag{3.5}$$

where the indices 1 and 2 refer to the stations forming a baseline, ZWD is the simulated Zenith Wet Delay, and $mf_{w,i}$ corresponds to the mapping functions at the *i*th station. The simulated observations are also disturbed by a source of white noise, n_w. The ZWD values are sampled based on the turbulence model introduced in Nilsson et al. (2007). The clock functions are modelled as having Allan Standard Deviation (ASD) and using a sum of random walk and integrated random walk. The clock simulations indicated that a frequency stability of 10^{-14} in ASD over a 50-minute period (the performance of a typical hydrogen maser) was a tipping point in the positional accuracy (Petrachenko et al., 2009, Pany et al., 2011). Based on the simulated results in Nilsson and Haas (2010) and Pany et al. (2011) troposphere was recognized as one of the main sources of stochastic error in the VLBI error budget.

The main characteristics of the new system is the shift from large and consequently relatively slow telescopes to smaller and fast-slewing telescopes observing in broadband mode. Another prominent paradigm shift is to have many stations operate two identical telescopes (twin-telescopes) per site. With this design it is possible mitigate slower slewing times with one telescope. This will also introduce new possibilities in scheduling and dealing with the troposphere. In case of two telescopes the slew rate of an individual telescope needs to be $5^\circ/s$ in azimuth. With only one telescope on site the azimuth slew rate must reach $12^\circ/s$ for similar performance in source switching interval. The VGOS system will consist of sites with one or two telescopes meeting the VGOS specifications. A minimum recommended number of telescopes for continuous EOP observation is 16, but the network size is intended to vary from 20 to 40 telescopes depending on the experiment. For example the reference frame maintenance sessions require a larger number of globally distributed telescopes. Based on simulations the accuracy of EOP and scale improved by 30 % when the network size was increased from 16 to 32 (Petrachenko et al., 2009). The low-cost approach to the telescope design makes it feasible for more sites to invest into building twin-telescopes. A standard VGOS telescope will have a size of approximately 12 m as opposed to the previous generation of telescopes with diameters from 20 m upwards. With faster telescopes it is possible to increase the number of observed sources, thus mitigating the issue with limited number of observations. Furthermore, smaller telescopes are less susceptible to deformation effects caused by their own weight, thermal changes, and rough weather conditions. This enhanced robustness will improve the stability of the telescope reference point, which needs be stable up to approximately 0.1 mm (Petrachenko et al., 2009).

The increased number of observations means that both the time available for observing on-source and moving to a new source have to be decreased. Shorter integration times will in turn reduce the signal-to-noise ratio (SNR). In order to obtain sufficient precision of the delay measurement the VGOS system will observe on four bands spanning a frequency range of 2.2–14 GHz. Each band will be 1024 MHz and further divided into channels. A likely channel bandwidth will be 32 MHz (Petrachenko et al., 2009, Baver et al., 2015). Further studies have since increased the low end of the frequency range from 2.2 GHz to 3 GHz for typical VGOS frequency sequences due to RFI (Baver et al., 2015). The broadband delay concept is being tested at the Goddard Geophysical and Astronomical Observatory (GGAO) by a proof-of-concept system currently under development (Baver et al., 2015). These tests will investigate how the concept of broadband delays will work in practice. Theoretical considerations have shown that broadband delays are sensitive to variations in source structure and RFI.

Data rates

Observing broadband delays will greatly increase the data rate requirements. In order to be able to detect a sufficient number of adequate sources the lower limit goal for sustained data rates is 4 Gbps. Moreover, the system has to be temporarily capable of handling burst rates up to 16–32 Gbps. These data rates are challenging for recording and data transfer. The still widely used Mark 5 series VLBI data system developed and MIT Haystack Observatory (Whitney, 2002) can handle data rates up to 4 Gbps (Mark 5C). Compared to its predecessor the latest item in the Mark-series, Mark 6, can handle sustained data rates up to 16 Gbps (Whitney and Lapsley, 2012). It also marks a move towards systems with higher modularity, with the use of inexpensive commercial off-the-shelf (COTS) components and easier upgrades (Whitney and Lapsley, 2012). An alternative COTS solution developed by within the NEXPReS[9] project is data streaming system Flexbuff/vlbi-streamer (Mujunen and Salminen, 2013). It differs from the fixed hardware solution of Mark 6 by being based on hardware specifications on a more general level.

Automated operations

The automation of the observing system and data acquisition chain is one of the main challenges in of VGOS. To realize the increased number of observation per time and continuous EOP monitoring, the VGOS system has to be heavily automated and have remote control capabilities. This essentially covers the whole data acquisition chain starting from scheduling and observations, correlation and fringe fitting, as well as the subsequent data analysis.

The increased data rates and the need for high level of automation also require upgrading the back-end in the signal processing chain. In recent years many stations have replaced their analogue back-end systems with a digital variant. The radio frequency signals coming from the receiver front-end are converted via intermediate frequency conversion to digital data streams by the VLBI back-end. Compared to the analogue systems the digital back-ends (DBE) have significant advantages. They have a great degree of flexibility and testability, because the functionality of the system can be tuned and replicated. DBEs are also less susceptible to environmental variations such as changes in temperatures and voltages. Moreover, DBEs are generally significantly cheaper than analogue back-ends, costing roughly one tenth of a legacy analogue system. The physical size is also greatly reduced, which helps transportation and installation on-site. DBEs are more easily upgraded and implemented along with other new hardware, which is optimal when the whole data acquisition chain is transferring from legacy S/X observations to VGOS observing modes.

[9] `http://www.nexpres.eu/`

A seamless operation of a VLBI network needs a common, data acquisition system-independent language in order to coordinate the observations and data generation. During the year 2014, based on the VLBI Experiment (VEX) format, an updated VEX2 format was released (Baver et al., 2015). The VEX format is devised to completely describe a VLBI experiment, including scheduling, data acquisition, and correlation. Furthermore, the widely used controller software for the VLBI data acquisition, the Field System (FS)[10], will have to be updated to meet the need for extended monitoring. The operators have to be able to review extensive performance diagnostics during the experiments to quickly assess and attend to possible problems (Niell et al., 2005).

The FS in its current form works in semi-automatic manner. When the observation schedule is running, it controls the telescope and recording process according to the pre-loaded procedure. However, this system still requires a considerable amount of manual input from the operator personnel. The observation schedules need to be downloaded to the FS computer and processed in order to extract the station-specific instruction set (procedure files). Moreover, with systems such as Mark 5 series, if the recorded data amount exceeds the size of available disk packs the operator needs to replace the disk packs. Furthermore, FS as such does not have any independently functioning troubleshoot/error correction procedure and at times manual input or soft/hard reset by the operator is needed. For continuous operations this level of input from on-site personnel is not a economically viable. Thus, VGOS needs a robust and as autonomous as possible monitoring and control system for the station operations. The monitoring will probably shift from station-wise operations to a more centralized system, which requires reliable and automatic reporting functionality from the FS or its replacement.

With VGOS the correlators are required to handle substantially larger amount of data compared to the legacy S/X system. The amount of data processed by the correlators as the number of active sites in the VGOS network rise is expected to increase from a current level of 58 TB/day (8 sites) up to 1037 TB/day by the year 2020 (24 sites) (Petrachenko et al., 2015). These numbers are based on a observation cycle of 30 s, with 7.5 s on-source time with a recording rate of 16 Gbps. If a correlator were to receive the full data rate from all stations in the network simultaneously, the network data rate calculated this way would have to be increased from a current level of 8 Gbps to 134 Gbps. This matches with a situation where all data transfer to a correlator would be handled online. The required high network data rates could prove to become a bottleneck in the VLBI observation chain, if necessary infrastructure is not readily available at the correlators. In case the stations would transfer the data exclusively on physical disk packs, the correlators would require an adequate number of playback units to handle playback of data. Moreover, by 2020 the network stations

[10] `http://lupus.gsfc.nasa.gov/fsdoc/fshome.html`

would require nearly one 48 TB module per day for sustained operations. In Petrachenko et al. (2015) the recommended correlator and data transfer capacities for future VGOS include the following aspects:

- The predicted number of over 3000 correlator cores in the coming years is not a certainty, and should the status should be re-assessed in the next few years.
- The Mark 6 VLBI data system is regarded as the most competitive system available. Correlators should have at least four Mark 6 units.
- Correlators should upgrade their network capacity to at least 10 Gbps, acknowledging that rates as high as 40 Gbps are needed in the future.
- Correlators should consider upgrading the internal network technology from the current 10 Gbps towards data rates of 40 Gbps.

When the data are correlated they are analysed to produce the EOP. With VGOS this will happen in near-real time. This means automating all aspects of the data analysis procedure. Currently the analysis process still contains multiple steps that are either semi-automatic or require manual input from the analyst. Firstly, to analyse the session the analyst has to obtain the observation data and all necessary auxiliary data (e.g. meteorological data and cable delay). With automated messages on finished observation, auxiliary data generation, and successful correlation and assuming these will be reliably produced and archived, this data acquisition step is likely trivial. However, to prevent bad or corrupted auxiliary data impairing the solution, the data have to be either pre-screened or checked for suspicious results. Up to this point this process has relied on various level of manual input from the analyst. Automating this process will remove one bottleneck in the analysis chain. Detecting abnormal values in local meteorological and cable data can be challenging, depending on the sampling interval of the data. For example, with standard IVS-R and IVS-INT sessions the weather and cable readings are recorded once per scan. With the INT sessions this leads to a relatively low number of data points. In absence of a good model for example for the cable delay, testing these values consistently for outliers can be difficult. The auxiliary values are then further interpolated to match the exact scan epochs. Because the adjustment process is non-linear it needs sufficiently accurate a priori values in order for the solution to converge. Usual a priori data include at least the EOP. Depending on the applied mapping functions further data might also be needed. The current S/X system produces delays which, due to bandwidth synthesis, contain ambiguities proportional to the channel separation. These need to be removed prior to ionosphere calibration. Some existing software packages can resolve ambiguities in automatic or semi-automatic mode (c5++ (Hobiger et al., 2010) and Calc/Solve/νSolve (Ma

et al., 1990, Bolotin et al., 2014), respectively). However, this task becomes more complicated with increased number of baselines.

Discontinuities in the station clock behaviour have to be taken care of by introducing clock breaks to the analysis. For this purpose there are automatic- and semi-automatic procedures, but consistent handling still requires human input. The data must also be processed with an outlier detection algorithm and rigorous cut-off limits for the outliers and re-weighting processes must be established. The automatic procedure must also be able to assess the solution quality and whether the intermediate tasks such as resolving ambiguities, ionosphere calibration, and clock breaks have been successful. Additionally, any other systematic or otherwise suspicious behaviour of a single station, sub-network, or the network in its entirety have to at least be flagged if not automatically corrected by e.g. excluding stations from the analysis. The analysis process usually involves, especially in case there are problems, investigating the correlator reports for the session. These are currently produced in human readable form. Automation however requires some type of reporting system/language that is able to convey any important information that arose during the correlation to the analysis algorithm. If necessary the analysis algorithm in turn then has to be able to adapt its actions based on these reports.

In addition to the analysis procedure the accuracy of results is influenced by the quality of the a priori data introduced into the analysis. This is especially important with observation modes that are designed to produce EOP results in near-real time. In this scenario it is usually necessary to use predicted values for the a prioris. Currently the IVS-INT sessions and their timeliness goals are closest to the continuous monitoring design of VGOS. The aspects of analysis automation and the impact of accuracy and application of a priori information is investigated in *Paper II* that is appended to this thesis.

Observing plan

The medium-term VGOS observing strategy foresees about 16 stations that will eventually operate in a continuous mode to produce near real-time EOP. Different scheduling strategies have been tested for VGOS observing modes. A standard approach is to maximize the number of stations per scan while minimizing the slewing time between these scans. By this method the observing time is maximized but the sky coverage is limited by the slewing times of the telescopes. An alternative scheduling method is to simultaneously observe sources on opposite sides on the sky that are visible to some part of the network at all times. This scheduling strategy aims at a uniform sky coverage by sampling sources in pairs with regular scan intervals (Petrachenko et al., 2009).

The current proposed VGOS observing plan anticipates to be operational 24/7 by the year 2020 (Petrachenko et al., 2014). During the preceding transition

stage the VGOS network is set to observe daily in four equally spaced 1-hour patches. Before this observation mode is implemented there are a number of planned exercise campaigns involving the new VGOS systems, which focus on different aspects of the continuous monitoring. This includes sustained 24-hour sessions, sustained daily EOP sessions in four 1-hour patches, and a combination of these two. The network performance has been simulated for 8, 16, and 30 stations observing in 4x1 h/24 h, 8x1 h/24 h, and 24 h modes, respectively. When simulating actual R1, R4, and CONT11 schedules in the same context, the network performance for UT1 reached CONT11 levels (2.0 μs) with the 8-station configuration. However, improvement of polar motion was more modest, with a 8-station setup performing slightly worse than IVS-R1 in x_p and y_p, and IVS-R4 in y_p. The VGOS observation time is increased considerably compared to IVS-R1, IVS-R4, and CONT11. However, the simulations also indicate sub-optimal scheduling, which is manifested in relative drop in observation time with network sizes larger than 8 stations. These times still surpass the old session types by a factor of approximately 3–5. The projected accuracies for the continuously operating network of 30 stations based on the simulations are below 1 μs for UT1, 10 μas for polar motion, and 0.1 ppb for scale. This marks an improvement of nearly an order of magnitude for each of these parameters when compared to current IVS-R1 and IVS-R4 sessions. With optimised schedules the observation time per station (simulated performance of 58.2 observations/hour/station) is also anticipated to improve closer to the VGOS target density of 120 observations/hour/station (Petrachenko et al., 2014).

3.4.3 VGOS data analysis challenges

The data produced by VGOS will present a set of new challenges in the data analysis. The session-based format of VLBI observations is deeply ingrained in many aspects of the geodetic VLBI product chain. When geodetic results are available on continuous basis the implications to data analysis have to be considered. To ensure consistent quality of the VLBI products, general guidelines are needed to address questions on what kind of products will be offered in the future. For example one has to consider what is the threshold in choosing between timeliness of the solution and the amount of data included in the solution. If the analysis is performed via a type of moving time window-method it needs to be decided whether the results are divided into averaged time periods based on calendar dates or whether it would be better to divide the results based on the network performance.

The shift to VGOS-capable observing systems will lead to the introduction of a large number of new hardware and data acquisition procedures. In order to guarantee that the system is performing on the expected level and to ensure the continuity of the long geodetic time series derived with the soon-to-be

legacy systems, it is necessary to compare the respective results. This will help in the detection of possible systematic biases between the old and new systems that could eventually propagate in to the final geodetic VLBI products. The cross-validation of the old and new data on many levels is important in order to verify the system functionality with respect to its components and to give an indication of possible sources for error. This means that it is important to test the new components on instrumental level, but also as a part of the whole system. The implementation of the broadband VGOS systems involves upgrading a wide range of equipment. If these upgrades are introduced in one big overhaul it complicates the possibilities to test the impact of individual components to the measurements. Furthermore, it is important to also verify the results on the end-product level, that is, the geodetic products. Testing elements in a system only component-wise or up to some point in the data stream might hide effects, which then later manifest in the actual data products that the system is built for. This aspect is also studied in *Paper I* appended to this thesis. The paper investigates the influence the implementation of a new digital backend (Digital Base-band Converter, DBBC) at OSO on the geodetic parameters.

3.5 VLBI delay model

As a consequence of the great distance to the observed radio sources, the signal arriving Earth can be physically described as a plane wave front. In general for sources further than $\approx$ 30 ly the curvature effects of the wave front can be ignored (Sovers et al., 1998). The baseline vector computed from the observed delays is a solution to a geometric problem. The observed delay is proportional to a scalar product of the baseline vector $\mathbf{b}$ and source vector $\hat{\mathbf{k}}$. The observation geometry is illustrated in Figure 3.4.

The delay model representing this observation geometry can be expressed in its basic form by

$$\tau = -\frac{1}{c}\,\mathbf{b} \cdot \hat{\mathbf{k}}, \tag{3.6}$$

where τ = t_2 - t_1 is the difference between observed signal arrival times at station 1 and 2. The numbering scheme follows the logic where 1 always refers to the station that receives the signal first. The geometric delay by definition assumes perfect observations in total vacuum between the source and the observing stations. The source vector is a unit vector perpendicular to the arriving wave front and pointing toward the source. It is defined in the Barycentric Celestial Reference System (BCRS). The baseline vector $\mathbf{b}$ is most naturally defined in a Terrestrial Reference System (TRS). However, in order to compute the scalar product the baseline vector $\mathbf{b}$ and source vector $\hat{\mathbf{k}}$ need to be transformed into

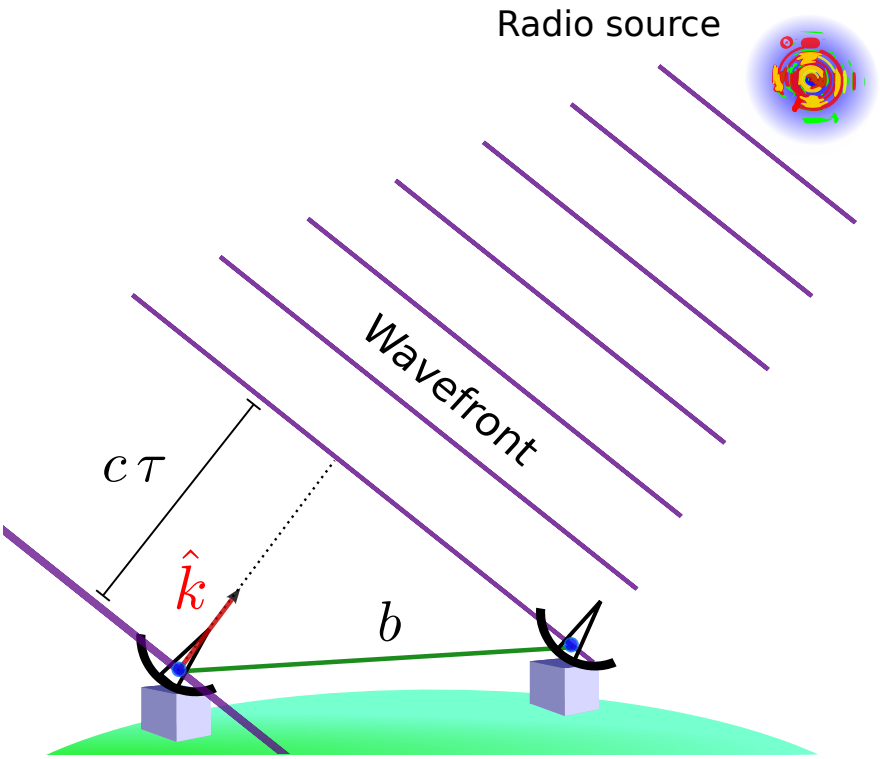

Figure 3.4: Basic observation geometry for single-baseline VLBI observation. A plane wave arrives from a radio source in direction $\hat{k}$ and is observed at two stations separated by a baseline b. The time-of-arrival delay of the signal between the two telescopes is τ and c is the speed of light in a vacuum.

the same basis. Thus **b** in Equation 3.6 represents the baseline vector transformed to BCRS. The observed delays produced by the correlator are assumed to be in the Terrestrial Time (TT) frame.

In practice the observed delay τ produced by the correlator includes the geometric delay and additional delay contributions from troposphere, ionosphere, instrumental effects, and station clocks. The baseline vector **b** at the signal time of arrival at station 1 (t_1) is defined as

$$\mathbf{b} = \mathbf{r}_2(t_1) - \mathbf{r}_1(t_1), \tag{3.7}$$

where $\mathbf{r}_1$ and $\mathbf{r}_2$ are the position vectors of stations 1 and 2 at time t_1, respectively. After the signal is detected at station 1 the plane wave signal traverses from station 1 to station 2. Because Earth is rotating, station 2 has moved from its location in space at time t_1 when the signal is finally detected at the station. As a result of this, the simplified geometric representation in Equation 3.6 must be

a complemented with a velocity parameter η_2 for station 2. The geometric delay is then expressed as

$$t_2 - t_1 = \frac{1}{c}\frac{1}{1 - \hat{\mathbf{k}} \cdot \eta_2}\,\hat{\mathbf{k}} \cdot \mathbf{b}. \tag{3.8}$$

Because the gravitational effects and the signal propagation are most naturally described in a BCRS frame, the baseline vector is transformed from ITRS to BCRS. First the locations of both stations are determined at the time t when the plane wave arrives at station 1. These ITRS coordinates have to be corrected for various geophysical effects discussed in more detail in Chapter 2. If not correctly modelled these variations will propagate into time-dependent changes of the baseline. On the other hand, at the same time it is also possible to detect the signal of some previously unmodeled geophysical phenomena via VLBI observations. Station movement due to tectonic motion is usually modelled as linear rates, which are estimated from long time-series of combined technique solutions. For VLBI, a priori station positions and velocities are provided by e.g. ITRF2008 (Altamimi et al., 2011) or the corresponding VLBI contribution VTRF2008 (Böckmann et al., 2010). Generally, the changes in the station positions are connected to the deformation of the Earth's crust, be it through tectonic or tidal motion.

Equation 3.8 is valid in a frame that is at rest relative to the solar system, i.e. BCRS. Formulating in GCRS the total delay is expressed as a sum of geometric delay, atmospheric delays, and other instrumental delays. The geometric delay consists of the vacuum delay and the geometric part of the atmospheric (tropospheric) delay. The vacuum delay in GCRS takes into account the gravitational delay caused the Sun, Moon, and planets, $\Delta\tau_{grav}$, computed in BCRS. It also includes the gravitational potential at the geocenter, U, which at the picosecond level needs only to include the potential of the Sun. In the latest IERS Conventions (Petit and Luzum, 2010) the delay is formulated within the general theory of relativity under the Parametrized Post-Newtonian (PPN) formalism, where γ = 1. The geometric delay is then given by

$$\tau^{21}_{geom} = \tau^{21}_{v}(\Delta\tau_{grav}, U, \gamma, \hat{\mathbf{K}}, \omega_1, \omega_2, \mathbf{b}, \mathbf{V}_{\oplus}) + \delta\tau_{trop1}\frac{\hat{\mathbf{K}} \cdot (\omega_2 - \omega_1)}{c}, \tag{3.9}$$

where τ^{21}_{v} is the vacuum delay between stations 1 and 2, $\hat{\mathbf{K}}$ is the non-aberrated unit source vector towards the source, ω_i is the geocentric velocity of the ith telescope, $\mathbf{V}_{\oplus}$ is the barycentric velocity of geocenter and $\delta\tau_{trop1}$ is the tropospheric propagation for the station 1, which receives the signal first. The total delay is then given by

$$\tau = \tau^{21}_{geom} - \delta\tau_{trop2}(t_1 - \frac{\hat{\mathbf{K}} \cdot \mathbf{b}}{c}, \mathbf{k}_2 - \delta\tau_{trop1}(\mathbf{k}_1) + \sum_n \tau_n, \tag{3.10}$$

where the troposphere delays are computed using the aberrated source vectors $\mathbf{k_i}$, and $\mathbf{b}$ is the baseline vector in GCRS. The sum for the τ_n term includes corrections to the delay caused by e.g. clocks, antenna deformation, axis offsets, and instrumental delays (Petit and Luzum, 2010).

3.5.1 Transformation from ITRS to GCRS

After the station positions at the moment of observation are corrected for the various loading effects, the baseline vector (i.e. station coordinates) is transformed from ITRS to GCRS via a series of rotations. In sequence these rotations transform the station coordinates according to

$$\mathbf{X}_{GCRS} = N(t)\ R(t)\ W(t)\mathbf{X}_{ITRS}, \tag{3.11}$$

where $W(t)$ (wobble) is a matrix combination of rotations representing polar motion, $R(t)$ is a rotation matrix for the diurnal rotation of the Earth around the Celestial Intermediate Pole (CIP), and $N(t)$ is the nutation-precession matrix which describes the orientation of Earth's axis of rotation in space. The time argument t (the signal time of arrival t_1 at station 1 in UTC referred to TT with respect to TT(J2000.0) (Petit and Luzum, 2010)) corresponds to

$$t = \frac{(TT - TT(J2000.0))_{days}}{36525}, \tag{3.12}$$

$$TT = t_1 + (\Delta_{TT-TAI} + N_{ls}), \tag{3.13}$$

where Δ_{TT-TAI} is defined as 32.184 s and N_{ls} is the number of leap seconds applied to UTC until epoch t_1. J2000.0 is the epoch Jan 1st 2000 12:00 UT (Petit and Luzum, 2010).

Following the International Astronomical Union (IAU) 2000 recommendations the transformation from ITRS to GCRS should be done with the CIP defined in the GCRS and ITRS, and the Earth Rotation Angle (ERA). This transformation is done via two intermediate systems, the Terrestrial Intermediate Reference System (TIRS) and the Celestial Intermediate Reference System (CIRS). For both systems a non-rotating reference longitude is defined on the CIP equator, the Celestial Intermediate Origin (CIO) and the Terrestrial Intermediate Origin (TIO) for the CIRS and TIRS, respectively. In the intermediate systems the z-axes are aligned with the CIP in that system and the x-axes to their respective reference longitudes. The expanded version of W is

$$\begin{aligned} W(t) &= R_3(-s')R_2(x_p)R_1(y_p) \\ &= \begin{bmatrix} \cos s' & -\sin s' & 0 \\ \sin s' & \cos s' & 0 \\ 0 & 0 & 1 \end{bmatrix} \begin{bmatrix} \cos x_p & 0 & -\sin x_p \\ 0 & 1 & 0 \\ \sin x_p & 0 & \cos x_p \end{bmatrix} \begin{bmatrix} 1 & 0 & 0 \\ 0 & \cos y_p & \sin y_p \\ 0 & -\sin y_p & \cos y_p \end{bmatrix}, \end{aligned} \tag{3.14}$$

where R_1, R_2, and R_3 are the conventional rotation matrices in the Cartesian coordinate system. The arguments for the first two rotations y_p and x_p are the polar motion coordinates for the CIP, respectively, and s′ is the Terrestrial Intermediate Origin (TIO) locator. The position of TIO with respect to the CIP equator is given by s′. Its value varies with time as a function of the polar motion coordinates following

$$s'(t) = \frac{1}{2} \int_{t_0}^{t} (x_p \dot{y}_p - \dot{x}_p y_p) dt. \tag{3.15}$$

The value of s' is determined by the large-scale variations in polar motion. With current mean values for annual and Chandler wobble terms the value of the TIO locator in μas is given by

$$s' = -47 \cdot t. \tag{3.16}$$

The W(t) rotation relates the ITRS coordinates to TIRS coordinates. The next rotation R(t) consists of

$$R(t) = R_3(-\text{ERA(UT1)}), \tag{3.17}$$

where ERA is defined as the angle between the CIO and TIO measured along the equator of the CIP and R_3 is a rotation matrix about the z-axis having the same form (with $-ERA(UT1)$ as an argument) as in Equation 3.14. It can be expressed with linear relation to UT1 via T_u(UT1) by

$$ERA(T_u) = 2\pi(0.7790572732640 + 1.00273781191135448 \cdot T_u), \tag{3.18}$$

with $T_u = (JD(\text{UT1}) - 2451545.0)$ i.e. the Julian Date value of UT1 referenced to J2000.0 (Capitaine et al., 2000). This rotation transforms the coordinates from the TIRS to the CIRS.

The final rotation, N(t), transforms the CIRS coordinates to the GCRS. Physically it represents the effects of precession and nutation. This transformation is given by combination of four rotations

$$N(T) = R_3(-E)\ R_2(-s)\ R_3(E)\ R_3(s), \tag{3.19}$$

where E and d define the coordinates of the CIP in the GCRS as

$$\mathbf{X}_{GCRS}^{CIP} = \begin{bmatrix} \sin d \cos E \\ \sin d \sin E \\ \cos d \end{bmatrix}, \tag{3.20}$$

while s is the CIO locator, that describes the movement of the CIO on the CIP equator between the reference epoch and t caused by nutation and precession.

Similar to s' the CIO locator s is a time-integral of a function of the related coordinates. It is given by

$$s(t) = -\int_{t_0}^{t} \frac{X(t)\dot{Y}(t) - Y(t)\dot{X}(t)}{1 - Z(t)} dt - (\sigma_0 N_0 - \Sigma_0 N_0), \tag{3.21}$$

where X, Y, and Z are the coordinates of the CIP in the GCRS. The offset-term is a constant, which includes the position of the CIO at J2000.0 (σ_0), x-origin of the GCRS (Σ_0), and the ascending node of the equator in the equator of the GCRS at J2000.0 (N_0). The rotations in Equation 3.19 can be expressed in terms of X and Y with $a = 1/(1 + \cos d) \approx 1/2 + 1/(8(X^2 + Y^2))$ (within 1 μas) as

$$N(t) = \begin{bmatrix} 1 - aX^2 & -aXY & X \\ -aXY & 1 - aY^2 & Y \\ -X & -Y & 1 - a(X^2 + Y^2) \end{bmatrix} \begin{bmatrix} \cos s & \sin s & 0 \\ -\sin s & \cos s & 0 \\ 0 & 0 & 1 \end{bmatrix}. \tag{3.22}$$

The values for X and Y can be expressed by the IAU 2006/2000A model developed from the nutation and precession series. The value for s can be estimated via the quantity $s + XY/2$, which is numerically derived from Equation 3.21 using the modelled values for X and Y (Petit and Luzum, 2010).

The CIP divides the motion of ITRS pole in GCRS into the terrestrial polar motion and celestial nutation-precession. By convention the nutation-precession includes variation that has a period of 2 days or larger and polar motion includes the terms with higher frequency.

3.5.2 Atmospheric delay

For stations on the Earth's surface the arriving radio signal has to pass through different atmospheric layers before it reaches the VLBI telescopes. The signal path is changed by the presence of neutral and charged parts in the atmosphere. The effect of the different layers can be modelled as changes in the signal arrival times. Detectable changes in the signal arrival times due to the propagation medium are mainly due to two distinct atmospheric layers, the ionosphere and the troposphere.

Ionospheric delay

The ionosphere is an atmospheric region that consists of electrically charged particles. Its extent can be categorized by the varying degree of plasma density in the atmosphere. It is driven by the sun, whose radiation excites the atoms and molecules in this layer. Since this radiation ionizes neutral atoms the medium will be populated with free electrons. This effect is amplified during day time, which pushes the lower layer of the ionosphere to a height of approximately

60 km. The upper layer of the ionosphere extends to an altitude of over 500 km. The ionosphere is classified into three main layers: D, E, and F. The D layer is mostly active and reaches its peak during daytime, diminishing during the night due to recombination of the free electrons, in which the ionized atoms and molecules are again paired with the free electrons. This number of free electrons is described with the measure of Total Electron Content (TEC), which gives a physical quantification of the ionosphere. Between 90–150 km lies the E layer, which is mainly composed of NO+ and O_2^+. The ionosphere density peaks in the F layer, which is dominated by O+ ions. The peak density is on the order of 10^6 particles per cm^3. Compared to the D and E layer, the F layer does not undergo similar reduction in magnitude during its day-night cycle, but is also strongest during daytime (Kelley, 2009).

The ionosphere is a dispersive medium for radio-magnetic radiation, that is, the refractive index of ionosphere varies with frequency. Following Sovers et al. (1998) the contribution τ_{iono} of the ionosphere to the phase delay, compared to a perfect vacuum, is given by

$$\tau_{pd}^{iono} = \frac{1}{c}\int [n(f) - 1]dl, \tag{3.23}$$

where $n(f)$ is the frequency dependent refractive index integrated over a distance element dl along the line of sight. The ionospheric phase delay for frequency f can be expressed by omnidirectional approximation

$$\tau_{pd}^{iono} = -\frac{q(STEC)}{f^2}, \tag{3.24}$$

where $q = \frac{c \cdot r_0 \cdot STEC}{2\pi}$ with speed of light c, classical electron radius r_0, and Slant Total Electron Content (STEC). The additive group delay due to the ionosphere is given by

$$\tau_{gd}^{iono} = \frac{q}{f^2}. \tag{3.25}$$

For X-band the typical ionospheric delay is approximately between 0.1 ns and 2 ns.

Tropospheric delay

The troposphere contains the atmospheric layers that extend approximately between 0–20 km. It contains most of the water vapour in the atmosphere and nearly all weather phenomena take place there. Electromagnetic waves passing through the troposphere are influenced by the changes in the refractive index of the medium. The propagating waves are delayed, refracted, and attenuated by the molecules and particles present in the troposphere. Opposed to ionosphere

the troposphere is generally considered electronically neutral. Because it spans the space above approximately 20 km of the station it has a depth-component that needs to be taken into account modelling-wise. This means that the delay caused by the troposphere is highly elevation dependent. For lower elevations the signal arriving at the station has traversed a considerably longer distance in the troposphere compared to a signal incoming from the zenith. The main influence mechanism of the troposphere is the presence of moist air. The changes in the refraction index are caused by permanent and induced dipole moments present in the atmospheric molecules. The most important contributor is the water vapour. This is because water molecules have a strong permanent dipole moment. On the other hand, the main components of the atmosphere, nitrogen and oxygen, only have induced dipole moments.

The signal path delay caused by the troposphere in addition to the vacuum path length is given by the integral

$$\tau_{trop} = \int_S (n-1)\, dS, \tag{3.26}$$

where S is propagation path of the signal. This path corresponds to the path on which the propagation time is minimized.

The changes in the refractivity caused by the permanent and induced dipole moments are proportional to functions of pressure and temperature of the refracting medium. The effect of pressure is divided into partial pressure parts that contain hydrostatic pressure constituents (dry air) and the water vapour part (wet air). Thus the delay is divided into a dry and wet part as well following

$$\tau_{trop} = 10^{-6} \int_S (N_h + N_w)\, dS, \tag{3.27}$$

where h and w indicate hydrostatic and wet, respectively. Due to the small scale of $(n-1)$ a scaled quantity $N = 10^6(n-1)$ called refractivity is usually used in the formulations instead of n. The separated dry and wet parts are further modelled via their zenith components. The tropospheric delay is divided into Zenith Hydrostatic Delay (ZHD) and Zenith Wet Delay (ZWD) and their associated mapping functions. The zenith delay describes the atmospheric delay along the vertical column above the station. The mapping function (mf) maps this value to an arbitrary elevation angle. The tropospheric delay model is thus

$$\tau_{trop} = mf_h(e)\ \text{ZHD} + mf_w(e)\ \text{ZWD}. \tag{3.28}$$

Because the elements of the dry part are close to hydrostatic equilibrium in Equation 3.27 its behaviour can be predicted relatively well. Consequently ZHD can be estimated as a function of total surface pressure, station latitude

and height (Saastamoinen, 1972). On sea level the magnitude of ZHD is approximately 2.3 m, while ZWD is on the order of tens of centimetres. The mapping functions which model these zenith delays along the propagation path utilise external data from meteorological observations, numerical weather models, ray-traced delays, and derived numerical models (Böhm et al., 2006a, Sovers et al., 1998). Generally, ZHD can be accounted for almost completely in the modelling (Böhm et al., 2006a). In Equation 3.9 the tropospheric term for station 1 is the hydrostatic contribution to the troposphere delay.

Equation 3.28 uses mapping functions, that only vary as a function of elevation. The azimuthally non-symmetric behaviour can be modelled via troposphere gradients. The troposphere delay is appended with a gradient term that is dependent on the azimuth, giving the following form for the tropospheric delay

$$\tau_{trop} = mf_h(e)\ \mathrm{ZHD} + mf_w(e)\ \mathrm{ZWD} + mf_{grad}(e)[\mathrm{G_n}\cos\alpha + \mathrm{G_e}\sin\alpha], \qquad (3.29)$$

where mf_{grad} is the gradient mapping function. $\mathrm{G_n}$ and $\mathrm{G_e}$ are the north and east gradients, respectively (MacMillan, 1995, Böhm and Schuh, 2007).

Because the wet part consists of shifting water vapour masses its behaviour is much more dynamic. The water vapour is subject to changes during the diurnal period connected to heating by the sun. Furthermore, weather patterns and atmospheric turbulence can cause large variations within a short timespan. Atmospheric turbulence can change the water vapour content on local level very rapidly, which both change the observing conditions but also introduce possible correlations on a local level. This effect of modelling atmospheric turbulence has been investigated in e.g. Nilsson and Haas (2010). The dynamic nature of the troposphere makes it very difficult to model, not to mention predict, its variation. The troposphere is not a dispersive medium, so it can not be eliminated by linear combination of observations on multiple two frequencies. It is regarded as one of the main error sources in VLBI today.

3.5.3 Mapping functions and weather models

The mapping functions that appear in the equation for the tropospheric delay (see Equation 3.28) are used to transform the delay from the zenith direction to a local slant delay for an elevation e. This implies a model that considers the atmosphere to be symmetric respective to the local azimuth. Geometrically the delay mapping is proportional to the distance travelled within this tropospheric layer, i.e. $mf(e) = 1/\sin(e)$. The projective mapping can be expressed as a continued fraction (Marini, 1972)

$$mf(e) = \cfrac{1}{\sin(e) + \cfrac{a}{\sin(e) + \cfrac{b}{\sin(e) + \cfrac{c}{\cdots}}}}, \tag{3.30}$$

where e is the elevation and a, b, c are coefficients of the mapping function, that need to be determined. Most mapping functions employ some form of this type of continued fraction, with varying number of terms used in the expansion, e.g. Davis et al. (1985), Herring (1992), Niell (1996), Böhm et al. (2006a). The mapping function coefficients can be determined from e.g. by fitting the model to results obtained with ray-tracing or radiosonde measurements. The following will discuss a selection of the troposphere mapping, which are relevant in the context of this thesis.

New Mapping Functions (NMF)

The New Mapping Functions (NMF) (Niell, 1996) use a form of continued fraction employed in Herring (1992) where

$$mf(e) = \cfrac{1 + \cfrac{a}{1 + \cfrac{b}{1 + c}}}{\sin(e) + \cfrac{a}{\sin(e) + \cfrac{b}{\sin(e) + c}}}. \tag{3.31}$$

For the hydrostatic part of the NMF the coefficients a_h, b_h, and c_h are parametrised as sinusoidal functions of latitude and time and corrected for changes in station height (a_{ht}, b_{ht}, c_{ht}). The wet part of NMF is based on only interpolating the latitude values. The coefficients ($a_{h,w}, b_{h,w}, c_{h,w}$) are determined for five equally spaced latitudes between 15° and 75° by ray-tracing for nine elevation angles from 3° to 90°. The phase was fixed to January 28. NMF results were validated by comparing the results to radiosonde data. The associated coefficient values can be found in Niell (1996). An apparent feature of the NMF is that it does not rely on any additional external data, but can be used to compute global mapping function values based on only on site latitude.

Vienna Mapping Functions

The Vienna Mapping Functions (VMF1) (Böhm et al., 2006a) are based on a form of continued fraction similar to Equation 3.31. The b and c coefficients for the hy-

drostatic mapping functions were determined using data from European Centre for Medium-Range Weather Forecasts (ECMWF) 40-year re-analysis data for the year 2001. The corresponding wet mapping function coefficients were fixed to corresponding values in NMF. The a coefficients are determined by a fit to ray-traced refractivity profiles, based on ECMWF data. The a coefficients are provided with a 6-hour time resolution on a $2.5^\circ \times 2.0^\circ$ latitude-longitude grids by the Vienna University of Technology (IGG Vienna, 2015). In order to use VMF1 the user needs access to pressure data and a coefficients. Depending on the required timeliness these are based on observed or forecast values. Based on the good performance of VMF1 with station height standard deviations the VMF1 is recommended for global applications in the IERS Conventions 2010.

Global Pressure and Temperature model and Global Mapping Functions

The Global Pressure and Temperature (GPT) model and the Global Mapping Functions (GMF) together form an empirical model, based on average ECMWF values (Böhm et al., 2006b). The GMF coefficients were determined by spherical harmonic expansion (degree and order 9) of the VMF1 parameters on a global grid. The a coefficients were based on monthly mean profiles of ECMWF ERA-40 data from 1999–2000. The original GMF/GPT model was upgraded in 2013 with a combined model GPT2 (Lagler et al., 2013). It is based on ECMWF ERA-interim data covering 2001–2010. In addition to annual and mean terms, compared to GMF/GPT the GPT2 includes semi-annual terms. Moreover, instead of fixing the phase to January 28 (as also in NMF) the phase is estimated. Furthermore, GPT2 provides mean, annual, and semi-annual terms for the lapse rate (as opposed to -6.5°C/km in GMF/GPT). The GPT2 data are provided on a $5^\circ \times 5^\circ$ global grid.

3.5.4 Station clocks

The station clocks (frequency standards) are used to generate the UTC time-tags for the observations used in the correlation. These time-tags need to be extremely accurate in order to be able to correlate the observations and model the delays accurately. Although the frequency standards at the stations are normally highly accurate hydrogen masers, these clocks are usually independent of one another and can exhibit relative drifts and jumps. The delay model needs to account for these variations in the station clocks. Synchronization of the station clocks can be monitored to some extent by utilizing the frequency information from GPS satellites. However, the accuracy of GPS clocks is not sufficient to realize the frequency standard for the VLBI observations. Typically the station clocks are modelled as quadratic functions (sometimes appended with piecewise linear modelling) during the observation interval. The clock delay on the

baseline between telescopes 1 and 2 is then given by

$$\tau_c = a_0 + a_1(t - t_0) + a_2(t - t_0)^2, \tag{3.32}$$

where the coefficients a_0, a_1, and a_2 are the constant, linear, and quadratic terms of the clock polynomial, respectively. The clock performance can be divided into two parts: stability in time and stability in frequency. A highly stable clock can exhibit large drifts over time while still having small error in frequency. This behaviour must be accounted for in different ways depending on the length of the observing session, by e.g. estimating the clock polynomial for smaller intervals. The clock delay constitutes one of the largest contributions to the total observed delay, thus it is important to handle it appropriately as unmodeled clock behaviour will propagate into the estimated geodetic parameters (Sovers et al., 1998).

Chapter 4

VLBI data processing

VLBI data processing is a procedure that involves multiple steps in which geodetic parameters and physical phenomena are estimated and investigated using the VLBI observables as input. The correlation and the related post-processing also involve various steps of processing and analysing the data. In the context of this chapter VLBI analysis refers to the analysis of post-processed VLBI data which is performed with a VLBI data analysis software.

VLBI data analysis is an intricate subject which involves modelling a complex set of phenomena related to signal-propagation, geophysical processed on Earth, and the evolution of geodetic parameters in time. It is usually in the VLBI analysis software where models are implemented to test and validate different hypotheses and experimental configurations. Furthermore, VLBI analysis software are also used by the correlator to compute the theoretical delays, which are needed as a priori values in the correlation process to align observations from the telescopes in the network (McCarthy and Petit, 2004).

Historically the available VLBI software have always had components that require human interaction in order to reach the highest accuracy in the geodetic products. Automation and simplification of the VLBI analysis procedure can be said to always have been a subject of interest within the software development. However, with the upcoming VGOS observations with greatly increased data quantities and continuous operations, the automation of the analysis process has moved from being an object of technical interest into a necessity. While many of the VLBI software packages offer good possibilities in processing the sessions in a semi-automatic fashion, they still require human input or validation in some of the key steps in the analysis chain. These include e.g. resolving ambiguities, detecting anomalous clock behaviour (clock breaks), or establishing whether the station had problems during observations, which are stated in the correlation report. Real-time analysis also introduces the aspect of availability of external data. VLBI analysis typically requires some a priori informa-

tion about station positions, EOP, instrumental delays, and weather conditions. Real-time processing means either these values have to be supplied in real-time (could be feasible for instrumental delays) or estimated from prediction models. In some cases even if the data, such as meteorological data, are available, they need to be amended by parameters that are generated e.g. via Numerical Weather Models (NWM). Since VLBI is the primary method used to determine the EOP the a priori information needs to be predicted or modelled to some degree. Thus it is necessary to investigate which factors are crucial for the solution quality when the time resolution and accuracy of the available external information is limited.

In a multi-layered system changes in the observation equipment may cause hard to model, unexpected biases or changes in instrumental precision. These changes can be investigated on an instrumental or system-wide levels. Even though the technical specifications of the components are normally known with exceptional detail it is important to also investigate whether there are any unexpected effects on the estimated parameters. In 2011, as a part of the preparation in the transition to VGOS, the Onsala Space Observatory installed a Digital Base-band Converter (DBBC). It was run in parallel with the then operational system consisting of the analogue Mark 4 rack. During a three-year period these systems were run in parallel to collect data with DBBC while the old and proven analogue system remained the operational system. During this period the performance of the DBBC could be assessed by running local zero-baseline tests. Additionally, the sessions recorded in parallel could be compared in order to investigate possible discrepancies in the observed delays and geodetic parameters.

These issues connected to the general process of transitioning into VGOS compliant operations are studied in *Papers I* and *II* appended to this thesis. The transition into operational use of DBBC at OSO is investigated in *Paper I*, where the results from the DBBC-analogue comparison are presented. The near-real time automated observation and analysis aspects are investigated in *Paper II*, presenting the results from investigation of the requirements for a priori information for automated near-real time analysis of IVS-INT1 sessions.

This chapter will give a general introduction to the various aspects of VLBI data processing such as the analysis software packages, VLBI data formats, auxiliary data, steps in the analysis process, differences in analysis approach when analysing different session types (e.g. Rapid-turnaround and INT-sessions), and automation. Moreover, the specific issues related to the VLBI analysis procedures, associated software, and analysis approaches used for the results of these two papers are discussed in more detail.

4.1 VLBI data formats

The VLBI data goes through multiple formats during the observation chain. The recorder format is read into the correlators, which produce the cross-correlation functions in a format read by the post-correlation software. Then the correlation and post-correlation process produces the VLBI observables, group delay, phase delay, phase delay rate, and amplitudes, and these data are typically stored into databases. There are various database formats available, which are to some degree dependent on the correlator/post-correlator software used and vice versa.

The most common formats used in geodetic VLBI are the Goddard Database Format i.e. Mark3-database (Mark3-DB) format (Gipson, 2012) and National Geodetic Survey (NGS) cards (Gordon, 2007). These two formats differ significantly in their structure and usual application in the standard VLBI data processing chain.

Mark3-DB is binary in format which together with the Calc/Solve VLBI analysis software (Ma et al., 1990) can be regarded as the primary combination used in creating the IVS VLBI data products. The databases contain the observational data and optionally complete sets of auxiliary info, such as geophysical models and meteorological data. IVS correlators, such as the Washington Correlator and the Bonn Correlator, participating in the regular IVS VLBI sessions (e.g. Rapid turnaround) produce their data in the Mark3-DB format. The K5-type GSI correlator (Japan) (Kurihara and Hara, 2015) initially produces databases in K5 format (KOMB), which can be subsequently converted into Mark3-DBs (Hobiger et al., 2008). The K5-format has also been used in an automated data processing chain from correlator to the VLBI analysis for near-real time estimation of UT1-UTC from INT2 sessions (Sekido et al., 2008).

NGS databases are formatted in ASCII and they contain only a subset of the data included in the more comprehensive binary database formats. If the binary databases contain cable delays and meteorological data, these are interpolated for the observation epochs in the NGS files. There are trade-offs when using this type of trimmed format. On the one hand some information is lost, but on the other hand the ASCII representation is directly human readable and parsing this data does not require extensive software implementations, but can be done with relative ease by using scripting languages or standard command line programs in Unix-like systems. The NGS format is supported by several software packages such as c5++ (Hobiger et al., 2010), the Vienna VLBI Software (VieVS) (Böhm et al., 2012), and OCCAM (Titov et al., 2004).

The official IVS VLBI data are currently released in Mark3-DB and NGS-formats. However, the information in these databases is not interchangeable. The databases use a numbering scheme called versions, which indicate the stage of the processing chain that the database represents. Normally this includes ver-

sions from one to four. Version numbers higher than four normally indicate that a modified/corrected version of the final database was produced. In practice Version-1 databases contain the correlator output. This data refers to the raw delay data, without any processing after the post-correlator output. The raw correlator output has one file for each observation. These are patched together into the Version-1 database. Version-2 databases have been processed with Calc (of Calc/Solve) to add information on model parameters, their partial derivatives, and theoretical delays. In Version-3 the Version-2 databases have been extended with auxiliary information, such as information from the station log-files. Version-4 database have been processed for the removal of group delay ambiguities, outliers, clock-breaks, station performance, and the application of external data. It is these Version-4 databases that represent the official IVS data and are converted to the NGS card format, which are subsequently used as the first input by many VLBI analysis software packages (Gipson, 2012).

The NGS databases (also called cards) are further structured into cards, which each correspond to one line in the database. The cards contain session information, auxiliary data, and observations using the following division:

1. Header: information on the source-database and version used in generating the NGS database: date (YYMMMMDD), database code (xx), version (####).
2. Sites: stations included in the database along with their Cartesian coordinates, axis type, and axis offset.
3. Sources: the radio sources observed in the sessions along with their J2000.0 coordinates in right ascension and declination using the IAU 1984 Nutation/Precession model.
4. Auxiliary parameters: reference frequency, group delay ambiguity spacing, delay and delay rate type (group/phase delay).
5. Data cards (data given in following cards are omitted if they are provided in the four cards above):
   (a) Baseline (stations 1 and 2), observed source, time of observation.
   (b) Observed delay and delay rate and their formal error, indicators for data quality, delay and delay rate type.
   (c) Correlation coefficient, fringe amplitude, and fringe phase and their formal errors.
   (d) System and antenna temperatures and their formal errors (sites 1 and 2).
   (e) One-way cable calibration corrections (sites 1 and 2), Water Vapour Radiometer (WVR) readings and formal errors (sites 1 and 2)

(f) Ambient atmospheric temperature, barometric pressure, and humidity (sites 1 and 2).

(g) Time difference to the reference epoch (date assigned to database in the filename/header), observation duration, a priori UT1-UTC offset (site 1), observation frequency, group delay ambiguity.

(h) Ionosphere delay and delay rate correction and their formal errors as well as ionosphere error flag.

(i) Same as observed delays card, but includes modified formal errors if applicable.

Compared to Version-4 Mark3-DB the contents of the NGS file poses limitations on the possible steps that the analyst can do in order to trace back in case of problems with the database. In case of Version-4 NGS-files the information on the number of ambiguity shifts has been lost. Thus it is not possible in practical sense to re-visit the ambiguities at this stage. The NGS format itself does not prevent resolving ambiguities, but if one wishes to use the official IVS products directly in NGS format then the user is limited to the Version-4. There are utilities to convert Mark3-DBs to NGS format, such as MK3TOOLS (Hobiger et al., 2008), which extract the Mark3-DB contents to NetCDF format and create the NGS based on the extracted data.

The Mark3-DB format will be eventually replaced with a new format called vgosDB (Gipson, 2012). Designed for the requirements of VGOS in mind, it is meant to handle the challenges with the new system, such as large amounts of data, new observables (broadband delays), and need for flexibility. It has been shown that vgosDB improves the processing time of large databases by nearly 50 % (Gipson, 2014). It will also assess many shortcomings of the Mark3-DB format. In the current processing chain the use of Mark3-DB format is baked-in with the use of Calc/Solve (Ma et al., 1990). The vgosDB is aimed to be easily implementable with existing software packages.

4.2 VLBI analysis software

VLBI analysis software packages are used to process the delay observables stored in databases produced by the correlator. They are used to estimate a wide range of geodetic parameters such as station positions and EOP. Furthermore, they are used to investigate various geophysical phenomena by e.g estimating geodynamical parameters such as Love numbers (Mathews et al., 1995, Haas and Schuh, 1996).

There are many software packages available for VLBI data analysis developed independently by multiple institutions. These include e.g. Calc/Solve

(Ma et al., 1990) and the Solve upgrade νSolve (Bolotin et al., 2014), c5++ (Hobiger et al., 2010), OCCAM (Titov et al., 2004), VieVS (Böhm et al., 2006a), and GEOSAT (Andersen, 2000). Most of these software packages are open-source and available either freely or by request. The software packages differ in their capabilities to perform different level of tasks necessary in the VLBI data analysis chain and combining VLBI with different space-geodetic methods such as GNSS and SLR. In general these software can be divided into two groups. Firstly, software that are able to process databases in order to solve group delay ambiguities and compute the ionosphere calibration. Secondly, software that needs databases which have had these procedures performed prior. Out of the listed software the ones capable of ambiguity resolution and ionosphere calibration are c5++ and Calc/Solve/νSolve. Because of the dependency of other software on ionosphere-free databases and its major role in creating the official IVS products the product chain has become especially dependent on the Calc/Solve software package. This situation is not optimal in terms of redundancy and solution validation. Furthermore, because Calc/Solve is the main software used for operational analysis, any updates to this infrastructure have to be rolled in sequentially and with great care. These two software, Calc/νSolve (Calc/Solve with Solve replaced by νSolve) and c5++, were used for the results obtained in *Papers I* and *II*, respectively. The following subsections discuss these used software in some more detail.

4.2.1 Calc/Solve and νSolve

Calc/Solve (Ma et al., 1990) is a VLBI analysis software package, which has been continuously developed for over 40 years at the Goddard Space Flight Center (GSFC). Due to this long development history the code base of Calc/Solve has been appended and modified continuously. The main parts of the program are written in Fortran-95. This type of extensive legacy code base developed over a long period of time may require extensive knowledge of the package, which can make it relatively difficult to independently include additional functionality to the program. In recent years a successor, νSolve, for the Solve-part of the package has been introduced. Currently under development, it represents a complete modernisation of the Solve package, with support for future data structures and VGOS observing modes. The native data format in Calc/Solve is the binary Mark3-DB, which can be further collected into superfiles for analysing multiple sessions in a combined solution. The program consists of two main parts, Calc and Solve.

Calc is responsible for computing the theoretical VLBI delay and delay rates for the observations. Moreover, it computes several of the partial delays used in the adjustment process, including EOP, station positions, and source coordinates. Calc includes most geophysical models, and writes information on e.g.

ocean loading, atmosphere loading, and tides (Fey et al., 2009). Calc11[1] (latest version at the time) is compatible with the latest IERS Conventions 2010.

Solve is a collection of programs intended for parameter adjustment and performance analysis. It takes databases processed with Calc as an input and performs a least-squares adjustment in order to estimate geodetic parameters. The database must include (i.e. be processed with Calc) the theoretical delays, partial derivatives, observed delays, and additional models and their partial derivatives.

Calc/Solve is controlled via various control-files, that include instructions on which databases to read, and enabling e.g. geophysical models. The typical Calc/Solve processing work flow in interactive mode includes the following steps

- Calc processing (latest version Calc11):
  - Process the Version-1 database with Calc
  - Add external info on cable calibration and meteorological data to the database
- Using Solve perform the adjustment:
  - Apply contributions from cable calibration, meteorological data, loading effects, tides
  - Solve X/S group delay ambiguities and perform ionosphere calibration
  - Perform and fine-tune the parameter adjustment on the ionosphere free database

The above steps form the basic outline for a typical VLBI data analysis with Calc/Solve. In general the steps remain similar when Solve is replaced with νSolve. Most of the parameter estimation options are found in both programs. When using Mark3-DB database format the processing with Calc11 is done in a similar manner regardless whether Solve or νSolve is used.

νSolve

Compared to Solve, νSolve has many of the options available as well as a compatibility mode, which attempts to recreate Solve-like solutions. Generally, it represents a major upgrade to the user interface. It features an upgraded plotting subsystem, which can be used to interactively perform tasks related to

[1] `http://gemini.gsfc.nasa.gov/solve/release/release_20140221.pdf`

session processing, such as resolving ambiguities, detecting clock breaks, evaluating station performance, and for estimated parameters displaying residuals. The estimation is done with Square-Root Information Filter (SFIR) (Bolotin et al., 2014). Parameters can be estimated as four types, which are 1) local, 2) arc, 3) piece-wise linear (PWL) functions, 4) and stochastic parameters. A local parameter is determined once for the whole sessions, an arc parameter estimates a constant parameter within user-specified time intervals. Piece-wise linear functions are linear functions estimated from the data with user specified intervals. Stochastic parameters model the time-variations as stochastic processes (Bolotin et al., 2014). The use of latter estimation type is still under development, thus mixing it with the other estimation methods can produce unpredictable results (νSolve version 0.1.6 Red Rue/Solar Fire). The automatic ambiguity resolution algorithm is derived from the standard Solve version, with the added capability of handling variable ambiguity spacing within baselines or one baseline in a session. The clock break detection is done in semi-automatic or manual mode. Individual observations and groups of observations can also be adjusted manually in the plotting subsystem. The parameters that can be estimated with νSolve include clock polynomial coefficients, ZWD, ZHD, tropospheric gradients, station positions, sources coordinates, EOP and their rates (excluding nutation angle rates), baseline vectors and clock offsets, and antenna axis offsets.

The νSolve software was used with Calc11 for the VLBI data analysis of the databases in *Paper I*.

4.2.2 c5++

The c5++ space-geodetic analysis software has been jointly developed by NICT, Japan Aerospace Exploration Agency (JAXA), and Hitotsubashi University. It is based on analysis software CONCERTO04, written in Java, which was able to process GPS, SLR, and satellite-tracking data. In c5++ the functionalities of CONCERTO04 were ported into C++ and the capability to analyse VLBI observations was added. The design philosophy of c5++ aims to make multi-technique combinations straightforward and robust. It is a collection of technique-specific libraries, which can be called from the main program. With this approach it is possible to ensure that the different techniques implement the same conventions for geophysical models. The current stable version of c5++ follows the latest IERS Conventions (Petit and Luzum, 2010). Consistently modelled observations can then be combined on either observation or normal equation level. For the user the operating principle of c5++ differs from e.g. interactive νSolve. c5++ does not include a Graphical User Interface (GUI), but is invoked purely through command line with a single binary. The analysis options are set via configuration files, which include all the necessary information to analyse a session. The configuration file points to geophysical models (stored in files)

which are included in the analysis. The parameter estimation options are also set in these files. Moreover, all the commands can be alternatively passed to the binary directly from the command line. In fact, the configuration file is essentially just a collection of command line parameters. Because of this design aspect c5++ is very suitable for controlling the program with external scripts. For VLBI observations c5++ is capable of directly processing data in NGS and K5 raw correlator output format. Furthermore, with associated MK3TOOLS it is possible to process Mark3-DB databases without Calc libraries (Hobiger et al., 2010). Recently a module for reading and writing databases in vgosDB data format has been developed for c5++ (Klopotek, 2015).

Due to its design, c5++ is well suited for automatic analysis of VLBI data. However, the solution is somewhat dependent on the success of the automated ambiguity and outlier detection algorithms, since the observations cannot be easily (i.e. without modifying the NGS database) adjusted or removed on an individual level. The adjustment procedure used in c5++ is an iterative one. The convergence criterion is determined by the ratio of the successive Weighted Root Mean Square (WRMS) errors of the fit. The cut-off criterion is defined by the user. The solution is iterated until the change in WRMS error ratios between successive runs is sufficiently close to 1. This condition assumes that the solution converges and does not e.g. oscillate around 1.

The ambiguity resolution and ionosphere calibration is done recursively. In the ambiguity resolution mode the non-ionosphere calibrated databases for X- and S-band are estimated with a simple parameter estimation configuration. The ambiguities are then assigned for each band according to the proper ambiguity spacing. The difference between theoretical and observed delay is modelled by a clock function, where the offset term is allowed to vary between S- and X-bands. This accounts for the different ionosphere on the bands. If a residual exceeds a threshold relative to the ambiguity spacing on the band it is shifted as an ambiguity. Once the ambiguities are resolved, c5++ creates a database in NGS format, which includes the ionosphere corrections.

The parameter estimation in c5++ is computed with Gauss-Markov least-squares adjustment. The VLBI component of c5++ can estimate EOP and LOD, station positions and velocities, source positions, ZWD, ZHD, station clocks, scale, and eccentricity. The cable delays and meteorological date are added via the configuration file through VLBI station logs. Because c5++ is directed for multiple techniques the results are formatted to Solution INdependent EXchange (SINEX) format. This feature enables the user to directly use the estimation output as input for subsequent analysis. The work flow of c5++ automated VLBI analysis processing is depicted in Figure 4.1.

The software package c5++ was applied to the automated analysis of INT1 databases and investigations in *Paper II*. The software was modified to include the capability to add simulated noise the estimated parameters.

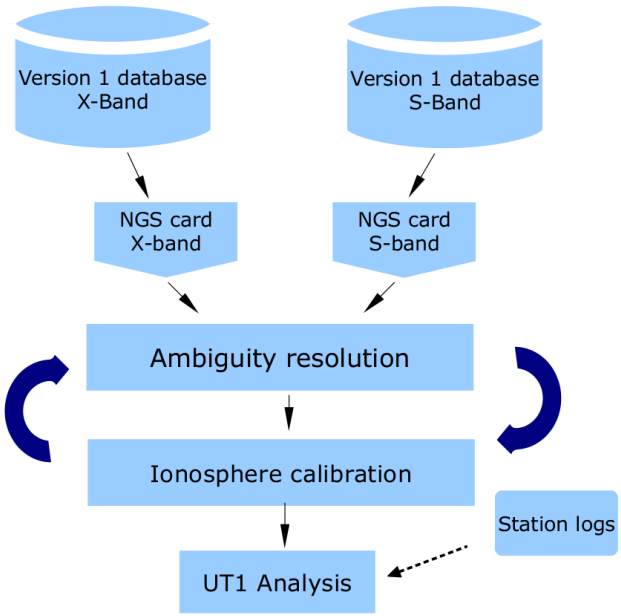

Figure 4.1: Flowchart of the automated VLBI data analysis process with c5++.

4.3 Processing VLBI sessions

Processing geodetic VLBI sessions to estimate geodetic parameters is a sequential operation. The required steps depend on the session type (1 h or 24 h) and whether we have access to a X-band database which already includes the ionosphere calibration (i.e. in IVS-numbering the database version is four or larger). The parameter estimation possibilities of 1-hour INT sessions are limited when compared to the 24-hour R1 and R4 sessions. This is due to the limited number of scans that can be completed in the time span of one hour. The typical data processing tasks differ in individual steps somewhat between c5++ and Calc/Solve, but the main processing flow and the end results are to a degree comparable within the two software packages. In the context of this thesis the database processing always starts with the correlator output, i.e. Version-1 databases. This means the analysis starts with processing the databases for ambiguity resolution. The main task in the analysis process is to form the difference of the reduced observed delay and the computed (theoretical) delay, and using this difference to estimate various geodetic parameters. This process is pictured in Figure 4.2. In the following sections the general steps and related issues of VLBI data processing are discussed. Furthermore, special aspects involved in the VLBI data analysis of the work presented in *Papers I* and *II* are discussed in connection with the introductions to analysis of different session types.

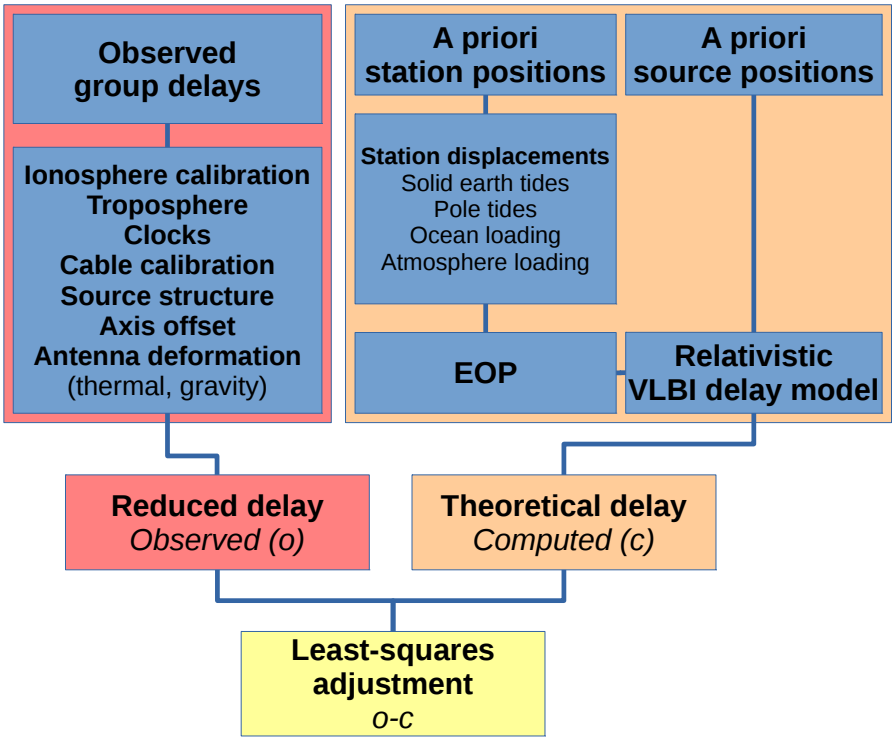

Figure 4.2: Schematics of the data flow in a typical VLBI data analysis. The process is divided into reducing the observed delay and computing the theoretical delay. The differences between observed and computed delays are used as an input to the parameter estimation, here with least-squares adjustment.

4.3.1 Resolving ambiguities

The dual-band observations on X- and S-band both contain an unknown number of group delay ambiguities. The ambiguities are an artefact of the multi-frequency bandwidth synthesis technique (Rogers, 1970), which is used to combine observations on different channels spanning the observed band. As discussed in Chapter 2, the group delay observable is given by $\tau_{gd} = \partial\phi/\partial\omega$. The multi-band group delay is thus determined as the gradient of the best-fit line of the phase samples in the frequency-phase domain. The group delay ambiguity spacing τ_{amb} is given by

$$\tau_{amb} = \frac{1}{\Delta f}, \tag{4.1}$$

where Δf is the greatest common divisor (gcd) between the frequency spacings. With a typical frequency setup the ambiguities in R1/R4 sessions for X- and S-band are 50 ns ($\Delta f = 20$ MHz) and 100 ns ($\Delta f = 10$ MHz), respectively.

The ambiguities must be resolved on both frequency bands prior computing the ionosphere correction for the dual-frequency observations. This process involves distributing the ambiguities between the inter-connected baselines. In an observation network of three or more stations the ambiguities must be distributed in a way that avoids triangle misclosures in the delays between the subsets of three stations.

The approach used in resolving the ambiguities differs between c5++ and Calc/Solve/νSolve. The Solve package supports both manual and automatic ambiguity shifting. The automatic ambiguity resolving utility in Solve is called GAMB. The ambiguity spacing in νSolve follows the process also implemented in Solve. The ambiguities can be solved interactively in semi-automatic iterative manner or adjusted individually for single observations.

The databases used for the DBBC-analogue comparison had to be resolved for ambiguities. This is because the databases were generated to include both the analogue and DBBC recorded data as separate stations and as such were Version-1 databases. These databases were made for R1 and CONT14 sessions and therefore contain several baselines each. Thus, the ambiguity resolution needed to be performed in a way that eliminates all the triangle misclosures between the baselines. The ambiguities for X- and S-band were resolved combining the automatic and manual modes in νSolve. First, automatic resolving of ambiguities was attempted on both bands. When this procedure stabilized (i.e. did not resolve any more ambiguities) or shifted certain data points cyclically between certain ambiguity number, the bands were screened manually. At this stage the triangle misclosure-condition was checked thoroughly. Furthermore, by comparing the difference in X- and S-band residuals it was possible to try to determine applied ambiguity shifts in unclear cases. The difference between X- and S-band observed delays should be in the range of up to a few centimetres. For comparison a typical X-band ambiguity spacing of 50 ns corresponds to approximately 14 m. In some cases the assignment of ambiguities can be itself ambiguous, e.g. in case with 50 ns ambiguity spacing where the residual will be either -25 ns or $+25$ ns. Because the databases contained baselines for both the analogue and the digital Onsala VLBI systems separately, care had to be taken to ensure that the ambiguities were resolved the same way for both stations so as not to introduce artificial differences in the number of applied ambiguities.

The ambiguity resolution processing for the INT1 sessions was done with c5++ in automated mode. This was a necessity since the analysed databases were Version-1 and due to the large number of databases. In total over 1800 databases covering a time period between 2001–2015 were processed. Manual ambiguity resolution in this case would be infeasibly time consuming. Hence for any session where the ambiguity resolution failed, large outliers in the WRMS error of the session and the estimated parameters would show up, which would be suppressed (on a session level) in further stages of the analysis. However, in

general the ambiguity resolution process in the INT sessions is more straightforward due to the small number of baselines (1–3).

4.3.2 Ionosphere calibration

To avoid modelling the ionospheric effects directly on X-band, the delays on the two S/X frequencies used in geodetic VLBI are formed into a linear combination. Recalling Equation 3.25, and adding the ionospheric effect to the respective delays τ_S and τ_Xa, the combined SX delay is given by

$$\tau_{gd}^{SX} = \underbrace{\frac{f_X^2}{f_X^2 - f_S^2}}_{c_1} \tau_{gd}^X - \underbrace{\frac{f_S^2}{f_X^2 - f_S^2}}_{c_2} \tau_{gd}^S. \tag{4.2}$$

Assuming no uncorrelated errors, the variance of the SX combination can be estimated by

$$\sigma_\tau^2 = c_1^2 \sigma_{\tau_X}^2 + c_2^2 \sigma_{\tau_S}^2, \tag{4.3}$$

where the STEC-dependent q has been eliminated. For the S/X frequencies on 2.3/8.4 GHz the c_1 and c_2 fractions are approximately 1.081 and 0.081.

4.3.3 External data

The external data used in VLBI data analysis can be divided into auxiliary data and a priori data for parameter estimation and modelling.

The auxiliary data are used for calibration input in order to model additional errors in the delays or derived parameters. Such data are the cable delay values and meteorological data that are stored in the station log files by the FS during the recording process. The cable delay values can be converted into time delay information that can be included in the observed delay part. Meteorological data can be utilised in the modelling of atmospheric delays.

The a priori data are used as initial values for the parameters in the analysis. The parameters are either fixed to these values or estimated. The estimation processes, such as least-squares estimation, used in VLBI data analysis need some form of a priori information of the involved parameters. For the solution to converge sometimes a reasonably accurate initial guess is needed, which is provided by the a priori values. Depending on the analysis and data availability the a priori values are typically provided by post-processed time-series or model predictions.

Additionally, the theoretical modelling include many geophysical models and instrumental models, which are calculated using precomputed parameters, e.g. ocean loading coefficients. Furthermore, technique combination can also

be regarded as an instance of using external data. An example for this are co-located Water Vapour Radiometer (WVR) observations, which can be potentially used to estimate the ZWD, and thus help to more accurately separate it from the estimated parameters.

Reference frames

In absence of discontinuities or response to geodynamical changes, such as after an earthquake, the station motions can be expected to be linear. Moreover, sources positions are provided by a current realization of the ICRF. In standard geodetic VLBI analysis the source positions are fixed to these a priori values. Thus, in general a priori information on the TRF and CRF do not pose major problems in VLBI. For TRF this is obviously different in case the station position is affected by an earthquake, which might affect the station position through co-seismic displacement and non-linear motion after the main event. Depending on the VLBI network structure this can have a big influence on the related data products. This was the case when the Tsukuba VLBI station (Wakasugi et al., 2015) was displaced due to the 2011 earthquake off the Pacific coast of Tōhoku. After the initial displacement the station is experiencing non-linear motion due to post-seismic relaxation. This affects the INT2 sessions in particular since the sessions consist only of one baseline, of which Tsukuba was the other station.

Earth orientation parameters

A priori data for the EOP are supplied in the form of multi-technique EOP time-series or predicted values based on both previous data and rapid solutions from other techniques such as GNSS. The IERS computes several multi-technique EOP products. Their accuracy, latency, and frequency depend on the techniques involved in the combination. The latency/frequency is connected to the availability and quality of the data from these different techniques.

The main IERS time-series product is the EOP C04 series (the latest version Bizouard and Gambis (2011) is consistent with ITRF2008 (Altamimi et al., 2011)), which combines contributions from VLBI, GNSS, SLR/LLR, and DORIS. However, these values are updated only twice per week, and they have a time lag of over 30 days. Thus, depending on the application, it is necessary to use EOP values that are predicted or taken from techniques that can provide rapid estimates on the values. For example the daily rapid EOP file[2] includes VLBI (1 and 24-hour), GPS observations, and modelling of Atmospheric Angular Momentum (AAM). The values are thus dependent on the number and the quality of the observations included in the estimation procedure. For example 24-hour VLBI sessions are regularly observed bi-weekly (Monday and Thursday), thus

[2] `http://datacenter.iers.org/eop/-/somos/5Rgv/getMeta/13/finals2000A.daily`

the time from previous 24-hour sessions varies between 0–3 days. One of the main VLBI products is UT1-UTC, for which variation is difficult to model and predict. The impact of EOP on the UT1-UTC estimates have been previously investigated in e.g. Malkin (2011) and Nothnagel and Schnell (2008). In the appended *Paper II* the impact of various analysis configurations and the quality of a priori data are investigated for the INT1 sessions, in particular in connection with polar motion and UT1-UTC.

If the EOP are not estimated during the processing or for near-real time VLBI analysis, some form of prediction of the a priori values is unavoidable. The last value covered in the long-term EOP C04 08 time series is always at least 30 days old. It only covers days starting from 30 days into the past, thus more recent values from daily EOP solutions or predictions are needed. IERS releases a weekly Bulletin A (IERS Rapid Service Prediction Centre, 2015), which contains EOP at a daily interval.

Meteorological data

Meteorological data that are used in the VLBI processing come from many sources. Typically such data include on-site observations made during the experiment and a range of Numerical Weather Models (NWM) and associated data sets. For example, when performing a VLBI experiment with FS the standard procedure is to record local weather data to a station log-file. These observations include temperature, barometric pressure, relative humidity, and wind speed and direction. This data is as accurate as the instrumentation at the individual stations. Generally speaking, the long term stability is not an issue with the locally observed weather data, but rather missing or corrupted data and sudden deviations from the trend. Separating suspicious values from data depicting real dynamics in the weather can be difficult. Depending on experiment length and the possible range of typical weather conditions at the time of observation at the telescope, it must be decided whether a value that exhibits large deviation from some implied trend represents a true variation or an erroneous observation. In the current IVS analysis procedures the weather data are screened either manually or semi-automatically (Gipson, 2015, Thorandt, 2015). For VLBI the most important meteorological parameter is the barometric pressure, because along with the station position it is the sole input parameter for the Saastamoinen model for the calculation of the ZHD (Saastamoinen, 1972). In addition to barometric pressure, the only other in situ observation utilised in a standard VLBI processing is the local temperature, used for antenna thermal deformation modelling. In order to automatically screen the observed data to some extent, a simplified approach is to check whether the observed quantities have physically reasonable values. For example, the pressure can be limited between the extrema values recorded on Earth. However, this still leaves the

possibility to have unrealistic pressure gradients between the measurements.

The handling of meteorological data in Calc/νSolve and c5++ are different. In the Calc work flow the weather information is included in the database after processing with Calc11 using the programs pwxcb and dbcal. The former reads in values from the station log-files and provides a graphical data editing interface. The program tries to automatically detect suspicious data points and optionally suppress them. The screened values are then included in the database using dbcal. In the subsequent νSolve processing the weather data can be enabled/disabled station-wise.

The software package c5++ uses meteorological data if they are found in the NGS database. The data are added in the same stage as the ambiguity estimation and ionosphere calibration. The station log-files are declared in the configuration file that sets up the ambiguity processing. These meteorological data are then included in the resulting NGS files. This means the that raw values from the station log-files are already interpolated to observation epochs at this stage. Moreover, obviously unphysical values due to instrument malfunction or corrupted log files, such as 0 mbar pressure are filtered out prior to including the data in the NGS database. The weather data time stamps in the station log-files can differ from the observation epochs in the NGS file. Singular large deviations in the raw data can, due to the interpolation, propagate into multiple observation epochs in the NGS file. The abnormal values can be in some cases harder to detect at this stage, if the large raw deviation is damped in the interpolation.

Phase calibration and cable delay

The VLBI observation system is not perfectly stable. The electronic length of the cables and signal path through various equipment can change in response to for example thermal expansion or physical forcing (e.g. cable wrapping). Thus, the signal is subjected to propagation delays when it travels through the system. In order to measure the changes in phase and frequency, a known calibration signal is injected together with the observed signal. In time domain the phase calibration signal is a tone repeating e.g. every 1 μs (Petrov, 2000). The number of pulses per second is dependent on the number of calibration tones that are wanted within the frequency range. The signal is typically inserted into the system close to the feed. Depending on the injection point the signal will then include contributions from the instruments that follow it in the signal chain. At the correlation this tone can be recovered and thus it is possible to determine the measured changes in phase and delay.

The phase calibration reference signal path needs to be monitored for changes in electrical length as well. This is done by cable calibration. A signal is sent to and back from the receiver. These values are recorded in the station log-files,

from which a cable delay can computed and included in the VLBI delay model. This is done similarly as the respective processes including the meteorological data in Calc/νSolve and c5++. The cable delay time tag is determined by the execution time of the command in the FS. Thus, for the parallel recording configuration in *Paper I* even though the same cable calibration signal is used for both backends, the cable delay values are not sampled in absolute synchronization. The time tags are determined by the system time in the respective recording systems, Mark 5A for the analogue and Mark 5B+ for the digital system configurations. Each configuration outputs individual station log-files, which contain the respective cable delay measurements. The impact of this difference in sampling is dependent on the noisiness of the cable calibration signal. This aspect of differences in the cable delays is addressed in *Paper I*.

A cable delay value is ideally measured for each observation during the experiment. In the experiment preparation and end stages the cable sign is measured by adding an additional bit of cable in the signal path and measuring the effect on the observed cable delay. The cable sign is needed to convert the cable delay values from the log-file into the corresponding group delay contribution.

As with the meteorological data, in the standard processing the cable delay values are also screened in manual or semi-automatic procedure. The cable delay values are similarly prone to errors such as corrupted log-files. Furthermore, it is possible that the log-files lack information on the cable sign, if the sign test was not performed even once during the preparation or finalizing stages. In this case with manual processing it is usually possible to check previously used cable sign values and manually add this missing information into the data. Normally the cable sign of at a station does not change from session to session, unless a result of instrumental changes.

Automatic detection of suspicious or erroneous cable delay data are more complicated than with the meteorological data. The nominal values for the cable delays are not so clear cut. The delays can be affected by the temperature, but also the wrapping of the cables when the telescopes is turning. For some telescopes this cable wrapping can manifest as changes in the cable delay behaviour. Thus, the delays are dependent on the azimuth and elevation of the source, and also the positions of the preceding sources, because this determines the level of wrapping in the cables, before the antenna has to e.g. turn $+365^\circ$ instead of -5° to unwrap the cables.

4.3.4 Parameter estimation

After reducing the observations and computing the theoretical delays, i.e. determining the observed$-$computed vector, the geodetic parameters are estimated by finding an extremum for some objective function, or by filtering methods. In νSolve and c5++ this is done in a least-squares adjustment. Assuming the obser-

vations in general have decent signal-to-noise ratios (SNR) (for VGOS the estimated minimum SNR to resolve the broadband delays is 10 (Petrachenko et al., 2009)) the main factors that influence the parameter estimation process are the number of observations and the network geometry. The observation schedules are typically designed to provide optimum premise (or at least a compromise) in terms of network geometry and number of observations for the parameter estimation. The choices made during the parameter estimation include choosing the estimated and fixed parameters, estimation interval and type, constraints and conditions, outlier rejection algorithms, weighting for estimated parameters and observations, selecting which a priori data are used and included in the estimation, the mapping functions, and source selection (quality flags and elevation cut-off).

The parametrisation depends on the target parameters and session types. For the various IVS EOP sessions there are standard configurations which are used at least as a usual starting point in the analysis. Generally, the parameter estimation is done in steps and iteratively, increasing the number of estimated parameters once crude and systematic errors are removed from the observations. For example in the ambiguity estimation or clock break detection the parametrisation is simplified only to include the largest contributors to the observed group delays, such as clock offsets. More intricate parametrisation is added as the data have first been processed for these more prominent errors. It is possible that the real variation in the parameters is so large and fast, that the parametrisation needs to include higher order terms and to decrease the estimation intervals. For example a quickly varying troposphere might benefit from estimating ZWD every 20 minutes instead of every hour. The room for adjustment in parametrisation is still largely connected to the number of observations. Each estimated parameter increases the number of unknowns and thus reduces the degrees of freedom (DOF) by one. The degree of freedom r is given by $r = n - u$, the difference between the number observations and unknowns. If the degree of freedom is zero the solution is determined. This case is sensitive to outliers and could become rank deficient, if the solution cannot decorrelate the unknown parameters. However, it is important to prevent to overparameterise the system in order to avoid the situation where the model is explaining observation noise instead of the true parameter values.

In the following the two most common parametrisation cases, the 24-hour and 1-hour sessions, are described. Moreover the parameter estimation involved with the data processing in *Papers I* and *II* are discussed with the corresponding session type (24 h/INT, respectively). These parametrisations apply for ambiguity-resolved and ionosphere calibrated data. The process of resolving ambiguities and ionosphere involves a simplified parametrisation.

24-hour sessions

The most common length for a VLBI observation session is 24 hours. This include for example the R1, R4, and T2 sessions. Due to the length and the number of observations in these sessions, it is typically possible to estimate a large number of parameters, including all EOP and station coordinates. Station clocks are estimated usually with a 60 minute interval. One station is selected as the reference clock, against which all the other station clocks are estimated. In general the only requirement in choosing the reference clock is that the frequency standard is known to be stable and not affected by some form of known (or unknown) problems. EOP and station coordinates are typically considered to have one value per 24-hour session. For datum definition it is possible to apply No-Net-Translation (NNT) and No-Net-Rotation (NNR) conditions for the source and station positions. As a rule of thumb the radio source coordinates are fixed to their a priori values e.g. ICRF2 (Fey et al., 2009), but if needed individual source positions may be estimated, e.g. in case of hard-to-handle influence of source structure. The troposphere and gradients are estimated depending on the participating stations. Generally, 1 to 2 hourly estimates are produced for the ZWD. The atmospheric gradients are usually estimated every 6 hours for a 24-hour session. Furthermore, the estimated parameters, such as troposphere delays, can be constrained in an absolute or relative sense. Tuning these constraints might help with sessions that have unusual behaviour in some of the estimated parameters or large gaps between observations.

The operational analysis of e.g. R1/R4 sessions also includes thorough outlier rejection and observation re-weighting procedures. The data processing for the DBBC-analogue comparison (*Paper I*) differs slightly from this type of analysis. The object of the study was to compare the results obtained from sessions where the data recorded with both digital and analogue backends at Onsala were correlated as their own stations, included in the same database. These stations are now referred according to 2-letter station code notation as as the 'On' (analogue) and 'Od' (digital).

The comparison was done both by comparing the observed delays and the geodetic parameters estimated from the sessions. The latter involves processing all included databases with Calc11 and analysed with νSolve (ver. 0.1.6 Red Rue/Solar Fire). For this Calc/νSolve combination the implemented mapping functions were the NMF. Since we are dealing with Version-1 databases, all sessions were initially processed for ambiguities, clock breaks, ionosphere calibration, and initial check of data quality. This process involves processing the sessions with increasing complexity in parametrisation, starting with only the clock polynomials.

In the final processing stage the On/Od stations were in turns excluded from the parameter estimation, thus producing a set of geodetic parameters associ-

ated with both stations separately. When estimating station positions in order to prevent the network to absorb the possible differences in the data, all the other stations were fixed to their a priori VTRF2008 (Böckmann et al., 2010) positions and velocities. Furthermore, stations with known discontinuities due to earthquakes (TIGO VLBI station and Tsukuba 32-m VLBI station, see e.g. Baver et al. (2015)) were excluded from the analysis. The parallelly recorded experiments included R1 and CONT14 sessions. The parametrisation was done in two modes: "Stapos" and "Full EOP".

1. Stapos: when On/Od station position was estimated only a subset of EOP was estimated.
2. Full EOP: When estimating the full set of EOP all station positions were fixed to a priori values.

The common parameter setup that was used for both modes is presented in Table 4.1. The mode-specific configuration are listed in Table 4.2.

Table 4.1: Common parametrisation setup used in the On–Od comparison. The "Local" estimation uses the whole set of observations to produce one estimate for the whole session.

Parameter	Estimation type
Station clocks	Quadratic polynomial, PWL 60 min interval
Zenith delays	PWL 60 min intervals
Atm. gradients	One PWL for session
Source positions	Fix to ICRF2
UT1-UTC rate	Local
Nutation angles	Local

For all the analysed sessions Wettzell was chosen as the reference clock. The cable delays and meteorological data were included in the databases prior to parameter estimation, and this information was used in the analysis. Because the On/Od data were recorded on separate Mark 5/FS systems, both station had their individual station log-files. However, in practice some of the log files for Od did not contain e.g. cable information because the it was not logged during the experiment. In this cases data from the On-log was used for both databases, instead. The PWL functions used in the processing were realised by B-splines. Moreover, the PWL functions are characterised by two values, the estimation interval and constraints to the variation of the parameters on these intervals. For these values the νSolve default settings were used. For ZWD and

Table 4.2: Differences between the two parametrisation modes ”Stapos” (left column) and ”Full EOP” (right column) in the On–Od comparison. The ”Local” estimation uses the whole set of observations to produce one estimate for the whole session.

	Mode: Stapos	Mode: Full EOP
Parameter	Estimation type	Estimation type
Station positions	On/Od local, rest fix to VTRF2008	Fix all to VTRF2008
UT1-UTC	USNO finals EOP	Local
Polar motion	USNO finals EOP	Local

clocks the constraints were 1.1992 cm/h and 72 ps/h, respectively. For gradients the constraints were so loose (29979245.8 cm/h) that essentially they were not applied.

1-hour Intensive sessions

The analysis of the INT sessions is limited by the number of observations, session length and the number of baselines. The INT sessions are designed for UT1-UTC estimation, which is the main target parameter from these sessions. Because of the limited number of observations in these sessions, the amount of estimated parameters is kept to a minimum to maximise the DOF. Moreover, the session length and baseline configuration is not sufficient to resolve polar motion or celestial pole offsets. The clock polynomial is estimated quadratically, which for a one-baseline configuration means 3 parameters (offset, rate, and a quadratic term) while the first station is used as the reference clock. The station positions and source positions are fixed to their a priori values. Generally these 6 parameters (3 clock coefficients, troposphere for both stations, UT1-UTC) comprise the default estimation setup for INT session. The benefit of estimating gradients is a compromise between a possibly better resolved troposphere and adding another parameter to the already weak system. Furthermore, the effect of estimating gradients during the relatively short time span of an INT duration can be limited. Using external information for gradient determination has been investigated in e.g. Böhm et al. (2010) and Teke et al. (2015), where it was found to have some promise for improvement for UT1-UTC estimation.

The investigation in *Paper II* concentrates on the INT1 sessions on the Kokee–Wettzell baseline. It is aimed at recognizing the important factors in UT1-UTC estimation with respect to external data in a near-real time automated config-

uration. Thus the parametrisation used in the analysis follows closely a "standard" setup used in INT UT1-UTC production. This parametrisation that was that was used in the analysis with c5++ is described in Table 4.3.

Table 4.3: Typical parametrisation for one-baseline observation geometry in INT analysis. The parametrisation described was used in the automated analysis of INT1 in c5++.

Parameter	Station #1 (Wettzell)	Station #2 (Kokee)
Station clock	Reference	Quadratic polynomial
Station position	Fix to ITRF2008	Fix to ITRF2008
Zenith Hydrostatic Delay	Fix	Fix
Zenith Wet Delay	Estimate 1 offset	Estimate 1 offset
Radio sources	Fix to ICRF2	
UT1-UTC	Estimate 1 offset	
Polar motion	Fix to a priori	
Nutation/precession	Fix to a priori	

Throughout the analysis with c5++ the modelling was done in accordance with the latest IERS conventions 2010 (Petit and Luzum, 2010). In the parameter estimation the clock function was computed as a simple quadratic polynomial without constraints. Because INT sessions have a duration of only 1 hour this clock model is likely sufficient to model the clock behaviour during the session. The UT1-UTC estimate was computed as one offset value on top of a quadratic polynomial interpolated from the a priori EOP (in this case IERS C04 08). ZHD was computed as one offset using a pressure value which was taken from either GPT2 or local pressure supplied by the station log file. The tropospheric delays were mapped using either GMF(GPT2) or VMF1. Generally the station positions and source coordinates were kept fixed to their a priori values. The same applies to the non-estimated EOP. An exception to this parametrisation was one aspect of the analysis, where the station position of the non-reference station (i.e. Kokee) was estimated in order to test different constraint levels. In general the investigation involved applying different configurations of a priori data. In addition to estimating the station position of Kokee the impact of external data was studied in terms of the external meteorological and cable delay data. The effect of the applied a priori EOP data was investigated by simulating the effect of having old/predicted EOP values. This was done by modifying the c5++ program to allow adding an additional noise to the applied a priori EOP. This way the reference EOP time series C04 08 was impaired to realistically

represent the use of inaccurate data. In practice this was done by using estimated accuracy levels for predicted polar motion and UT1-UTC a priori based on IERS Bulletin A. These standard deviations were used as a seed for values drawn from a Gaussian distribution, which were added to the reference a priori values. The process was repeated in a Monte Carlo simulation, 20 times per session for 36 standard deviation levels. This number of iterations, combined with the large number of sessions (1669 included in the Monte Carlo simulation) ensured that the sample is representative.

Chapter 5

Results and discussion

The previous chapters described to some detail the processing chain involved in geodetic VLBI data analysis and the related data products. This was expressed both in general context as well as related to the research carried out for this thesis and the appended *Papers I* and *II*. In this chapter the general results from this work are summarised and discussed.

5.1 Comparing VLBI experiments with analogue and digital backends at Onsala Space Observatory

The parallelly recorded sessions at Onsala during the testing phase of the DBBC equipment included several R1, EUR, T2, and R&D-sessions. These sessions are listed in Table 5.1. Some of the data from these sessions were correlated on-site at Onsala with the DiFX software correlator (Deller et al., 2007). Furthermore, a subset of these sessions were correlated at Bonn (Bernhart et al., 2015) to produce databases, which included both the analogue- and digital-based data as separate Onsala-stations, denoted as ”On” and ”Od”, respectively. These sessions formed the basis of the comparison for the observed delays and geodetic parameters. They are listed in Table 5.2.

The raw correlator delays involving the On and Od baselines were inspected by using a third station (Wettzell, Wz) from the observing network to form a subset baseline-triangle. The observed group delays on these baselines were screened for outliers using the 3-σ rule with respect to the mean delay on the baseline. The median absolute values for the On–Wz–Od triangle misclosures in group delays for the R1 and CONT14 were 6.5 ps and 3.2 ps, respectively. The corresponding values for the median formal errors were 14.7 ps and 9.4 ps. An example of misclosure histograms for CONT14 are illustrated in Figures 5.1 and 5.2. This indicates that the correlated group delays were within the

Table 5.1: Sessions recorded in parallel with the analogue Mark 4 system and the DBBC.

R1 sessions	R1.553, R1.563, R1.566, R1.567, R1.569, R1.570, R1.572
	R1.573, R1.585, R1.591, R1.592, R1.598, R1.600, R1.601
	R1.602, R1.604, R1.612, R1.615, R1.616, R1.615, R1.616
RD sessions	RD.12.01, RD.13.01, RD.13.03, RD.13.06
EUR sessions	EUR.118, EUR.120, EUR.123, EUR.125
T2 sessions	T2.090, T2.093, T2.094
CONT14	Complete campaign
	C14.01–C14.15

Table 5.2: Databases that include data from On and Od as separate stations.

Database date	Session code
12-Dec-10	IVS-R1.563
13-Jan-02	IVS-R1.566
13-Jan-07	IVS-R1.567
13-Jul-01	IVS-R1.592
13-Nov-18	IVS-R1.612
14-May-09	CONT14.04
14-May-10	CONT14.05
14-May-11	CONT14.06
14-May-13	CONT14.08
14-May-15	CONT14.10

error limits of the observations. The cable delay differences from the On and Od station log files were found to be normally distributed, with most values between ± 5 ps. This indicates that the cable delays did not contribute any biases to the observations, when read from the individual log files. In general the geodetic parameters derived from the On and Od solutions agreed with each other within the respective formal errors for the differences. The results from the R1 sessions in terms of EOP were affected by the weakened network ge-

ometry due to excluding the earthquake-affected stations completely from the analysis. Compared to the very large network of size CONT14 in terms of number of stations, the exclusion of these stations relatively weakened the network geometry of the R1 sessions more. Some discrepancies could be explained by remaining triangle misclosures between On, Od, and a third stations, that were not detected during coarse outlier search. In general the results showed that there were no obvious biases between the On and Od data, but most variation in the differences were scattered around the zero-line both within and between the sessions.

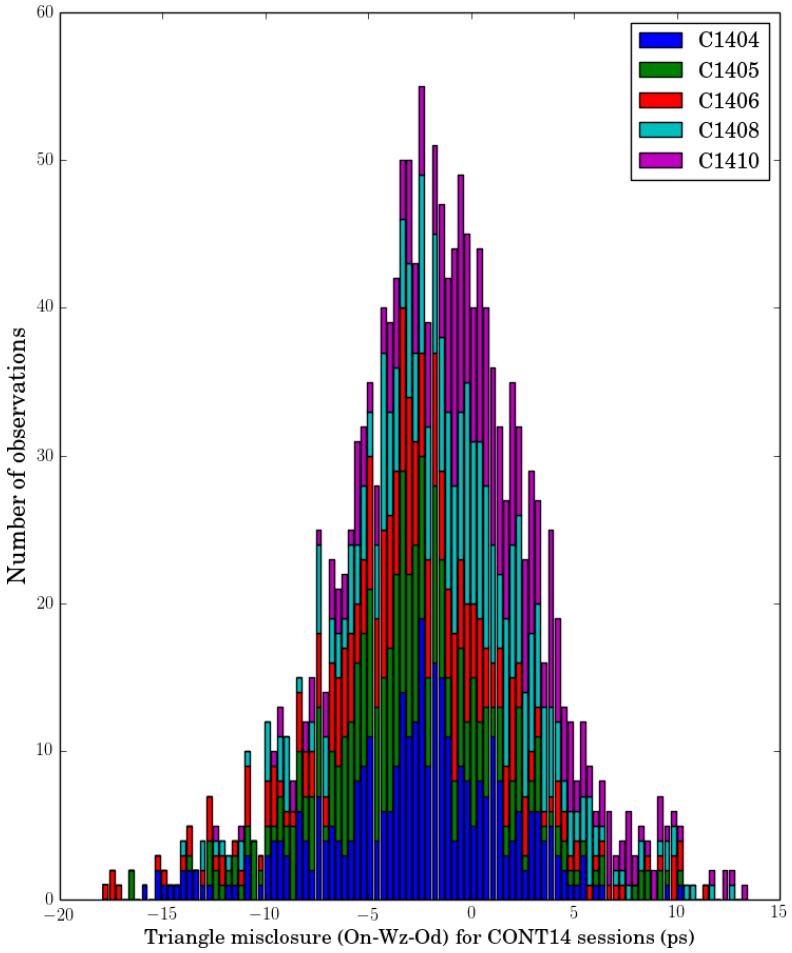

Figure 5.1: Triangle misclosures for the observed group delays (On–Wz–Od).

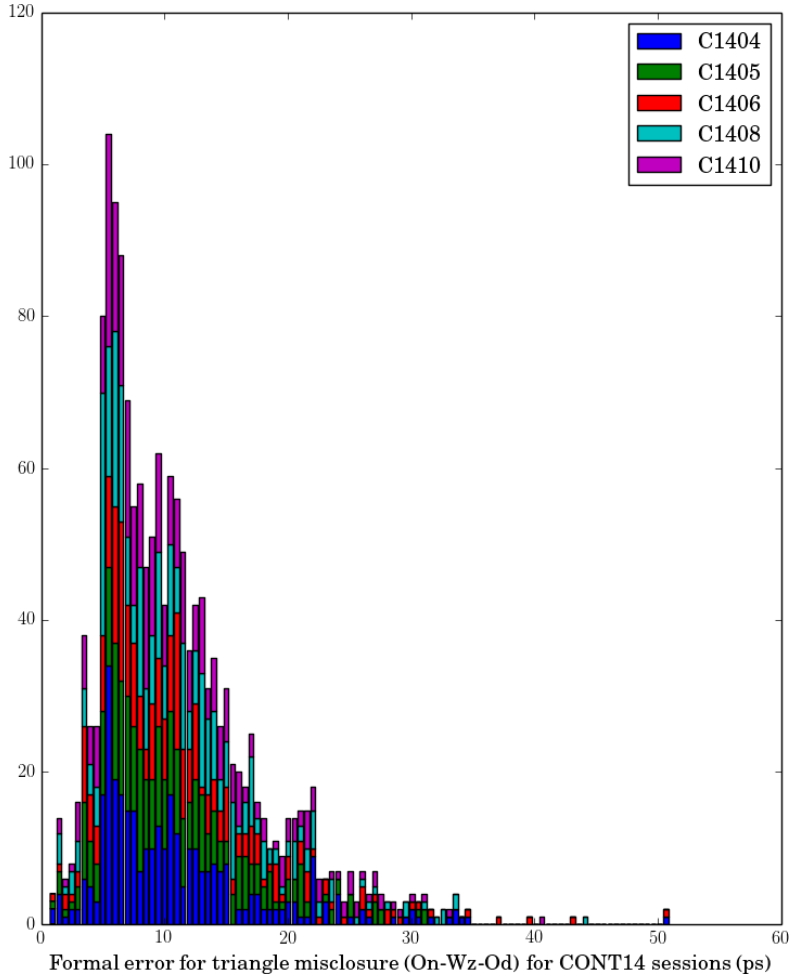

Figure 5.2: Formal errors of the observed group delays for the triangle misclosure (On–Wz–Od).

5.2 On the impact of a priori information on INT1 sessions

The impact of applying different a priori information and analysis procedures were assessed by investigating the UT1-UTC estimates with respect to IERS C04 08 derived from observations on the Kokee–Wettzell baseline. One of the aims of the study was to introduce an estimation procedure that would correspond to the situation where the UT1-UTC estimate could be produced in an automated near-real time fashion. This meant analysing the impact of the different analysis choices on databases that correspond to the correlator output. The different analysis options included assessing the impact of mapping functions, use of external data (cable delays from station log files), in situ meteorological

data (measured local barometric pressure) versus models (GPT2), studying the impact of estimated station positions, and impact of a priori EOP data. The UT1-UTC estimates were computed with respect to the C04 08 EOP time series, which in this case can be regarded as the best estimate reference. This makes it possible to infer the effectiveness of the different analysis configurations by comparing the respective results within each other. If not otherwise mentioned, the UT1-UTC estimates discussed in the following refer to the residuals with respect the C04 08 series.

In order to have a temporally extensive and procedurally consistent data set the sessions were selected based on availability and scheduling. The initial inclusion criteria was to use all the sessions between 2001 and 2015 where a Version-1 database was available and Kokee–Wettzell was the only scheduled baseline. This lead to a data set of 1669 databases. These databases were processed with c5++ software package in automated mode to resolve ambiguities and to calibrate ionospheric effects.

The impact of mapping functions, local meteorological data, and cable delays were cross-investigated by estimating UT1-UTC using the four different analysis configurations. The sessions were analysed by turning on/off the station log-files and using either VMF1 or GMF(GPT2) mapping functions. When the station log-files were not used the pressure data for both mapping functions were provided by the GPT2 values. The four analysis configurations are listed in Table 5.3.

Table 5.3: The four analysis strategies used to study the impact of mapping function selection and applying external data.

Strategy	Mapping function	Pressure data	Cable delay
A	VMF1	station log-files	station log-files
B	GMF(GPT2)	station log-files	station log-files
C	VMF1	GPT2	not used
D	GMF(GPT2)	GPT2	not used

Based on the UT1-UTC WRMS values obtained using these four strategies it was found that the use of external data or the choice of mapping function has a markedly small effect on the UT1-UTC estimated from INT1 sessions. The improvement in WRMS when in situ data were used was far below 1 μs. The difference in WRMS between the mapping functions when the same set of external data were used (using/not-using station log-files) was diminishingly small (0.01–0.02 μs). The use of external data also reduced the number of sessions which passed the adopted crude outlier rejection limits, indicating that in some cases a rudimentary automatic screening of the external data was not

adequate. In the end the use of external data did improve the UT1-UTC accuracy slightly, but this requires that the external data are reliable. The automatic processing was also in some cases hampered by ill-formatted data, which was likely due to program/hardware malfunction or a combination of the two. The UT1-UTC time series and associated WRMS values computed using the four strategies are shown in Figures 5.3 and 5.4.

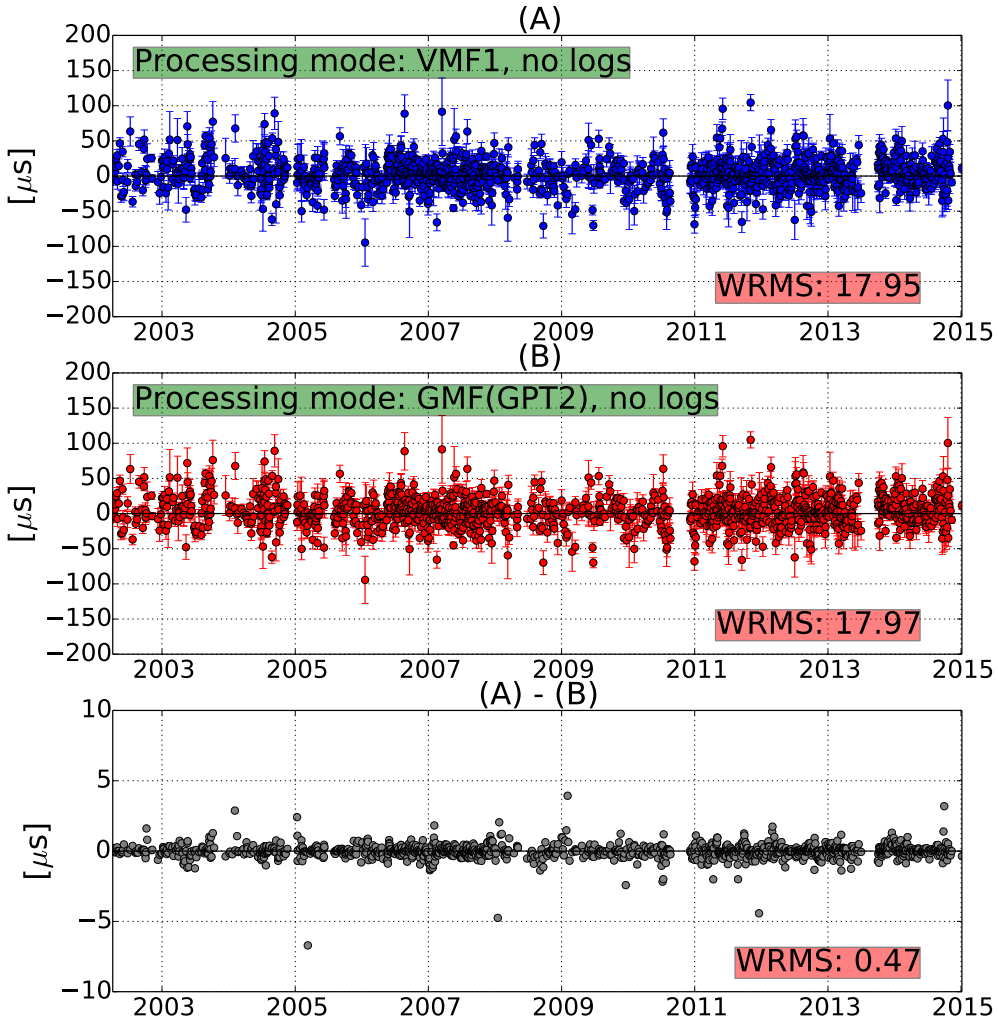

Figure 5.3: Processing without external data included in the log files: UT1-UTC residuals from processing with VMF1 (A) and GMF(GPT2) (B). The bottom row: difference of time series (A) and (B).

Estimating a constrained station position for the non-reference station did not lead to any improvement in terms of UT1-UTC. On the other hand, when

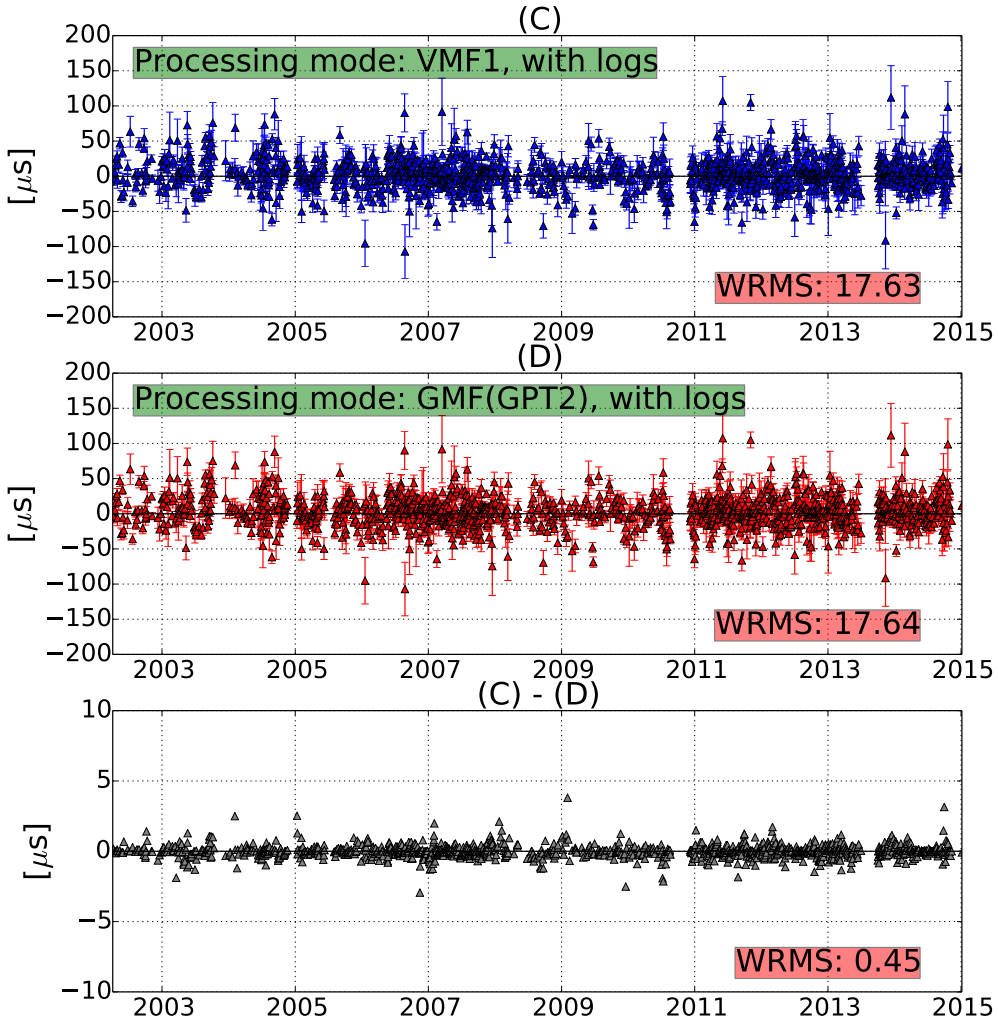

Figure 5.4: Processing with external data included in the log files: UT1-UTC residuals from processing with VMF1 (C) and GMF(GPT2) (D). The bottom row: the difference of time series (C) and (D).

strong constraints for the station position were applied, the inclusion of the extra parameter did not have a significant adverse effect either. The mean degree of freedom in the 6 unknowns parametrisation setup was 14, varying between 4 and 28.

This leaves the a priori EOP as candidates through which the UT1-UTC estimates could be improved. In their present form UT1-UTC is the only EOP that can be estimated from the INT sessions. For near-real time applications this immediately implies that predicted EOP data are required. The influence of Ce-

lestial Pole Offsets (CPO) on UT1-UTC is relatively small. According to Malkin (2011) neglecting CPO models may lead to UT1-UTC biases of approximately 1.4 μs. The impact of inaccuracies in a priori polar motion an UT1-UTC were studied using Monte Carlo simulations. A detailed explanation of the simulation process is provided in *Paper II*. In its main points, the predicted accuracy for the polar motion and UT1-UTC were estimated, respectively, using

$$\sigma_{X_p}, \sigma_{Y_p} = 680 \cdot D^{0.80}, \tag{5.1}$$

and

$$\sigma_{UT1} = 250 \cdot D^{0.75}, \tag{5.2}$$

where D is the days elapsed from the release of IERS Bulletin A (IERS Rapid Service Prediction Centre, 2015). Noise terms for 36 values of D were sampled from a Gaussian distribution using the expressions in Equations 5.1 and 5.2, which were used as offset to the a priori values. The sampling was done 20 times for each session.

The a priori UT1-UTC accuracy was found not be a significant issue in the estimation process. Even very outdated a priori UT1-UTC did not affect the convergence of UT1-UTC, because the least-squares adjustment remained in the linear neighbourhood for the UT1-UTC with respect to the a priori values. Outdated polar motion values were however found to be the main factor which quickly degraded the accuracy of the UT1-UTC estimates. This is in agreement with previous studies, that have shown that there exist a directly proportional effect between polar motion offsets and UT1-UTC estimates (Nothnagel and Schnell, 2008). With their present level of accuracy the a priori polar motion values can not be older than 6 hours in order to provide an UT1-UTC accuracy below 20 μs. Figure 5.5 illustrates the increase of UT1-UTC WRMS as the estimated accuracy of the a priori polar motion values decrease.

5.3 Discussion and future scenarios

The world of geodetic VLBI is in a state of transition. An increasing number of stations are building new telescopes and implementing related instrumentation compatible with the requirements for VGOS. When a large number of upgrades are implemented in quick succession it is possible that some bias effects or other disturbances are overlooked. Hence it is important to analyse the effects of instrumental changes in diverse and comprehensive way, covering the whole VLBI product chain.

Once fully operational the new VGOS system will have unprecedented capabilities for continuous space-geodetic observations. However, while a detailed road map to operational VGOS operations has been emerging in the recent years

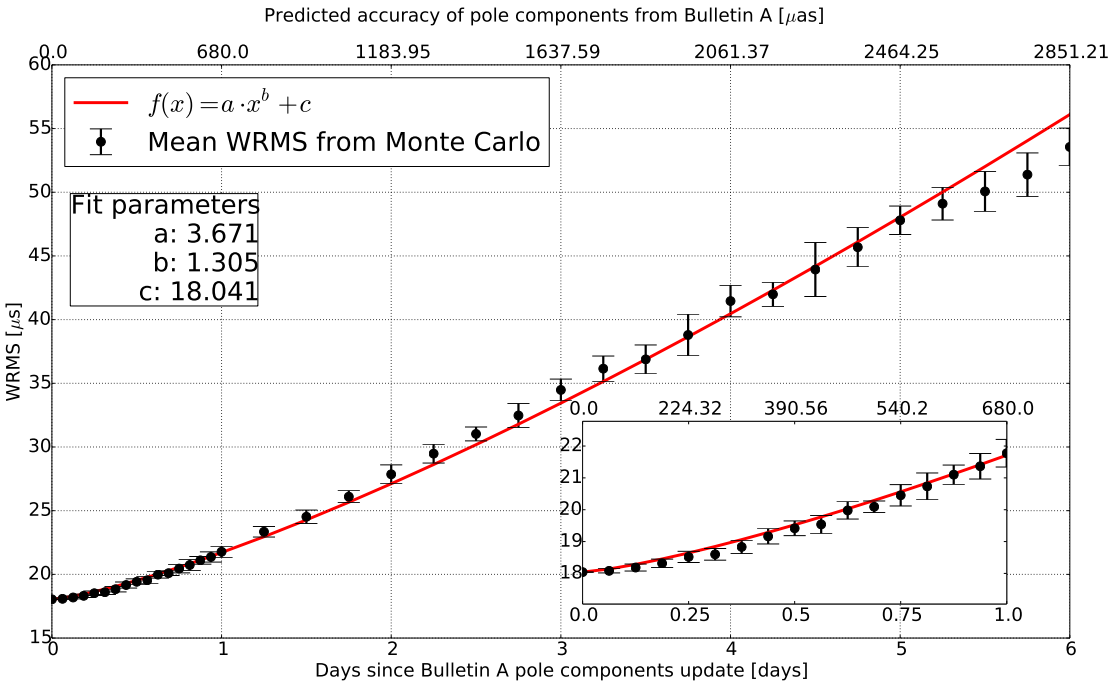

Figure 5.5: Mean WRMS of UT1-UTC residuals with respect to C04. The X-axis shows days elapsed since the Bulletin A epoch (bottom) and corresponding polar motion accuracy (top).

(see e.g. Petrachenko et al. (2014)) a full transition still lies a long way ahead. In the meantime geodetic VLBI must be able to provide high-quality data products, such as daily UT1-UTC, for e.g. the scientific, technical, and commercial sectors. Furthermore, one of the core missions for geodetic VLBI is also to establish long-term monitoring of parameters and phenomena such as nutation and plate tectonics.

VGOS will be a largely automated monitoring system working in near-real time. However, currently the turnaround time requirements for R1 and R4 sessions for EOP determination are not even close to these type of latency levels. These sessions are carried out bi-weekly and the target maximum latency is over two weeks. The INT sessions can be thought of as a type of a stepping stone between the old fashioned session-based VLBI to continuous monitoring. Executing the INT observation schedule requires daily input in the form of scheduling, station operations, correlation, and data analysis, to name a few.

It is evident that reliable and consistent operations call for a high-level automation, even in the case of the hourly intensives. Lessons learned in automating the existing VLBI procedures are valuable in all upcoming observation tasks that need to be automated. Identifying the significant contributors to the over-

all noise-floor and systematic errors can both help in the development of the analysis strategies for the upcoming observing system as well as the improve the already existing observing programs.

The INT sessions have over time proven to be particularly resistant to efforts of improving their accuracy. The short observation interval combined with an overall low number of observations set conditions that fundamentally limit the available potential for improvement. However, sometimes limited resources can lead to imaginative solutions, which can be useful for future applications as well. Recognizing both the existence and reason for the bottlenecks is important in assessing whether they could be an issue within a different context. For the current noise-levels in automated near-real time INT processing, the issues with cable delay and meteorological data mainly concern the capability to filter the data in case of outliers or otherwise unreliable data. In general, the relative impact of either applying reliable cable delay and meteorological data or ignoring them both, is small on the UT1-UTC from INT sessions. However, with smaller overall noise floor the relative importance of these data could significantly increase. The strong observation networks of VGOS may alleviate the issues experienced with needing to fix EOP to inaccurate values a priori values. The system as whole will still depend on its ability to process data automatically and respond in case the results indicate a problem. Adaptive automatic parameter estimation methods have the potential to become important, when large numbers of observations are constantly streamed for processing. The bandwidth increases associated with VGOS are also going to put the correlators under a new type of pressure. If the correlators cannot handle the amount of incoming data for real-time processing, it might be necessary to use some form pre-correlation metrics to decide which observations will be prioritised.

Overall it is important to recognize the key components of a system that need to be improved in order to optimally serve the end-user of the data products. This includes both purely scientific and more practically oriented target audiences alike.

Bibliography

Altamimi, Z., Collilieux, X. and Métivier, L. (2011), 'ITRF2008: an improved solution of the international terrestrial reference frame', *Journal of Geodesy* **85**(8), 457–473.

Andersen, P. (2000), 'Multi-level arc combination with stochastic parameters', *Journal of Geodesy* **74**(7-8), 531–551.

Barry, R. G. and Chorley, R. J. (1992), *Atmosphere, weather, and climate*, Cambridge University Press.

Battrick, B., ed. (2005), *Global Earth Observation System of Systems (GEOSS): 10-year Implementation Plan Reference Document*, ESA Publications Division, ESTEC, Netherlands.

Baver, K. D., Behrend, D. and Armstrong, K. L., eds (2013), *International VLBI Service for Geodesy and Astrometry 2012 Annual Report*, NASA/TP-2013-217511.

Baver, K. D., Behrend, D. and Armstrong, K. L., eds (2014), *International VLBI Service for Geodesy and Astrometry 2013 Annual Report*, NASA/TP-2014-217522.

Baver, K. D., Behrend, D. and Armstrong, K. L., eds (2015), *International VLBI Service for Geodesy and Astrometry 2014 Annual Report*, NASA/TP-2015-217532.

Bernhart, S., Alef, W., Bertarini, A., La Porta, L., Müskens, A., Rottmann, H. and Roy, A. (2013), 'The Bonn Astro/Geo Correlator', *in* K. D. Baver, D. Behrend and K. L. Armstrong, eds, 'International VLBI Service for Geodesy and Astrometry 2012 Annual Report', NASA/TP-2014-217522, pp. 209–212.

Bernhart, S., Alef, W., Bertarini, A., Bruni, G., La Porta, L., Müskens, A., Rottmann, H., Roy, A. and Tuccari, G. (2015), 'The Bonn Astro/Geo Correlator', *in* K. D. Baver, D. Behrend and K. L. Armstrong, eds, 'International VLBI Service for Geodesy and Astrometry 2014 Annual Report', NASA/TP-2015-217532, pp. 161–163.

Bindoff, N.L., Willebrand, J., Artale, V., Cazenave, A., Gregory, J., Gulev, S., Hanawa, K., Le Quéré, C., Levitus, S., Nojiri, Y., Shum, C.K., Talley, L.D. and Unnikrishnan, A. (2007), 'Observations: oceanic climate change and sea level', *in* S. Solomon, D. Qin, M. Manning, Z. Chen, M. Marquis, K.B. Averyt, M. Tignor and H.L. Miller, eds, 'Climate change 2007: the physical science basis. Contribution of Working Group I to the Fourth Assessment Report of the Intergovernmental Panel on Climate Change', Cambridge University Press, pp. 385–432.

Bizouard, C. and Gambis, D. (2011), 'IERS C04 08',
available from: `https://hpiers.obspm.fr/iers/eop/eopc04/C04.guide.pdf`. The combined solution C04 for Earth Orientation Parameters consistent with International Terrestrial Reference Frame 2008. Accessed: 2015-12-28.

Böckmann, S., Artz, T. and Nothnagel, A. (2010), 'VLBI terrestrial reference frame contributions to ITRF2008', *Journal of Geodesy* **84**, 201–219.

Böhm, J., Werl, B. and Schuh, H. (2006a), 'Troposphere mapping functions for GPS and very long baseline interferometry from European Centre for Medium-Range Weather Forecasts operational analysis data', *Journal of Geophysical Research: Solid Earth (1978–2012)* **111**(B2).

Böhm, J., Niell, A., Tregoning, P. and Schuh, H. (2006b), 'Global Mapping Function (GMF): A new empirical mapping function based on numerical weather model data', *Geophysical Research Letters* **33**(7).

Böhm, J. and Schuh, H. (2007), 'Troposphere gradients from the ECMWF in VLBI analysis', *Journal of Geodesy* **81**(6-8), 403–408.

Böhm, J., Hobiger, T., Ichikawa, R., Kondo, T., Koyama, Y., Pany, A., Schuh, H. and Teke, K. (2010), 'Asymmetric tropospheric delays from numerical weather models for UT1 determination from VLBI Intensive sessions on the baseline Wettzell–Tsukuba', *Journal of Geodesy* **84**(5), 319–325.

Böhm, J., Böhm, S., Nilsson, T., Pany, A., Plank, L., Spicakova, H., Teke, K. and Schuh, H. (2012), 'The new Vienna VLBI software VieVS', *in* 'Geodesy for Planet Earth', Springer, pp. 1007–1011.

Bolotin, S., Baver, K., Gipson, J., Gordon, D. and MacMillan, D. (2014), 'The VLBI Data Analysis Software νSolve: Development Progress and Plans for the Future', *in* K. D. Baver, D. Behrend and K. L. Armstrong, eds, 'IVS 2014 General Meeting Proceedings "VGOS: The New VLBI Network"', Science Press, Beijing, pp. 253–257.

Bourda, G., Charlot, P. and Collioud, A. (2015), 'Aligning VLBI and Gaia Extragalactic Celestial Reference Frames', *in* 'Proceedings of 22nd European VLBI for Geodesy and Astrometry (EVGA) Working Meeting', pp. 220–225.

Capitaine, N., Guinot, B. and McCarthy, D. D. (2000), 'Definition of the celestial ephemeris origin and of UT1 in the international celestial reference frame', *Astronomy and Astrophysics* **355**, 398–405.

Capitaine, N. and Wallace, P. T. (2006), 'High precision methods for locating the celestial intermediate pole and origin', *Astronomy and Astrophysics* **450**(2), 855–872.

Capitaine, N. and Soffel, M. (2015), 'On the definition and use of the ecliptic in modern astronomy', *arXiv preprint arXiv:1501.05534* .
URL: *http://syrte.obspm.fr/jsr/journees2014/pdf/Capitaine.pdf*

Chao, B., Dong, D., Liu, H. and Herring, T. (1991), 'Libration in the Earth's rotation', *Geophysical Research Letters* **18**(11), 2007–2010.

Chernicoff, S. (1999), *Geology: an introduction to physical geology*, Houghton Mifflin Harcourt (HMH).

Cook, J., Nuccitelli, D., Green, S. A., Richardson, M., Winkler, B., Painting, R., Way, R., Jacobs, P. and Skuce, A. (2013), 'Quantifying the consensus on anthropogenic global warming in the scientific literature', *Environmental Research Letters* **8**(2), 024024.

Davis, J., Herring, T., Shapiro, I., Rogers, A. and Elgered, G. (1985), 'Geodesy by radio interferometry: Effects of atmospheric modeling errors on estimates of baseline length', *Radio Science* **20**(6), 1593–1607.

Deller, A., Tingay, S., Bailes, M. and West, C. (2007), 'DiFX: A Software Correlator for Very Long Baseline Interferometry Using Multiprocessor Computing Environments', *Publications of the Astronomical Society of the Pacific* **119**(853), 318–336.

Desai, S. D. (2002), 'Observing the pole tide with satellite altimetry', *Journal of Geophysical Research: Oceans (1978–2012)* **107**(C11), 7–1.

Dick, W. R. and Thaller, D., eds (2014), *IERS Annual Report 2013*, Verlag des Bundesamts für Kartographie und Geodäsie, Frankfurt am Main.

Fey, A., Gordon, D. and Jacobs, C. S., eds (2009), *The Second Realization of the International Celestial Reference Frame by Very Long Baseline Interferometry, Presented on behalf of the IERS / IVS Working Group*, IERS Technical Note 35, Verlag des Bundesamts für Kartographie und Geodäsie, Frankfurt am Main.

Gipson, J. (2010), 'An introduction to Sked', *in* D. Behrend and K. D. Baver, eds, 'IVS 2010 General Meeting Proceedings VLBI2010: From Vision to Reality', NASA/CP-2010-215864, pp. 77–84.

Gipson, J. (2012), 'IVS Working Group 4: VLBI Data Structures', *in* D. Behrend and K. D. Baver, eds, 'IVS 2012 General Meeting Proceedings "Launching the Next-Generation IVS Network"', NASA/CP-2012-217504, pp. 212–221.

Gipson, J. (2014), 'IVS Working Group IV and the New Open Format Database', *in* K. D. Baver, D. Behrend and K. L. Armstrong, eds, 'IVS 2014 General Meeting Proceedings "VGOS: The New VLBI Network"', Science Press, Beijing, pp. 248–252.

Gipson, J. (2015), Personal communication.

Gordon, D. (2005), 'Using the VLBA For Geodesy and Astrometry', *in* J. Romney and M. Reid, eds, 'Future Directions in High Resolution Astronomy: The 10th Anniversary of the VLBA, ASP Conference Proceedings', Vol. 340 of *ASP Conference Series*, p. 496.

Gordon, D. (2007), 'NGS Format for VLBI Data Transfer – Revised June 11, 2007', available from: `http://lacerta.gsfc.nasa.gov/mk5/help/dbngs_format.txt`. Accessed: 2015-12-17.

Haas, R. and Schuh, H. (1996), 'Determination of frequency dependent Love and Shida numbers from VLBI data', *Geophysical Research Letters* **23**(12), 1509–1512.
URL: *http://dx.doi.org/10.1029/96GL00903*

Hartmann, D. L., Klein Tank, A. M. G., Rusticucci, M., Alexander, L.V., Brönnimann, S., Charabi, Y., Dentener, F. J., Dlugokencky, E. J., Easterling, D. R., Kaplan, A., Soden, B. J., Thorne, P.W., Wild, M. and Zhai, P. M. (2014), 'Observations: atmosphere and surface', *in* T. F. Stocker, D. Qin, G.-K. Plattner, M. Tignor, S. K. Allen, J. Boschung, A. Nauels, Y. Xia, V. Bex and P. M. Midgley, eds, 'Climate change 2013: The Physical Science Basis Contribution of Working Group I to the Fifth Assessment Report of the Intergovernmental Panel on Climate Change', Cambridge University Press,

Hase, H., Behrend, D., Ma, C., Petrachenko, B., Schuh, H. and Whitney, A. (2012), 'The emerging VGOS network of the IVS', *in* D. Behrend and K. D. Baver, eds, 'IVS 2012 General Meeting Proceedings "Launching the Next-Generation IVS Network"', NASA/CP-2012-217504, pp. 8–12.

Herring, T. (1992), 'Modeling atmospheric delays in the analysis of space geodetic data', *in* J. C. De Munck and T. A. Spoelstra, eds. 'Proceedings of Refraction

of Transatmospheric signals in Geodesy', Vol. 36, Netherlands Geodetic Commission Publications on Geodesy, pp. 157–164.

Hobiger, T., Koyama, Y. and Kondo, T. (2008), 'MK3TOOLS - Seamless Interfaces for the Creation of VLBI Databases from Post-Correlation Output', *in* A. Finkelstein and D. Behrend, eds, 'IVS 2008 General Meeting Proceedings', Nauka, St. Petersburg, pp. 153–156.

Hobiger, T., Otsubo, T., Sekido, M., Gotoh, T., Kubooka, T. and Takiguchi, H. (2010), 'Fully automated VLBI analysis with c5++ for ultra-rapid determination of UT1', *Earth, Planets and Space* **62**(12), 933–937.

IERS Rapid Service Prediction Centre (2015), 'IERS Bulletin A', available from: `http://hpiers.obspm.fr/eoppc/bul/bulb/explanatory.html`. Accessed: 2015-12-17.

IGG Vienna (2015), 'Institute of Geodesy and Geophysics at the Vienna University of Technology, Archive of troposphere delay parameters.', available from: `http://ggosatm.hg.tuwien.ac.at/DELAY/SITE/VLBI/`. Accessed: 2015-12-17.

Jacobs, C. S., Arias, F., Boboltz, D., Böhm, J., Bolotin, S., Bourda, G., Charlot, P., De Witt, A., Fey, A., Gaume, R., Gordon, D., Heinkelmann, R., Lamber, S., Ma, C., Malkin, Z., Nothnagel, A., Seitz, M., Skurikhina, E., Souchay, J. and Titov, O. (2013), 'The ICRF-3: Proposed Roadmap to the Next Generation International Celestial Reference Frame', *Journées Systemes de Référence Spatio-Temporels, Paris* **16**.

Karttunen, H., Kröger, P., Oja, H., Poutanen, M. and Donner, K. J., eds (2007), *Fundamental astronomy*, 5 edn, Springer Science & Business Media.

Kelley, M. C. (2009), *The Earth's Ionosphere: Plasma Physics & Electrodynamics*, Vol. 96, Academic press.

Klopotek, G. (2015). Personal communication.

Krasna, H., Böhm, J. and Schuh, H. (2013), 'Free core nutation observed by VLBI', *Astronomy and Astrophysics* **555**, A29.

Kurihara, S. and Hara, T. (2015), 'Tsukuba VLBI correlator', *in* K. D. Baver, D. Behrend and K. L. Armstrong, eds, 'International VLBI Service for Geodesy and Astrometry 2014 Annual Report', NASA/TP-2015-217532, pp. 175–178.

Lagler, K., Schindelegger, M., Böhm, J., Krasna, H. and Nilsson, T. (2013), 'GPT2: Empirical slant delay model for radio space geodetic techniques', *Geophysical Research Letters* **Vol. 40 (6)**, 1069–1073.

Lambeck, K. (1988), *Geophysical geodesy: the slow deformations of the earth*, Oxford, England: Clarendon Press; New York: Oxford University Press.

Ma, C., Sauber J. M., Bell L. J., Clark, T., Gordon, D., Himwich W. E. and Ryan J. W. (1990), 'Measurement of horizontal motions in Alaska using very long baseline interferometry', *Journal of Geophysical Research: Solid Earth* **95**(B13), 21991–22011.

MacMillan, D. S. (1995), 'Atmospheric gradients from very long baseline interferometry observations', *Geophysical Research Letters* **22**(9), 1041–1044.
URL: *http://dx.doi.org/10.1029/95GL00887*

Malkin, Z. (2007), 'Empiric models of the Earths free core nutation', *Solar System Research* **41**(6), 492–497.

Malkin, Z. (2011), 'The impact of celestial pole offset modelling on VLBI UT1 intensive results', *Journal of Geodesy* **85**(9), 617–622.

Marini, J. W. (1972), 'Correction of satellite tracking data for an arbitrary tropospheric profile', *Radio Science* **7**(2), 223–231.

Mathews, P. M., Buffett, B. A. and Shapiro, I. I. (1995), 'Love numbers for a rotating spheroidal Earth New definitions and numerical values', *Geophysical Research Letters* **22**(5), 579–582.
URL: *http://dx.doi.org/10.1029/95GL00161*

McCarthy, D. D. and Petit, G., eds (2004), *IERS Conventions (2003)*, IERS Technical Note 32, Verlag des Bundesamts für Kartographie und Geodäsie, Frankfurt am Main.

Mujunen, A. and Salminen, T. (2013), 'Final report on Networked Storage on Demand', Technical report, The Joint Institute for VLBI in Europe.

Niell, A. (1996), 'Global mapping functions for the atmosphere delay at radio wavelengths', *Journal of Geophysical Research: Solid Earth (1978–2012)* **101**(B2), 3227–3246.

Niell, A., Whitney, A., Petrachenko, B., Schlüter, W., Vandenberg, N., Hase, H., Koyama, Y., Ma, C., Schuh, H. and Tuccari, G. (2005), 'VLBI2010: current and future requirements for geodetic VLBI systems', *International VLBI Service for Geodesy and Astrometry* .
URL: *http://ivscc.gsfc.nasa.gov/about/wg/wg3/IVS_WG3_report_050916.pdf*

Nilsson, T., Haas, R. and Elgered, G. (2007), 'Simulations of atmospheric path delays using turbulence models', *in* J. Böhm, A. Pany and H. Schuh, eds, 'Proceedings of the 18th European VLBI for geodesy and astrometry working

meeting', Vol. 79, Geowissenschaftliche Mitteilungen, Schriftenreihe der Studienrichtung Vermessung und Geoinformation, Technische Universitat Wien, pp. 175–180.

Nilsson, T. and Haas, R. (2010), 'Impact of atmospheric turbulence on geodetic very long baseline interferometry', *Journal of Geophysical Research: Solid Earth (1978–2012)* **115**(B3).

Nothnagel, A. and Schnell, D. (2008), 'The impact of errors in polar motion and nutation on UT1 determinations from VLBI Intensive observations', *Journal of Geodesy* **82**(12), 863–869.

Pany, A., Böhm, J., MacMillan, D., Schuh, H., Nilsson, T. and Wresnik, J. (2011), 'Monte Carlo simulations of the impact of troposphere, clock and measurement errors on the repeatability of VLBI positions', *Journal of Geodesy* **85**(1), 39–50.

Parselia, E., Nilsson, T., Heinkelmann, R., Gebauer, A., Klügel, T., Schreiber, U. and Schuh, H. (2014), 'Earth Rotation Determination by Combining Ring Laser Gyroscopes and VLBI', *in* K. D. Baver, D. Behrend and K. L. Armstrong, eds, 'IVS 2014 General Meeting Proceedings "VGOS: The New VLBI Network"', Science Press, Beijing, pp. 495–499.

Peixoto, J. P. and Oort, A. H. (1992), *Physics of climate*, New York, NY (The United States of America); American Institute of Physics.

Petit, G. and Luzum, B., eds (2010), *IERS Conventions (2010)*, IERS Technical Note 36, Verlag des Bundesamts für Kartographie und Geodäsie, Frankfurt am Main.

Petrachenko, B., Niell, A., Behrend, D., Corey, B., Böhm, J., Charlot, P., Collioud, A., Gipson, J., Haas, R., Hobiger, T., Koyama, Y., MacMillan, D., Malkin, Z., Nilsson, T., Pany, A., Tuccari, G., Whitney, A. and Wresnik, J. (2009), 'Design aspects of the VLBI2010 system'. Progress report of the IVS VLBI2010 committee, NASA/TM-2009-214180.

Petrachenko, B., Behrend, D., Gipson, J., Hase, H., Ma, C., MacMillan, D., Niell, A., Nothnagel, A. and Zhang, X. (2014), 'VGOS Observing Plan', *in* K. D. Baver, D. Behrend and K. L. Armstrong, eds, 'IVS 2014 General Meeting Proceedings "VGOS: The New VLBI Network"', Science Press, Beijing, pp. 16–19.

Petrachenko, B., Bertarini, A., Alef, W., Behrend, D., Cappallo, R., Hase, H., Ma, C., Niell, A., Nothnagel, A. and Xhang, X. (2015), 'VGOS Data Transmission and Correlation Plan', *in* K. D. Baver, D. Behrend and K. L. Armstrong, eds, 'International VLBI Service for Geodesy and Astrometry 2014 Annual Report', NASA/TP-2015-217532, pp. 11–19.

Petrov, L. (2000), 'Instrumental errors of geodetic VLBI', *in* N. R. Vanderberg and K. D. Baver, eds, 'IVS 2000 General Meeting Proceedings', NASA/CP-2000-209893, pp. 230–235.

Petrov, L. and Boy, J.-P. (2004), 'Study of the atmospheric pressure loading signal in very long baseline interferometry observations', *Journal of Geophysical Research: Solid Earth (1978–2012)* **109**(B3).

Plag, H., Beutler, G., Forsberg, R., Ma, C., Neilan, R., Pearlman, M., Richter, B. and Zerbini, S. (2005), 'The Global Geodetic Observing System (GGOS): observing the dynamics of the Earth system'.

Plag, H.-P. and Pearlman, M. (2009), *Global geodetic observing system: meeting the requirements of a global society on a changing planet in 2020*, Springer Science & Business Media.

Ratcliffe, J. A. (1972), *An introduction to the ionosphere and magnetosphere*, Cambridge University Press.

Rogers, A. E. (1970), 'Very long baseline interferometry with large effective bandwidth for phase-delay measurements', *Radio Science* **5**(10), 1239–1247.

Saastamoinen, J. (1972), 'Atmospheric correction for the troposphere and stratosphere in radio ranging satellites', *The use of artificial satellites for geodesy* pp. 247–251.

Scherneck, H.-G. (1999), 'Explanatory supplement to the section local site displacement due to ocean loading of the iers conventions (1996)', *Explanatory Supplement to the IERS Conventions (1996)* pp. 6–7.

Schuh, H. and Behrend, D. (2012), 'VLBI: a fascinating technique for geodesy and astrometry', *Journal of Geodynamics* **61**, 68–80.

Sekido, M., Takiguchi, H., Koyama, Y., Kondo, T., Haas, R., Wagner, J., Ritakari, J., Kurihara, S. and Kokado, K. (2008), 'Ultra-rapid UT1 measurement by e-VLBI', *Earth, Planets and Space* **60**(8), 865–870.

Souchay, J. and Feissel-Vernier, M., eds (2006), *The International Celestial Reference System and Frame - ICRS Center Report for 2001-2004*, IERS Technical Note 34, Verlag des Bundesamts für Kartographie und Geodäsie, Frankfurt am Main.

Sovers, O. J., Fanselow, J. L. and Jacobs, C. S. (1998), 'Astrometry and geodesy with radio interferometry: experiments, models, results', *Reviews of Modern Physics* **70**(4), 1393.

Sun, J., Pany, A., Nilsson, T., Böhm, J. and Schuh, H. (2011), 'Status and future plans for the VieVS scheduling package', *in* 'Proceedings of 20th European VLBI for Geodesy and Astrometry (EVGA) Working Meeting', pp. 44–48.

Teke, K., Böhm, J., Madzak, M., Kwak, Y. and Steigenberger, P. (2015), 'GNSS zenith delays and gradients in the analysis of VLBI Intensive sessions', *Advances in Space Research* **56**(8), 1667–1676.

Thompson, A. R., Moran, J. M. and Swenson Jr, G. W. (2008), *Interferometry and synthesis in radio astronomy*, John Wiley & Sons.

Thorandt, V. (2015), Personal communication.

Titov, O., Tesmer, V. and Böhm, J. (2004), 'OCCAM v. 6.0 software for VLBI data analysis', *in* N. R. Vanderberg and K. D. Baver, eds, 'IVS 2004 General Meeting Proceedings', NASA/CP-2004-212255, pp. 267–271.

Titov, O., Lambert, S. and Gontier, A.-M. (2011), 'VLBI measurement of the secular aberration drift', *Astronomy and Astrophysics* **529**, A91.

Torge, W. and Müller, J. (2012), *Geodesy*, 4 edn, Walter de Gruyter.

Tuccari, G. (2004), 'DBBC - a Wide Band Digital Base Band Converter', *in* N. R. Vanderberg and K. D. Baver, eds, 'IVS 2004 General Meeting Proceedings', NASA/CP-2004-212255, pp. 234–237.

Tuccari, G., Buttaccio, S., Nicotra, G., Xiang, Y. and Wunderlich, M. (2006), 'DBBC - A Flexible Platform for VLBI Data Processing', *in* D. Behrend and K. D. Baver, eds, 'IVS 2006 General Meeting Proceedings', NASA/CP-2006-214140, pp. 185–189.

Tuccari, G., Alef, W., Bertarini, A., Buttaccio, S., Comoretto, G., Graham, D., Neidhardt, A., Platania P.R., Russo, A., Roy, A., Wunderlich, M., Zeitlhöfler, R. and Xiang, Y. (2010), 'DBBC2 backend: Status and development plan', *in* D. Behrend and K. D. Baver, eds, 'IVS 2010 General Meeting Proceedings "VLBI2010: From Vision to Reality"', NASA/CP-2010-215864, pp. 392–395.

Tuccari, G., Alef, W., Buttaccio, S., Casey, S., Felke, A., Lindqvist, M. and Wunderlich, M. (2014), 'DBBC3: An EVN and VGOS All-inclusive VLBI System', *in* K. D. Baver, D. Behrend and K. L. Armstrong, eds, 'IVS 2014 General Meeting Proceedings "VGOS: The New VLBI Network"', Science Press, Beijing, pp. 86–90.

Vandenberg, N. R. (1999), *SKED: Interactive/Automatic Scheduling Program*, NVI, Inc. NASA/Goddard Space Flight Center Space Geodesy Program.

Vaughan, D. G., Comiso, J. C., Allison, I., Carrasco, J., Kaser, G., Kwok, R., Mote, P., Murray, T., Paul, F., Ren, J., Rignot, E., Solomina, O., Steffen, K. and Zhang, T. (2013), 'Observations: Cryosphere', *in* T. F. Stocker, D. Qin, G.-K. Plattne, M. Tignor, S. K. Allen, J. Boschung, A. Nauels, Y. Xia, V. Bex and P. M.

Midgley, eds, 'Climate change 2013: The Physical Science Basis Contribution of Working Group I to the Fifth Assessment Report of the Intergovernmental Panel on Climate Change', Cambridge University Press, Cambridge, United Kingdom and New York, NY, USA.

Wakasugi, T., Kawabata, R., Kurihara, S., Fukuzaki, Y., Kuroda, J., Wada, K., Mizuno, S. and Ishida, T. (2015), 'Tsukuba 32-m VLBI Station', *in* K. D. Baver, D. Behrend and K. L. Armstrong, eds, 'International VLBI Service for Geodesy and Astrometry 2014 Annual Report', NASA/TP-2015-217532, pp. 124–127.

Whitney, A. R. (1993), 'The Mark IV VLBI Data-Acquisition and Correlation System', *in* 'Developments in Astrometry and their Impact on Astrophysics and Geodynamics', Springer, pp. 151–157.

Whitney, A. R. (2002), 'Mark 5 Disc-Based Gbps VLBI Data System', *in* N. R. Vanderberg and K. D. Baver, eds, 'IVS 2002 General Meeting Proceedings', NASA/CP-2002-210002, pp. 132–136.

Whitney, A. R. (2004), 'The Mark 5B VLBI Data System', *in* N. R. Vanderberg and K. D. Baver, eds, 'IVS 2004 General Meeting Proceedings', NASA/CP-2004-212255, pp. 177–181.

Whitney, A., Ruszczyk, C., Romney, J. and Owens, K. (2010), 'The Mark 5C VLBI Data System', *in* D. Behrend and K. D. Baver, eds, 'IVS 2010 General Meeting Proceedings "VLBI2010: From Vision to Reality"', NASA/CP-2010-215864, pp. 373–377.

Whitney, A. and Lapsley, D. (2012), 'Mark 6 Next-Generation VLBI Data System', *in* D. Behrend and K. D. Baver, eds, 'IVS 2012 General Meeting Proceedings "Launching the Next-Generation IVS Network"', NASA/CP-2012-217504, pp. 86–90.